



Poly(A) Polymerase 1 (PAPS1) influences organ size and pathogen response in *Arabidopsis thaliana*

Dissertation

zur Erlangung des akademischen Grades

doctor rerum naturalium (Dr. rer. nat.)

eingereicht an der

Mathematisch-Naturwissenschaftlichen Fakultät der Universität Potsdam

Institut für Biochemie und Biologie

von

Gerda Trost

geboren am 27.01.1985 in Halberstadt

Potsdam, April 2014

Published online at the
Institutional Repository of the University of Potsdam:
URL <http://opus.kobv.de/ubp/volltexte/2014/7234/>
URN <urn:nbn:de:kobv:517-opus-72345>
<http://nbn-resolving.de/urn:nbn:de:kobv:517-opus-72345>

Table of contents

Summary	4
Zusammenfassung	5
Acknowledgements.....	6
List of Figures	7
List of Tables	8
1. Introduction	9
1.1. Growth is a genetically tightly controlled process.....	9
1.1.1. Mechanisms of plant organ growth.....	9
1.1.2. Genetic regulation of plant organ growth	10
1.1.3. Role of phytohormones in plant growth.....	13
1.2. Nuclear polyadenylation is a conserved mechanism amongst eukaryotes.....	15
1.2.1. Polyadenylation <i>cis</i> -elements	17
1.2.2. Polyadenylation trans-factors.....	17
1.2.3. Canonical Poly(A) Polymerases (cPAP)	19
1.2.4. cPAPs in plants	21
1.2.5. Control of mRNA poly(A) tail length	22
1.2.6. Alternative polyadenylation.....	23
1.3. Plants have a variety of mechanisms to react on biotic stress	24
1.3.1. Pathogen recognition and reaction in plants – PTI and ETI	25
1.3.2. EDS1/PAD4/SAG101 mediated signalling	27
1.3.3. Phytohormone crosstalk in plant immunity	28
1.3.4. Role of polyadenylation/deadenylation proteins in plant immunity	30
1.4. Aim of this study	31
2. Results.....	32
2.1 Target specificity among nuclear poly(A) polymerases in plants modulates organ growth and pathogen response	32
2.2. Arabidopsis poly(A) polymerase PAPS1 limits founder-cell recruitment to organ primordia and suppresses the salicylic acid-independent pathogen response downstream of EDS1/PAD4	68
2.3. Additional characterization of the <i>paps1-1</i> mutants.....	101
2.3.1. Double mutants with <i>ahg2-1</i> are embryo-lethal	101
2.3.2. The BR pathway is not affected in <i>paps1-1</i> mutants	101
.....	103
2.3.3. redox-sensitive GFP reveals more oxidized chloroplasts in <i>paps1-1</i> mutants.....	104

Table of contents

2.3.4. RNA sequencing	107
2.3.5. Methods and Material	110
3. Discussion.....	114
3.1. Why is the <i>PAPS1</i> function different in flowers and leaves?	114
3.2. The ectopic pathogen response in <i>paps1</i> mutant leaves	117
3.3. Influence of <i>paps</i> mutations on deadenylation and RNA decay.....	120
3.4. Functional specialization amongst <i>PAPS</i> in <i>Arabidopsis</i>	122
Appendix A: Cloning strategies	124
Appendix B: Instruments	126
Abbreviations.....	127
References	130

Summary

Polyadenylation of pre-mRNAs is critical for efficient nuclear export, stability, and translation of the mature mRNAs, and thus for gene expression. The bulk of pre-mRNAs are processed by canonical nuclear poly(A) polymerase (PAPS). Both vertebrate and higher-plant genomes encode more than one isoform of this enzyme, and these are coexpressed in different tissues. However, in neither case is it known whether the isoforms fulfill different functions or polyadenylate distinct subsets of pre-mRNAs. This thesis shows that the three canonical nuclear PAPS isoforms in *Arabidopsis* are functionally specialized owing to their evolutionarily divergent C-terminal domains. A moderate loss-of-function mutant in PAPS1 leads to increase in floral organ size, whereas leaf size is reduced. A strong loss-of-function mutation causes a male gametophytic defect, whereas a weak allele leads to reduced leaf growth. By contrast, plants lacking both PAPS2 and PAPS4 function are viable with wild-type leaf growth. Polyadenylation of *SMALL AUXIN UP RNA (SAUR)* mRNAs depends specifically on PAPS1 function. The resulting reduction in SAUR activity in *paps1* mutants contributes to their reduced leaf growth, providing a causal link between polyadenylation of specific pre-mRNAs by a particular PAPS isoform and plant growth. Additionally, opposite effects of PAPS1 on leaf and flower growth reflect the different identities of these organs. The overgrowth of *paps1* mutant petals is due to increased recruitment of founder cells into early organ primordia whereas the reduced leaf size is due to an ectopic pathogen response. This constitutive immune response leads to increased resistance to the biotrophic oomycete *Hyaloperonospora arabidopsidis* and reflects activation of the salicylic acid-independent signalling pathway downstream of ENHANCED DISEASE SUSCEPTIBILITY1 (EDS1)/PHYTOALEXIN DEFICIENT4 (PAD4). Immune responses are accompanied by intracellular redox changes. Consistent with this, the redox-status of the chloroplast is altered in *paps1-1* mutants. The molecular effects of the *paps1-1* mutation were analysed using an RNA sequencing approach that distinguishes between long- and short tailed mRNA. The results shown here suggest the existence of an additional layer of regulation in plants and possibly vertebrate gene expression, whereby the relative activities of canonical nuclear PAPS isoforms control *de novo* synthesized poly(A) tail length and hence expression of specific subsets of mRNAs.

Zusammenfassung

Polyadenylierung von prä-mRNAs ist entscheidend für den Export aus dem Zellkern, die Stabilität und die Translation der reifen mRNAs und dadurch für die Genexpression. Der Großteil der mRNAs wird durch sogenannte canonische Poly(A) Polymerasen (cPAPS) prozessiert. Die Genome von sowohl Wirbeltieren als auch Pflanzen kodieren mehr als eine Isoform dieser Enzyme, welche gleichzeitig in verschiedenen Geweben exprimiert werden. Es ist jedoch kein Beispiel bekannt, das zeigt, ob die verschiedenen Isoformen unterschiedliche Funktionen einnehmen bzw. verschiedene Untergruppen von mRNAs polyadenylieren. Diese Arbeit zeigt, dass drei canonische PAPS Isoformen in *Arabidopsis thaliana* aufgrund ihrer evolutionär unterschiedlichen C-terminalen Domänen spezialisierte Funktionen haben. Eine schwache Verlust-Mutation im *PAPS1* Gen bewirkt eine Vergrößerung der Blütenorgane, während die Blattgröße vermindert ist. Eine starke Verlust-Mutation bewirkt zusätzlich einen Defekt der männlichen Keimzellen. Im Gegenzug dazu sind Mutanten des *PAPS2* oder *PAPS4* Gens gesund und zeigen ein normales Wachstum. Polyadenylierung von *SMALL AUXIN UP RNA (SAUR)* mRNAs hängt spezifisch von der Funktion von PAPS1 ab. Die daraus entstehende Reduzierung der SAUR Aktivität in den *paps1* Mutanten trägt zur Verringerung der Blattgröße bei und stellt eine kausale Verbindung zwischen Polyadenylierung spezifischer mRNAs durch bestimmte PAPS Isoformen und Pflanzenwachstum dar. Zusätzlich spiegeln die unterschiedlichen Effekte von PAPS1 auf Blüten und Blätter die Identitäten dieser Organe wieder. Das übermäßige Wachstum der mutanten Petalen beruht auf einer erhöhten Anzahl an Gründer-Zellen im frühen Primordium, wohingegen die verminderte Blattgröße auf eine ektopische Pathogen Antwort zurückzuführen ist. Diese konstitutive Immunantwort bewirkt eine erhöhte Resistenz der Mutanten gegenüber dem biotrophen Oomyceten *Hyaloperonospora arabidopsidis* und reflektiert die Aktivierung des Salizylsäure unabhängigen Signalweges von ENHANCED DISEASE SUSCEPTIBILITY1 (EDS1)/PHYTOALEXIN DEFICIENT4 (PAD4). Immunantworten sind von Veränderungen des intrazellulären Redoxpotenzials gekennzeichnet. Damit übereinstimmend zeigen die Chloroplasten der *paps1-1* Mutanten ein verändertes Redoxpotenzial. Zur genaueren Aufklärung der molekularen Effekte der *paps1-1* mutation wurde eine RNA-Sequenzierungsmethode verwendet, die zwischen mRNAs mit langem oder kurzem Poly(A) Schwanz unterscheidet. Die Aktivitäten der verschiedenen canonischen PAPS Isoformen kontrollieren die Länge des neu synthetisierten poly(A) Schwanzes und damit die Expression spezifischer Untergruppen von mRNAs. Dadurch lassen die hier gezeigten Ergebnisse eine weitere Ebene der Genregulierung in Pflanzen, und möglicherweise auch in anderen Eukaryoten, vermuten.

Acknowledgements

Pursuing a PhD is both a painful and enjoyable experience. It's just like climbing a high peak, step by step, accompanied with bitterness, hardship, frustration, encouragement and trust with so many people's kind help.

I would like to thank my supervisor Prof. Dr. Michael Lenhard for giving me the opportunity to work in his group. He always offered me advice, patiently supervised me and always guided me in the right direction. I've learned a lot from him especially critical thinking about problems or questions and he has always had an open ear when problems arose.

I would like to thank all members of the Lenhard laboratory for fruitful seminar-discussions. I am especially thankful to Peggy Lange for her support with the lab work and caring for my plants during my holidays and to Lang Son Vi, who started over with this project and who helped me so much during the first time. Special thanks to Dr. Anahid Powell and Moritz Jöst, who were very nice office neighbours that always helped me with practical and theoretical advice; to Hjördis Czesnick, a friend from my undergraduate studies, for discussion and for making the lab-life more blitheful. Thanks to Dr. Christian Kappel for (sometimes too) critical views on the project from the statistical point of view and for his help with the statistical evaluation. Thanks to the student helpers Jill Kant, Kathrin König, Anna Ramming and Ben Kolbe who helped me a lot with the work in the lab.

I would like to thank Nguyen Huu Cuong for being my badminton partner and all the other lab members for nice trips and BBQ evenings in Golm. Thanks to the people from Berlin for making the train-journeys less lonely.

I am thankful to Dr. Armin Schlereth, Dr. Patrick Giavalisco and Dr. Otto Baumann who offered my kind help with new instruments and methods to improve my research.

Lastly, I would like to thank my partner Thomas, my parents and my sister for their support and encouragement throughout the whole time.

List of Figures

Fig. 1.1	Molecular mechanisms regulating leaf size	13
Fig. 1.2	Schematic overview of the eukaryotic 3' end processing machineries (Figure taken from (Millevoi and Vagner, 2010))	18
Fig. 1.3	Intron/exon map of the four PAPS genes in <i>Arabidopsis</i>	23
Fig. 1.4	Zig Zag model of PTI and ETI	25

Figures in Chapter 2.1

Fig. 1	Loss of PAPS1 function leads to altered organ growth	41
Fig. 2	Three nuclear PAPS isoforms in <i>A. thaliana</i> fulfill distinct functions	43
Fig. 3	Defective polyadenylation of <i>SAUR</i> mRNAs in <i>paps1</i> contributes to reduced leaf growth	45
Fig. 4	Reduced leaf growth in <i>paps1</i> is partly due to an <i>EDS1</i> -dependent pathogen response	49
Fig. S1	Molecular characterization of <i>PAPS1</i> and transgenic complementation of the <i>paps1-1</i> mutant	56
Fig. S2	Molecular characterization of <i>PAPS</i> isoforms in <i>Arabidopsis thaliana</i>	57
Fig. S3	Polyadenylation, but not 3'-end cleavage of <i>SAUR</i> mRNAs is affected in <i>paps1</i> mutants	58
Fig. S4	Nuclear polyadenylation of <i>SAUR</i> transcripts is defective in <i>paps1-1</i> mutants, but polyadenylation is partially rescued in plants expressing the chimeric PAPS4 ^N -PAPS1 ^C protein	60
Fig. S5	Interaction between <i>PAPS1</i> , <i>SAUR19</i> and <i>DST2</i>	61
Fig. S6	The constitutive pathogen response in <i>paps1-1</i> mutant leaves depends on <i>PAD4</i> activity	62

Figures in Chapter 2.2

Fig. 1	An allelic series of <i>paps1</i> mutations	76
Fig. 2	<i>PAPS1</i> activity is modulated by organ-identity	79
Fig. 3	<i>PAPS1</i> acts autonomously at the level of individual organs	81
Fig. 4	More founder cells contribute to <i>paps1-1</i> mutant than to wild-type petal primordia	83
Fig. 5	<i>paps1</i> mutants are more resistant to the biotrophic oomycete <i>Hyaloperonospora arabidopsidis</i>	86
Fig. 6	The constitutive immune response in <i>paps1-1</i> mutants depends on <i>EDS1/PAD4</i> but not <i>NPR1</i>	89
Fig. 7	SA levels are unaltered in <i>paps1</i> mutants	90
Fig. S1	Molecular characterization of <i>paps1</i> mutant alleles	99

List of Figures and Tables

Fig. S2	<i>paps1-1</i> mutants do not accumulate hydrogen peroxide	100
Fig. S3	The constitutive immune response in <i>paps1-1</i> is independent of <i>JAR</i> and <i>PAD3</i> activities	100

Figures in Chapter 2.3

Fig. 2.1	<i>paps1-1 ahg2-1</i> double mutants are embryolethal	104
Fig. 2.2	The constitutive immune response in <i>paps1-1</i> is independent of <i>BRI1</i>	104
Fig. 2.3	phenotypic similarities of <i>paps1-1</i> to <i>snc1</i> mutants	105
Fig. 2.4	Quantification of roGFP2 fluorescence in <i>paps1-1</i> and <i>Ler</i> leaves in cytoplasm and plastids	106
Fig. 2.5	Cytoplasmic roGFP fluorescence in <i>Col-0</i> and <i>paps1-1</i> leaves	107
Fig. 2.6	Plastidal roGFP fluorescence in <i>Col-0</i> and <i>paps1-1</i> leaves	108
Fig. 2.7	qPCR abundance of three control RNAs in the fractionated mRNA pools	110
Fig. 2.8	long/short mRNA ratios of 8 control genes in the fractionated mRNA pools	111

List of Tables

Table 1	Factors of the <i>Arabidopsis thaliana</i> 3'-end processing complex (after Hunt <i>et al.</i> , 2008)	18
---------	--	----

1. Introduction

1.1. Growth is a genetically tightly controlled process

As sessile organisms plants must cope with ever changing environmental conditions and it is obvious that every species has adapted to its environment with a characteristic size and shape of its organs. This holds true even for closely related species (Mizukami, 2001). However, plants belonging to the same species grow, under the same environmental conditions, to the same size and pass these characteristics to the next generation. The emergence of these heritable, species-specific growth patterns of the different plant organs is a genetically tightly controlled process and involves the interaction of many factors which either enhance or restrict growth. In recent years, much progress has been made on elucidating the genetic basis of organ size control in plants, mainly by analyzing the model plant *Arabidopsis thaliana* (*Arabidopsis* hereafter).

1.1.1. Mechanisms of plant organ growth

Plant development is characterized by so called indeterminate growth, where a vegetative meristem keeps on producing leaf primordia until it undergoes the transition into the inflorescence meristem that produces the floral meristems, which then initiate floral organs. The initiated organ primordia grow to a genetically determined size and shape, within the limits of phenotypic plasticity. Hence, leaf growth can be best described as the progression of five overlapping and linked phases: an initiation phase, a cell division phase, a transition phase, a cell expansion phase and a meristemoid division phase (Gonzalez *et al.*, 2012). The cell proliferation phase is characterized by mitotic cell division and accumulating of cytoplasmic mass to the size of the mother cell followed by another division. During the cell expansion phase cells stop proliferating and only grow by expansion. To investigate the influence of cell proliferation on organ size cyclin proteins are very useful markers, because they show expression patterns that are specific to certain phases of the cell cycle (Hemerley *et al.*, 1992; Ferreira *et al.*, 1994a, b). The *Arabidopsis* cyclin *cyc1At*, whose transcript is most abundant during G2 and M phase (Hemerly *et al.*, Shaul 1996), was fused to the β -glucuronidase (GUS) reporter. Its expression was investigated to follow the spatial and temporal patterns of cell division in developing *Arabidopsis* leaves. Shortly after leaf initiation, cell division occurs throughout the whole primordium, while in later stages it becomes restricted to defined regions in the leaf in a basiplastic manner (maturation/proliferation arrest processes from tip to base) (Donnelly *et al.*, 1999; Nath *et al.*, 2003). However, recent studies on the development of the third leaf of *Arabidopsis*

Introduction

have shown that on day 8 and 9 the leaf consists entirely of proliferating cells. On day 10 cells start to expand at the tip of the leaf and this gradient of expansion and proliferation persists through days 11 and 12 (transition period). After day 12 the proliferation zone disappears and cells only grow by expansion. These findings were also verified molecularly and it was shown that the expression of genes involved in general transcription, DNA synthesis, cell cycle and translation decreases, whereas the expression of genes involved in photosynthesis, cell wall synthesis, secondary metabolism and transport increases during the transition period. The activation of cell expansion comes along with and is dependent on the leaf greening. Inhibition of chloroplast differentiation by norflurazon showed, that retrograde signals from the chloroplasts are key factors driving the transition from cell proliferation to cell expansion (Andriankaja *et al.*, 2012; Kawade *et al.*, 2010).

1.1.2. Genetic regulation of plant organ growth

Growth by cell proliferation and later by cell expansion is a genetically tightly regulated process that gives the different organs their final size and shape. In the past decade, many factors have been identified regulating cell proliferation, cell expansion or the transition between both in a positive or negative manner (reviewed in (Gonzalez *et al.*, 2012; Hepworth and Lenhard, 2013) (Fig. 1.1).

The shoot apical meristem (SAM), a group of cells that retains its ability to proliferate, enables the plant to grow in an indeterminate manner. In *Arabidopsis*, the size of the SAM is only about 50 μm and gives rise to precursors, that develop into lateral organs such as leaves and branches. Its size is controlled by the antagonistic action of the *CLAVATA (CLV) 1,2* and *3* genes with *WUSCHEL (WUS)* to maintain a pluripotent stem cell population. The stem cells express the *CLV3* gene encoding a mobile signal that can diffuse to the adjacent organizing centre, where it is recognized by either a homodimer of the leucine-rich-repeat (LRR) receptor kinase CLV1 (Lenhard and Laux, 2003), or a tetramer consisting of two molecules of the receptor-like kinases CLV2 and two molecules of the CORYNE protein (Muller *et al.*, 2008; Bleckmann *et al.*, 2010).

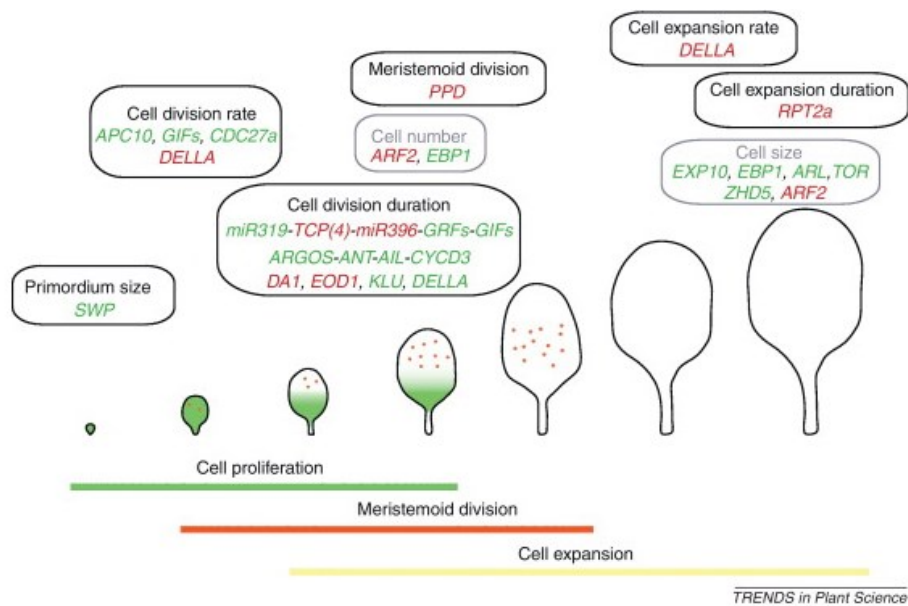


Fig. 1.1: Molecular mechanisms regulating leaf size. The different processes occurring during leaf development (cell division and cell expansion) are represented. The different events that could influence the final leaf size (primordium size, cell division or expansion rate, cell division or expansion duration, and meristemoid division) and genes involved in positive (green) or negative (red) regulation are shown. Abbreviations: *SWP* (*STRUWWELPETER*), *APC10* (*ANAPHASE PROMOTING COMPLEX10*), *GIF* (*GRF-INTERACTING FACTOR*), *CDC27a* (*CELL DIVISION CYCLE PROTEIN 27 HOMOLOG A*), *TCP* (*TEOSINTE BRANCHED1/CYCLOIDEA/PCF*), *GRF* (*GROWTH-REGULATING FACTOR*), *ARGOS* (*AUXIN-REGULATED GENE INVOLVED IN ORGAN SIZE*), *ANT* (*AINTEGUMENTA*), *AIL* (*AINTEGUMENTA-LIKE*), *CYCD3* (*CYCLIN D3*), *EOD1* (*ENHANCER OF DA1-1*), *ARF2* (*AUXIN RESPONSE FACTOR2*), *KLU* (*KLUH*), *EXP10* (*EXPANSIN10*), *EBP1* (*ErbB-3 EPIDERMAL GROWTH FACTOR RECEPTOR BINDING PROTEIN*), *PPD* (*PEAPOD*), *RPT2a* (*REGULATORY PARTICLE AAA-ATPASE 2a*), *ARL* (*ARGOS-LIKE*), *TOR* (*TARGET OF RAPAMYCIN*) and *ZHD5* (*ZINC FINGER HOMEODOMAIN5*). (from Gonzalez *et al.*, 2012)

The perception of *CLV3* then triggers signaling to repress *WUS* expression and therefore restricts stem cell fate (Bleckmann and Simon, 2009). *WUS* itself can move to the stem cells and promotes stem-cell fate and *CLV3* expression, building up a negative feed-back loop that defines the size of the stem cell population in the SAM (Schoof *et al.*, 2000; Brand *et al.*, 2002).

Phyllotaxis is the regular positioning of lateral organs around a stem (Kuhlemeier, 2007). Already in the 19th century Hofmeister made the following statement: new organ primordia are placed in the widest available gap in the meristem, as far away as possible from existing primordia (Hofmeister, 1868). Experimental evidence collected in the past decades has shown that the development of leaf primordium from the precursor cells produced by the SAM requires the establishment of a local auxin maximum at the site of initiation (Reinhardt *et al.*, 2003). The emerging leaf functions as an auxin sink, depleting its surrounding of auxin and forcing the following organ anlage to develop at a distinct position. The formation of auxin maxima is enabled by directed transport through the *PIN1* efflux protein (Benková *et al.*, 2003; Reinhardt *et al.*, 2006) into the emerging leaf. However, the fact that *pin1* mutants produce leaves nonrandomly in the vegetative phase suggests a *PIN1* independent mechanism of leaf initiation (Guenot *et al.*, 2012).

Introduction

The resulting leaf primordium continues growing by cell proliferation. The final organ size is determined by the number of cells produced during the proliferation phase (Korner *et al.*, 1989; Meyerowitz, 1997) and regulation of the cell cycle is therefore crucial to limit the cell proliferation phase. For example, destruction of A- and B-type cyclins (Marrocco *et al.*, 2010; Sullivan and Morgan, 2007) by overexpression of the APC10 subunit of the anaphase-promoting complex/cyclosome (APC/C) leads to an increased rate of cell division and the production of larger leaves (Eloy *et al.*, 2011). Not only regulation of the proliferation rate, but also regulation of the timing of proliferation arrest is a crucial step in growth control. Many factors have been unravelled in the last years shedding light on this step. For example the transcription factors GROWTH REGULATING FACTOR 1 (GRF1), 2 (GRF2) and 5 (GRF5) are involved in promoting cell proliferation (Gonzalez *et al.*, 2010; Horiguchi *et al.*, 2005; Kim *et al.*, 2003). GRFs in turn are regulated by *miR396*. *miR396* overexpressing plants produce narrower leaves with fewer cells (Liu *et al.*, 2009; Rodriguez *et al.*, 2010; Wang *et al.*, 2011). *miR396* is upregulated by class II members of the TEOSINTE-BRANCHED1/CYCLOIDEA/PCF (TCP) family (CIN-TCPs) (Rodriguez *et al.*, 2010). While class II TCPs function in cell cycle arrest, class I TCPs appear to promote proliferation (Kieffer *et al.*, 2011). Recent studies have shown that CIN-TCPs also modulate several hormone pathways such as cytokinin (Efroni *et al.*, 2013) or GA signaling (Steiner *et al.*, 2012). Other factors that control the duration of cell division are e.g. DA1, an ubiquitin receptor that restricts cell proliferation (Li *et al.*, 2008), the E3 ligase BIG BROTHER (BB) (Disch *et al.*, 2006) that negatively regulates the duration of cell proliferation in leaves and petals or the cytochrome P450 *KLUH*, that likely produces a mobile growth-promoting signal (Anastasiou *et al.*, 2007).

After the proliferation phase has finished, the cells continue growing by cell expansion. This occurs mainly by cell wall loosening, expansion through the turgor pressure and *de-novo* synthesis of cell wall components (Cosgrove, 2005). During the cell expansion phase, most cells start to differentiate; however, some cells, called meristemoids, still undergo several rounds of cell division. These cells will form specific cell types such as stomatal guard cells or vascular cells (Fisher and Turner, 2007; Nadeau and Sack, 2002; Peterson *et al.*, 2010). When regulation of cell proliferation is disturbed, a phenomenon called 'compensation' can be observed, i. e. a cell proliferation defect in developing leaf primordia triggers excessive cell expansion. As a result, final leaf size is less reduced compared to what would be expected from the reduction in leaf cell numbers as for example in the *AINTEGUMENTA* (*ant*) mutants (Mizukami and Fischer, 2000) (reviewed in (Horiguchi and Tsukaya, 2011)). After the vegetative growth period has ended, *Arabidopsis* plants start to flower. Transition to flowering is regulated by many factors, e.g. day length, temperature or leaf number, and hundreds of transcripts are affected in their expression in the shoot apex (Pullen *et al.*, 2013).

1.1.3. Role of phytohormones in plant growth

Phytohormones regulate plant growth from cell division in the meristem to organ initiation and development. The most well studied phytohormone influencing growth and development in plants is auxin. It was discovered as the hormone involved in bending of coleoptiles towards light. It acidifies the cell wall, which increases its extensibility, allowing cell elongation in the shoot (for review see (Chen and Baluška, 2013)). Although auxin sensing, signaling and regulation has been studied extensively, new insights are unraveled continuously. Recent studies have for example shown that *SMALL AUXIN UP RNAs (SAURs)* in particular *SAUR19-24* promote cell expansion in *Arabidopsis* leaves (Spartz *et al.*, 2012), yet the mechanism remains elusive.

Cytokinins are plant growth promoting hormones involved in the specification of embryonic cells, maintenance of meristematic cells, shoot formation and development of vasculature. They promote growth by stimulating cell proliferation. Elevation of endogenous cytokinin levels in *Arabidopsis* results in overexpression of the KNOTTED homeobox transcription factor homologs *KNAT1* and *SHOOT MERISTEMLESS (STM)* that are important in the regulation of meristem function (Rupp *et al.*, 1999). The reduction of cytokinin levels by overexpressing the cytokinin oxidase results in a strong retardation of shoot development due to delayed proliferation (Werner *et al.*, 2001).

Jasmonates (JAs) have been shown to inhibit plant growth, but the mechanisms are not well understood (for a review on JA biosynthesis and signaling see [Wasternack and Hause, 2013]). The effects of methyl jasmonate (MeJA) on leaf growth regulation were investigated in *Arabidopsis* in allene oxide synthase and *coi1-16B* (for *coronatine insensitive1*) mutants, exhibiting altered JA synthesis and perception, respectively. It was shown, that MeJA delays the switch from the mitotic cell cycle to the endoreduplication cycle, which accompanies cell expansion, in a COI1-dependent manner and inhibits the mitotic cycle itself, arresting cells in G1 phase prior to the S-phase transition (Noir *et al.*, 2013). Additionally class I and class II TCP proteins regulate leaf development antagonistically via the jasmonate signaling pathway (Danisman *et al.*, 2012)

Another group of phytohormones that are important growth and developmental regulators are giberellins (GAs). Mutants impaired in GA biosynthesis or signaling often show moderate to severe dwarf phenotypes as for example the *ga1-3* mutant in *Arabidopsis* (Koorneef and Vanderveen, 1980) or the *brd1* mutant in rice (Mori *et al.*, 2002). GAs regulate cell elongation and cell proliferation by stimulation of the destruction of growth-repressing DELLA proteins. It was for example shown, that the DELLA protein RGA regulates the activity of *STUNTED (STU)*, a member of the receptor-like cytoplasmic kinase (RLCK) VI family genes that plays a role in cell proliferation (Lee *et al.*, 2012). GAs act in various tissues, including hypocotyls, stamens, stems and roots (Yang *et al.*, 1996; Cowling and Harberd, 1999; Cheng *et al.*, 2004; Ubeda-Tomas *et al.*, 2008).

Introduction

Besides its roles in fruit ripening, seed germination, senescence and abscission, the gaseous hormone ethylene (ET) also plays a role in cell expansion and cell differentiation. It induces lateral cell expansion by causing a reorientation of the cell wall microtubules (Yuan *et al.*, 1994). A recent finding demonstrated the destruction of GA and therefore stabilization of DELLAs by ETHYLENE RESPONSE FACTOR 5 (ERF5) and ERF6, demonstrating the crosstalk between GAs and ethylene (Dubois *et al.*, 2013).

abscisic acid (ABA) plays a major role in seed maturation and dormancy as well as drought tolerance and stomata closure. It promotes root and inhibits shoot growth, but these effects are strongly dependent on the water status of the plant (for review see Leung and Giraudat, 1998).

The last class of phytohormones to be mentioned here are the brassinosteroids (BRs). These plant steroids take over critical roles during various plant growth processes, including control of cell proliferation and cell elongation (for review see Fridman and Savaldi-Goldstein, 2013). The BR deficient mutants *det2* (*de-etiolated2*) and *cpd* (*constitutive photomorphogenesis and dwarfism*) grow under normal light conditions as dark-green dwarfs due to a reduction in cell size and intercellular spaces and they have reduced apical dominance (Chory *et al.*, 1991; Szekeres *et al.*, 1996).

1.2. Nuclear polyadenylation is a conserved mechanism amongst eukaryotes

In all eukaryotic cells, DNA is transcribed by Polymerase II into pre-messenger RNA that serves as transport form of the genetic information from the nucleus to the cytoplasm. Prior to export, several modifications must happen to the pre-mRNA including splicing, 5'-capping, editing and 3'-end processing. mRNA 3'-end processing is part of this network of different pathways, making it possible to control gene expression. The 3'-end cleavage and addition of the poly (A) tail is performed by a multi-enzymatic complex, termed the 3'-end processing complex. This complex is in physical interaction with the transcription and splicing machinery. It was for example shown in yeast (*Saccharomyces cerevisiae*), that promoter and terminator regions are juxtaposed by interaction of transcription factor IIB (TFIIB) with the poly(A) polymerase and cleavage factor 1 (CF1), and that the resulting gene loops facilitate transcription reinitiation by the same molecule of RNAP II (Medler *et al.*, 2011; Al Husini *et al.*, 2013). Furthermore, the phosphorylated carboxy-terminal domain (CTD) of PolII serves as a 'delivering' platform for polyadenylation factors (Hirose and Manley, 1998). Splicing and polyadenylation are interconnected by regulating splicing of the terminal intron through physical interaction of the components of the 3'-end processing complex with the spliceosome. Furthermore, it was shown, that the cleavage and polyadenylation specificity factor 1 (CPSF1) regulates alternative splicing of interleukin 7 receptor (IL7R) exon 6. These and other examples imply the involvement of more than 80 proteins from different pathways of RNA biogenesis and maturation in a complex network to regulate gene expression (Nagaike *et al.*, 2011; Niwa and Berget 1991; Cooke *et al.*, 1999; Lutz *et al.*, 1996; Kyburz *et al.*, 2006, Evsyukova *et al.*, 2013, Shi *et al.*, 2009).

The resulting poly(A) tail has various important functions. It promotes the transport of mRNA from the nucleus to the cytoplasm (Vinciguerra and Stutz, 2004). Addition of the poly(A) tail and subsequent binding of the poly(A) binding protein (PAB) confers mRNA stability in the cytoplasm and protects it from degradation (Wickens *et al.*, 1997; Ford *et al.*, 1997). Furthermore the poly(A) tail and PABP interact with the methyl cap at the 5'-end of the mRNA to promote translation (Wickens *et al.*, 1997; Sachs *et al.*, 1997; Wilusz *et al.*, 2004; Chekanova and Belostotsky, 2006).

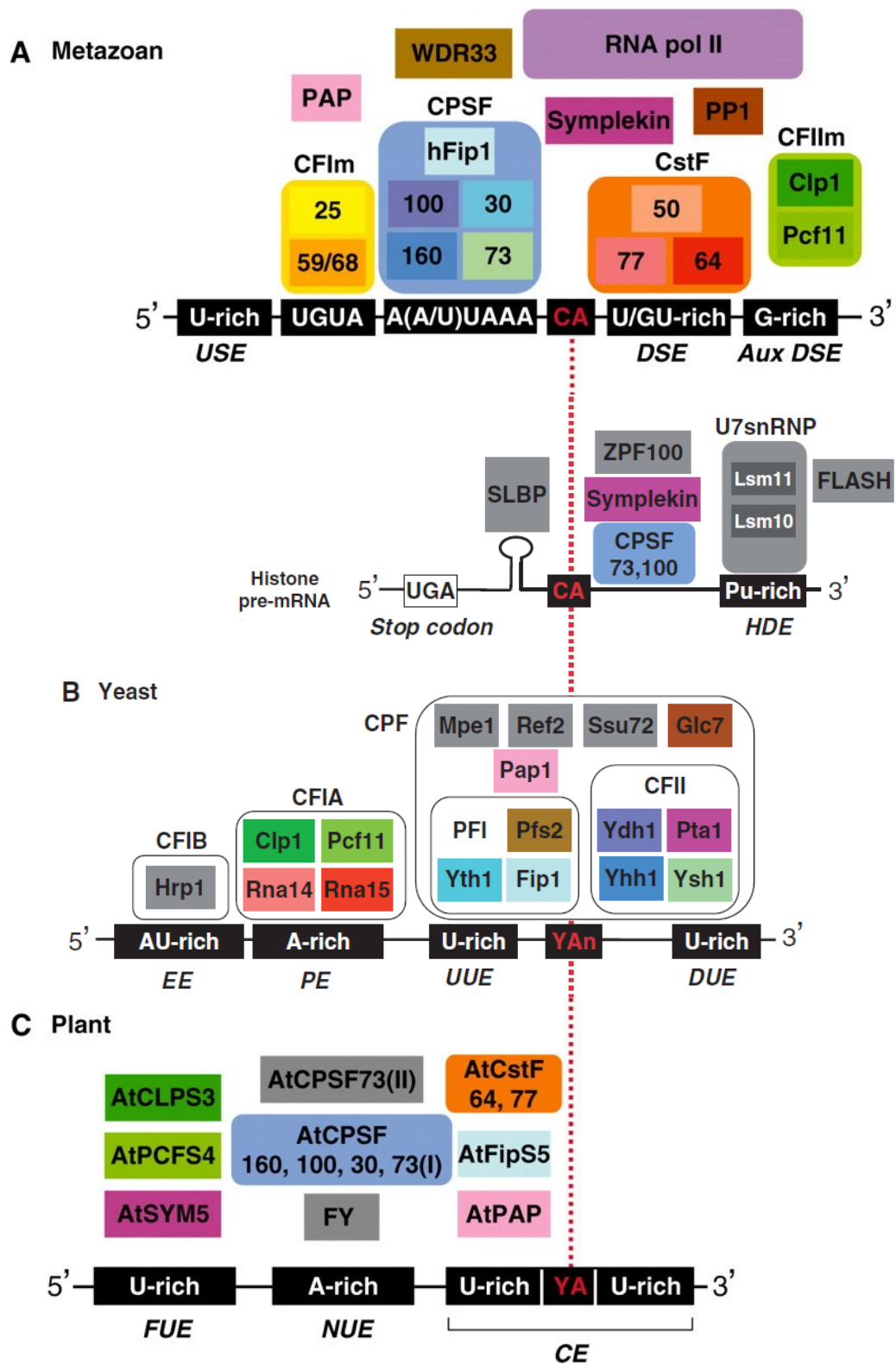


Fig. 1.2: Schematic overview of the eukaryotic 3'-end processing machineries (figure taken from Millevoi and Vagner, 2010)

1.2.1. Polyadenylation *cis*-elements

Cis-regulatory elements are sequence elements on the DNA or RNA that regulate the expression of genes located in their vicinity. The 3'-end cleavage site (CS) in mammals is the conserved dinucleotide CA (Sheets *et al.*, 1990). Around 10 to 30 basepairs (bp) upstream of the CS is the polyadenylation signal (PAS) that has the conserved sequence A(A/U)UAAA in the majority of all mammalian mRNAs (reviewed in Tian *et al.*, 2005; Millevoi and Vagner, 2010; and references herein) followed by a UGUA motif that serves as binding site for CFIm (see section 1.2.2 |Brown and Gilmartin, 2003|). Further upstream, the U-rich upstream sequence element (USE) serves as an anchor for the 3'-end processing machinery by recruiting other factors (see Millevoi and Vagner, 2010). 30 nucleotides downstream of the CS, the downstream sequence element (DSE) can be found. This element is U/UG rich and associates with CstF. The following auxiliary downstream element (AuxDSE) is G-rich and recruits regulatory factors, which enhance 3' end formation (Chen and Wilusz, 1998 and others) (Fig. 1.2).

Polyadenylation signals in plants are much more diverse (Rothnie, 1996; Li and Hunt, 1997; Rothnie *et al.*, 2001; Loke *et al.*, 2005). The Cleavage element (CE) consists of the CS, a pyrimidine-adenosine dinucleotide, surrounded by 5 to 10 bp long U-rich regions. Upstream of the CE, the Near Upstream element (NUE) and the Far Upstream Element (FUE) can be found. The NUE spans 6 to 10 nucleotides and is located 10 to 40 nt upstream of the CE. The sequence of the NUE is typically A and T rich, but the conserved mammalian motif AAUAAA can be found in only 10% of 8000 examined UTRs (Loke *et al.*, 2005). The FUE spans 60 to 100 nt and is located 25 to 160 bp upstream from the CS. The FUE is very variable in sequence as well but also generally A and U rich (Fig. 1.2). In addition to sequence properties, secondary structures in the 3'-UTR may also play a role in polyadenylation site choice (Loke *et al.*, 2005).

1.2.2. Polyadenylation *trans*-factors

3'-end processing is a two-step nuclear process that involves an endonucleolytic cleavage of the transcribed pre-mRNA followed by the addition of the poly(A) tail. The 3'-end processing machinery is a multienzymatic complex and plants express homologues of almost all factors acting in humans and yeast (for review see |Millevoi and Vagner, 2010| and included references).

The mammalian 3'-end processing machinery consists of the following subunits: Cleavage and polyadenylation specificity factor (CPSF, containing five subunits: CPSF-30, -73, -100, -160, hFip1); Cleavage stimulation factor (CstF, containing 3 subunits: CstF-50, -77, -64); Cleavage Factor I (CFIm subunits: CFIm-68, CFIm-25); Cleavage Factor II (CFIIm subunits hClp1, hPcf11) and symplekin (for review see Mandel *et al.*, 2008). Binding of the PAS by CPSF-160 and the DSE by Cstf-64 positions the

Introduction

3'-end processing machinery on the pre-mRNA, directing the endoribonuclease CPSF-73 close to the cleavage site. Interaction between the CstF subunits and CPSF is mediated by CstF-77, thus stabilizing the whole complex. The poly(A) polymerase (PAP, will be discussed in detail in section 1.2.3) is recruited to the complex by binding by CPSF-160 and CFIm-25. Subsequent polyadenylation is carried out by the PAP with involvement of CPSF and the emerging poly(A) tail is bound by nuclear poly(A) binding protein II (PABII or PABNP1). The binding of the PABN1 to the RNA is unstable and upon nuclear export it is replaced by the cytosolic poly(A) binding protein (PABC) (Thuresson *et al.*, 1994; Manley, 1995; Murthy and Manley, 1995; Kim and Lee, 2001; Mangus *et al.*, 2003; Kuhn and Wahle, 2004). Additional factors are involved in modulating the efficiency or stability of the 3'-end processing complex that will not be discussed further here (see Millevoi and Vagner, 2010) (Fig. 1.2). Much progress has been made in the past decade to shed light on the plant 3'-end processing mechanism, mainly by identifying mammalian and yeast 3'-end processing complex homologues. Plant poly(A) polymerases have been identified in many plant species, including maize, wheat, thale cress, rice and others (Mans and Huff, 1975; Berry and Sachar, 1982; Addepalli *et al.*, 2004, Hunt *et al.*, 2012). Other *Arabidopsis* 3'-end processing complex subunits and their mammalian homologues and functions are listed in Table 1.

The interactions between the different 3'-end processing complex factors have been examined by yeast-two hybrid assays (Hunt *et al.*, 2008). These experiments discovered three theoretical complexes around FIPS5, CPSF100 and a putative CFIm-like complex (CLP5 and CPSF orthologs) bridged by CPSF30, CFIS2 and three CSTF subunits. The four PAPS and PABN isoforms are all part of the FIPS5 complex and PAPS2 is also directly linked to CPSF100 subcomplex. Furthermore it was shown that FY physically interacts with CPSF160 and CPSF100 (Manzano *et al.*, 2009).

The fact that many single-gene encoded mammalian polyadenylation *trans*-factors have more than one homologue in *Arabidopsis* (Table 1) suggests the possibility that there are different 3'-end processing complexes in plants, fulfilling different functions.

Table 1: Factors of the *Arabidopsis thaliana* 3'-end processing complex (after Hunt *et al.*, 2008).

mammals	function	AGI code	Name
CPSF160	Binds AAUAAA	At5g51660	CPSF160
CPSF100	Unknown	At5g23880	CPSF100, ESP5
CPSF73a	Endonuclease	At1g61010	CPSF73-I
CPSF73b	Similar to CPSF73a	At2g01730	CPSF73-II, FEG
CPSF30	RNA binding, endonuclease	At1g30460	CPSF30, OXT6
Cstf77	Scaffold for Cstf64 and Cstf50, bridge to CPSF	At1g17760	CSTF77
Cstf64	Binds to DSE	At1g71800	CSTF64
Cstf50		At5g60940	CSTF50
hPfs2	RNA binding	At5g1348B	FY
PAP	Creates poly(A) tail	At1g17980 At2g25850 At3g06560 At4g32850	PAPS1 PAPS2 PAPS3 PAPS4
hFip1	Interacts with PAP, regulates CPSF30 activity	At3g66652 At5g58040	FIPS3 FIPS5
CFIm-25	Cleavage factor, interacts with RNA	At4g25550 At4g29820	CFIS2 CFIS1
hClp1	RNA Kinase	At3g04680 At5g39930	CLPS3 CLPS5
hPcf1	Interacts with CstF	At1g66500 At4g04885 At5g43620	PCFS1 PCFS4 PCFS5
PAB cytoplasmic	Binds poly(A) tail, controls length	At1g34140 At4g34110 At1g22760 At2g23350 At1g71770 At3g16380 At2g36660 At1g49760	PAB1 PAB2 PAB3 PAB4 PAB5 PAB6 PAB7 PAB8
PABN nuclear	Binds poly(A) tail, controls length	At5g65260 At5g51120 At5g10350	PABN1 PABN2 PABN3
Symplekin	Part of CPSF	At5g10350 At1g27590 At1g27595	ESP4, SYM5 SYM1 SYM2

1.2.3. Canonical Poly(A) Polymerases (cPAP)

One of the central proteins in the 3'-end processing complex is the poly(A) polymerase (PAP or PAPS in plants). PAPs belong to the DNA polymerase β subfamily (Holm and Sander, 1995; Martin and Keller, 1996) and retain adenylyltransferase activity and nucleotide specificity when separated from the complex (Edmonds, 1990). Crystal structures of the bovine and yeast PAPs have shown that they possess a modular organization with a nucleotide binding N-terminal domain, a central catalytic domain and an RNA-binding region that overlaps with a nuclear localization signal (NLS) near the C-terminus (Raabe *et al.*, 1991; Martin *et al.*, 1999; Martin *et al.*, 2000; Bard *et al.*, 2000). The active

Introduction

site, with two divalent cations, is located at the bottom of a large cleft between the N- and C-terminal domains, near the interface between the N-terminal and middle domains. Structural and biochemical data suggest that PAPs are induced-fit enzymes to select for the right nucleotide (Balbo *et al.*, 2005). They act via a two-metal-ion catalytic mechanism and add adenosine monophosphates to the free 3'-hydroxyl group of the mRNA in a catalytic cycle (Steitz, 1998). PAPs are categorized in canonical and non-canonical PAPs. Canonical PAPs (cPAPs) share high similarity with the bovine and yeast PAP and polyadenylate predominantly mRNA, while non-canonical PAPs (ncPAPs) are not so closely related to the bovine and yeast PAP and show remarkably diversity in substrate and nucleotide specificity (Schmidt and Norbury, 2010). For example the Trf4 ncPAP in *Saccharomyces cerevisiae* is part of the TRAMP complex. TRAMP mediated polyadenylation of aberrant and other short-lived nuclear noncoding RNAs targets them for degradation by the RNA exosome (Haracska *et al.*, 2005; Vanacova *et al.*, 2005)

cPAPs are highly conserved enzymes that can be found throughout all eukaryotic organisms. While only one cPAP is encoded in the *Saccharomyces cerevisiae* (Pap1p (Ligner *et al.*, 1990)) and *Drosophila melanogaster* genomes (Junge *et al.*, 2002), three can be found in mammals termed PAPOLA (PAP α) (Raabe *et al.*, 1991; Wahle *et al.*, 1991), PAPOLB (PAP β) (Kashiwabara *et al.*, 2000) and PAPOLG (PAP γ) (Kyriakopoulou *et al.*, 2001; Perumal *et al.*, 2001; Topalian *et al.*, 2001). PAP α and PAP γ are very similar nuclear localized proteins with an extended C-terminal domain that contains two nuclear localization sequence (NLS) motifs. In contrast, PAP β contains only one degenerated NLS motif, is cytosolic and testis-specific.

PAPs are regulated post-transcriptionally and post-translationally. For example, human PAP α exists in multiple forms due to extensive alternative splicing (Zhao and Manley, 1996). Numerous post-translational modifications occur on the C-terminal domain of PAP α and PAP γ in vertebrates. Hyperphosphorylation of the PAP regulatory domain represses its activity (Colgan *et al.*, 1996; 1998), while hypophosphorylation leads to hyperactivity of the PAP (Mouland *et al.*, 2002). Additionally, acetylation of the C-terminal domain compromises nuclear localization and inhibits the interaction between PAP and cleavage factor I subunit 25 (CFI25m) in COS cell lines (Shimazu *et al.*, 2007). Furthermore, PAP sumoylation is required for nuclear localization and contributes to PAP stability (Vethantham *et al.*, 2007).

1.2.4. cPAPs in plants

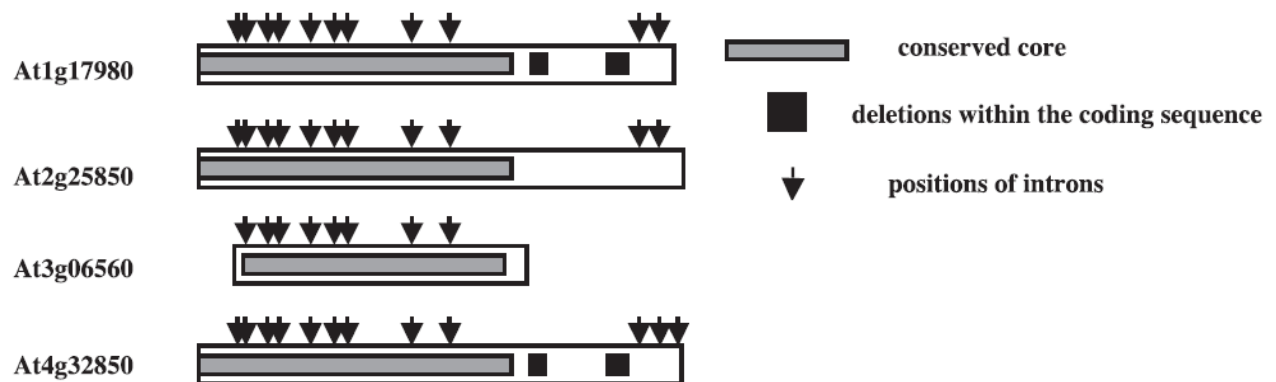


Fig. 1.3: Intron/exon map of the four PAPS genes in *Arabidopsis*. The longest protein-coding regions from each of the *Arabidopsis* PAPS genes are illustrated as rectangular boxes. The portion of the encoded proteins that is conserved in these, and other eukaryotic PAPS is shown as a dark bar within the coding region. The small black boxes in the chromosome I and IV depictions denote deletions relative to the chromosome II gene (Addepalli *et al.*, 2004)

The model plant *Arabidopsis thaliana* possesses four canonical poly(A) polymerases (PAPS) termed PAPS1 (At1g17980), PAPS2 (At2g25850), PAPS3 (At3g06560) and PAPS4 (At4g32850) according to the chromosomes they are encoded on (Addepalli *et al.*, 2004). All of them are believed to be essential enzymes, since no T-DNA mutants could be found (Meeks *et al.*, 2009). All four PAPS possess a conserved core that is also present in other eukaryotic PAPS (Fig. 1.3). PAPS1, PAPS2 and PAPS4 possess a NLS and an extended C-terminal domain and are localized exclusively to the nucleus. In contrast, PAPS3 lacks these domains and is located in the cytoplasm, therefore resembling mammalian PAP β (Meeks *et al.*, 2009). The C-terminal domains of the three longer PAPS are rather dissimilar between them and also very different from the C-terminal domains of PAPS from other organisms (Addepalli *et al.*, 2004). The presence of S/T-rich regions within this domain suggests that phosphorylation/dephosphorylation of the c-terminal domain may occur in plants as well (Verma and Sachar, 1994; Hunt *et al.*, 2000; Addepalli *et al.*, 2004). Alternative splicing was observed in all four PAPS, each introducing a premature stop codon resulting in truncated protein. *PAPS1* mRNA retains the sixth intron in flower cells (Addepalli *et al.*, 2004). *PAPS2* alternative mRNA keeps additional 20 nt from intron 6 in stem and root cells (Hunt *et al.*, 2000; Addepalli *et al.*, 2004), *PAPS3* mRNA shows inclusion of intron 7, predominantly in roots and flowers and *PAPS4* alternative splicing occurs within a cryptic splice sites between exon 6 and 10 with the longer mRNA being not present in roots (Addepalli *et al.*, 2004). *PAPS1*, *PAPS2* and *PAPS4* are expressed ubiquitously in all tissues during all developmental stages while *PAPS3* is only highly expressed in floral organs (Addepalli *et al.*, 2004; Meeks *et al.*, 2009).

1.2.5. Control of mRNA poly(A) tail length

Since the poly(A) tail has various important biological functions, it is conceivable that regulation of poly(A) tail length could be used to control gene expression. The length of the poly(A) tail can be regulated by either synthesis in the nucleus or degradation in the cytoplasm. Average or steady-state poly(A) tail lengths therefore always reflect the balance between *de novo* adenylation and deadenylation. It was shown that different species have different average poly(A) tail lengths of their mRNAs reaching from a few adenosines (As) in yeast (Brown and Sachs, 1998) to ~250 in mammals (Sawicki *et al.*, 1977; Wahle, 1995). In plants, the average poly(A) tail length is not clear. Furthermore, the steady-state poly(A) tail length is very variable as it was shown by genome-wide analysis (Meijer *et al.*, 2007; Beilharz and Preiss, 2007; Subtelny *et al.*, 2014).

In mammals, the final length of the poly(A) tail is reached by increasing the processivity of PAP by CPSF, PABPN1 and hFip1 as PAP alone is unable to produce tails of defined length (Wahle, 1991; Wahle, 1995; Kaufmann *et al.*, 2004). CPSF binds the AAUAAA signal, recruits PAP to the RNA template by direct interaction and anchors it to the mRNA (Kerwitz *et al.*, 2003). Once the minimal binding site for PABPN1 (12 adenosines) is synthesized it joins the complex, increasing the processivity of the PAP by 150-fold (Wahle, 1995). Binding of the emerging poly(A) tail by additional PABPN1s builds up a fold back-structure within the 3'-end processing complex to sustain the connection between the three proteins. When the length of the poly(A) tail exceeds 250 nucleotides (nt) the connection between CPSF, PABPN1 and PAP can no longer be maintained. Hence PAP is only stimulated by PABPN1, therefore losing its processivity and polyadenylation comes to an end (Kühn *et al.*, 2009). However, there are also exceptions to the 250 A rule present in mammals. It has been shown, that *Xenopus laevis* serum albumin mRNA has exceptionally short poly(A) tails, ranging from only 12 to 17 nt (Schoenberg *et al.*, 1989). A sequence element termed poly(A) limiting element (PLE) in the terminal exon is responsible for this regulation (Das Gupta *et al.*, 1998). Surprisingly, reporter-genes mRNAs containing PLEs accumulate, are efficiently recruited to polyribosomes and final protein levels do not differ from PLE-lacking mRNAs (Peng *et al.*, 2005; Shi *et al.*, 2009). A recent report showed that median poly(A) tail lengths in *Arabidopsis* are around 50 nucleotides in length (Subtelny *et al.*, 2014). To date, no data is available about poly(A) tail length regulation in plants but the presence of homologues of all mammalian poly(A) factors and the importance of the 3'-end processing in all eukaryotes suggests a similar mechanism.

After export to the cytoplasm, the mRNA is protected from different degradation mechanisms by its poly(A) tail and the 5'-guanosine cap. To achieve degradation, there are two possible ways. Either the 5'-cap is removed by a process known as decapping, which allows the mRNA body to be degraded in the 5'→3' direction by the XRN1 exoribonuclease, a nuclear protein that degrades

aberrant RNAs. Or the unprotected 3'-end is attacked by a large complex of 3'→5' exonucleases known as the exosome. The exosome is cytoplasmic and degrades mRNAs. There are three major deadenylases in eukaryotes: the CCR4-POP2-Not (carbon-catabolite repressor) complex, PAN (poly(A) nuclease) and PARN (poly(A) specific ribonuclease) complex (reviewed in [Garneau *et al.*, 2007; Goldstorm and Wickens, 2008; Wahle and Winkler; 2013]). Deadenylation in mammalian cells is a biphasic process. In the first phase, the PAN2-PAN3 complex synchronously shortens the poly(A) tail to ~110 nt whereas in the second phase, catalysed by the CCR4-Not complex, mRNAs become highly heterogeneous in the lengths of their poly(A) tails, ranging from ~110 nt to ~20 nt (Yamashita *et al.*, 2005). Deadenylases are often associated with multisubunit complexes and form homo- or heterodimers or multimers and therefore provide a complex regulatory potential (Goldstorm and Wickens, 2008). They are regulated by transcription rate (Green and Besharse, 1996) or intercellular localization (Yamashita *et al.*, 2005; Wagner *et al.*, 2007). A unique feature of PARN is, that its activity is dependent on the presence of a 5'-cap on the mRNA (Dehlin *et al.*, 2000; Gao *et al.*, 2000; Martinez *et al.*, 2001). Interestingly, the PABP can activate deadenylation by recruiting PAN2-PAN3 in yeast to trim off poly(A) tails from pre-mRNAs (~80 nt) to mRNA specific poly(A) tails (55-70 nt) (Brown and Sachs, 1998). Homologues of most of the mammalian and yeast deadenylases have been identified in plants (reviewed in [Abbasi *et al.*, 2013]). As in other eukaryotes, CCR4 is the main cytoplasmic deadenylase while PARN deadenylates only a subset of transcripts in *Arabidopsis* (Reverdatto *et al.*, 2004). Additionally, a recent study showed that PARN directly regulates the poly(A) tail of mitochondrial RNAs (Hirayama *et al.*, 2013). These findings suggest a distinct regulation of deadenylation for different transcripts in *Arabidopsis*. The third deadenylase complex, PAN, has not been examined in *Arabidopsis* yet.

1.2.6. Alternative polyadenylation

A large proportion of genes contains more than one polyadenylation site, a phenomenon termed alternative polyadenylation (APA). Several studies have shown, that 30% of mouse and 50% of human (Tian *et al.*, 2005; Ozsolak *et al.*, 2010) and the majority of genes in plants (up to 82% in rice and 74% in *Arabidopsis*) contain more than one polyadenylation site (Shen *et al.*, 2011; Wu *et al.*, 2011, Sherstnev *et al.*, 2012). This fact already implies the great regulatory potential of APA by determining the coding and regulatory regions of an mRNA (Lutz and Moreira, 2011; Xing and Li, 2011). APA may cause incorrect definition of the 3'-end on an mRNA leading to a truncation of the mRNA and/or resulting protein (Xing and Li, 2010). APA might also cause inclusion or exclusion of specific sequence elements (e.g. miRNA target sites) to control mRNA turnover (Mayr and Bartel, 2009). One well characterized example for APA is the regulation of *FLOWERING LOCUS C (FLC)* by the RNA binding protein FCA and the spen family protein FPA (Liu *et al.*, 2010; Hornyik *et al.*, 2010). A

Introduction

promoter situated downstream of the polyA site of the *FLC* sense gene and on the opposite strand generates antisense transcripts that have alternative polyA sites. Two classes of transcript arise from this: the class I antisense transcript PAS is opposite to the terminal *FLC* intron, whereas class II antisense transcripts have the PAS opposite to the *FLC* promoter. Both, FCA and FPA associate with *FLC* mRNA downstream of the antisense class I poly(A) site and promote its usage. This short antisense transcript functions in silencing of *FLC*, thus promoting flowering (Horniyik *et al.*, 2010; Liu *et al.*, 2010). Additionally, both proteins promote the proximal poly(A) site selection (within the first intron of the pre-mRNA) in their own mRNA, negatively autoregulating their own expression (Quesada *et al.*, 2003; Horniyik *et al.*, 2010).

As mentioned before, plants possess very variable poly(A) signals situated in exons, introns, 3'-UTRs or 5'-UTRs (Wu *et al.*, 2011). To date, no auxiliary downstream element has been identified that can explain the choice between the different sites. However, it was recently shown that a protein of the 3'-end processing complex, AtCPSF30 (see section 1.2.2), is involved in redox-potential dependent poly(A) site choice (Thomas *et al.*, 2013). This fact implies the specific regulation of poly(A)-site choice under different conditions or in different developmental stages and underlines the regulatory potential of APA.

(reviewed in [Elkon *et al.*, 2013], for plant APA see [Xing and Li, 2010; Hunt, 2012]).

1.3. Plants have a variety of mechanisms to react on biotic stress

As sessile organisms plants have to face a variety of environmental factors that they cannot escape by moving. Not only abiotic factors like temperature or water supply influence plant life, they also have to defend their space against other plants and share it with billions of microorganisms, including pathogens. The basal, or nonhost, resistance to invasive pathogens is the first crucial protective layer. Without it, plants become hyper-susceptible to even mild infections and are less likely to survive in a competitive environment. The next level of defense mechanisms is the expression of plant 'resistance' (*R*) genes, which encode components that allow the recognition and response of plants to specialized pathogens. The pathogen's counterpart inducing the expression of *R* genes was referred to as the avirulence (*Avr*) gene. However, recent studies have shown that *R* genes do not only recognize the presence of the pathogen itself, but the changes of the pathogen's targets in the host (Chisholm *et al.*, 2006; Jones and Dangl, 2006). Unlike animals, plants lack an adaptive immune system (Ausubel 2005), but plants are equipped with a sophisticated immune system for the recognition of invading pathogens, transmission of alarm signals, and rapid activation of efficient defense responses that limit infection.

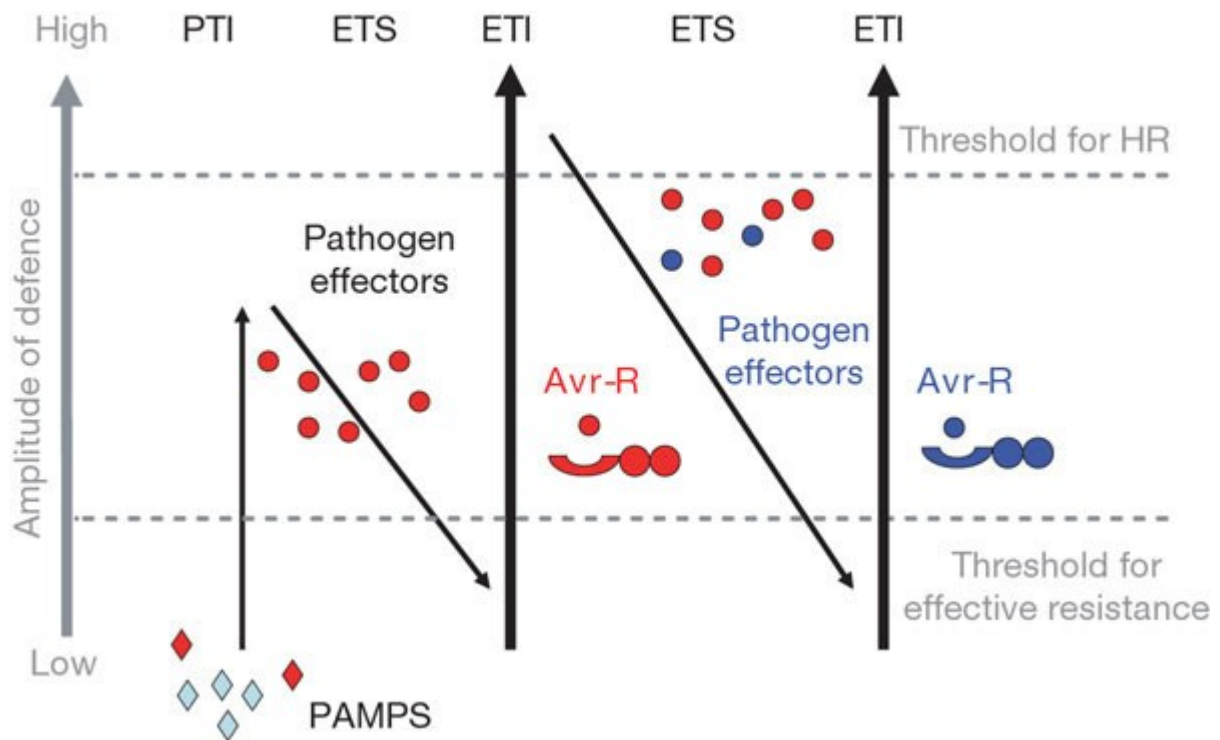


Fig. 1.4: In this scheme, the ultimate amplitude of disease resistance or susceptibility is proportional to [PTI – ETS + ETI]. In phase 1, plants detect microbial/pathogen-associated molecular patterns (MAMPs/PAMPs, red diamonds) via PRRs to trigger PAMP-triggered immunity (PTI). In phase 2, successful pathogens deliver effectors that interfere with PTI, or otherwise enable pathogen nutrition and dispersal, resulting in effector-triggered susceptibility (ETS). In phase 3, one effector (indicated in red) is recognized by an NB-LRR protein, activating effector-triggered immunity (ETI), an amplified version of PTI that often passes a threshold for induction of hypersensitive cell death (HR). In phase 4, pathogen isolates are selected that have lost the red effector, and perhaps gained new effectors through horizontal gene flow (in blue)—these can help pathogens to suppress ETI. Selection favours new plant NB-LRR alleles that can recognize one of the newly acquired effectors, resulting again in ETI (from Jones and Dangl, 2006).

1.3.1. Pathogen recognition and reaction in plants – PTI and ETI

A simple but elegant model of innate immunity in plant pathogen interactions is depicted by the so-called zigzag model introduced by Jones and Dangl (2006) (Fig. 1.4). This model proposes that the first line of active plant defense is formed by pattern recognition receptors (PRRs) that recognize pathogen-associated molecular patterns (PAMPs) (Janeway, 1989) and activate pattern-triggered immunity (PTI). PAMPs are highly conserved molecules within a class of microbes that have an essential function in microbial fitness or survival, so cannot be easily lost in evolution (Medzhitov and Janeway, 1997). The best known examples of PAMPs include lipopolysaccharide (LPS) of gram-negative bacteria, peptidoglycan of gram-positive bacteria (reviewed in [Boller, 1995]) and flagellin (Felix *et al.*, 1999). The first PRR identified in plants is the *FLS2* gene from *Arabidopsis* (Gómez-Gómez and Boller, 2000), a transmembrane protein that is responsible for the recognition of the bacterial elicitor flagellin (in particular a highly conserved 22-amino-acid epitope, flg22). Intercellular responses associated with PTI include rapid ion fluxes across the plasma membranes, MAP kinase

Introduction

activation, production of reactive oxygen species (ROS), cell wall reinforcement and rapid changes in gene expression (Zipfel, 2008). Successful pathogens are able to overcome PTI by inserting effectors into the plant cell that suppress PTI responses, resulting in effector-triggered susceptibility (ETS). Plants in turn have reacted to this by evolving cytoplasmic R-proteins that recognize the presence or activity of an effector. The majority of these R proteins are intracellular receptor proteins of the nucleotide-binding leucine-rich-repeat (NB-LRR) type that activate so-called effector-triggered immunity (ETI). NB-LRRs belong to a subfamily of proteins within the STAND (signal transduction ATPase with numerous domains) superfamily that also contains regulators of immunity, inflammation and apoptosis in animals (Ye and Ting, 2008; Lukasik and Takken, 2009). The N-terminal domain usually exhibits either a toll/interleukin-1 receptor (TIR) domain or a coiled-coil domain (CC), which influences the requirement for distinct downstream signaling components (Aarts *et al.*, 1998). Typically, the ability to induce ETI is pathogen strain- or race-specific. It is associated with an increase of cytosolic Ca^{2+} levels, programmed cell death in the plant (the so called hypersensitive response [HR]), and 'priming' of the surrounding tissue to react on the diseases (the so called systemic acquired resistance [SAR]). However, some studies have shown that also PTI can induce HR in plants (e.g. flg22 in *Arabidopsis*) (Naito *et al.*, 2007). Although PTI and ETI share many signaling components, it is believed that ETI occurs more quickly, more prolonged and more robust than PTI, suggesting that PTI is a weak variant of ETI. Both PTI and ETI trigger massive reprogramming of the transcriptome (Tao *et al.*, 2003; Navarro *et al.*, 2004). A key component involved in the transcriptional regulation of immune-response genes is NONEXPRESSOR OF PATHOGENESIS RELATED GENES 1 (NPR1). A salicylic acid (SA)-triggered change of the intracellular redox state causes release of the disulfite bonds in the NPR1 oligomer by the activity of the thioredoxins TRX-H3 and TRX-H5 (Tada *et al.*, 2008). Released NPR1 monomers subsequently translocate from the cytoplasm to the nucleus (Kinkema *et al.*, 2000). There, NPR1 recruits transcription factors to the promoters of defense-related genes including the *PATHOGENESIS-RELATED 1 (PR1)* gene (Dong, 2004). In this ongoing evolutionary battle, pathogens are forced to evolve other effectors, which suppress the ETI in the host in turn forcing the plant to evolve new resistance strategies.

1.3.2. EDS1/PAD4/SAG101 mediated signalling

ENHANCED DISEASE SUSCEPTIBILITY 1 (EDS1) and its interacting partners, PHYTOALEXIN DEFICIENT 4 (PAD4) and SENESCENCE ASSOCIATED GENE 101 (SAG101) are plant-specific proteins that constitute a regulatory hub that is essential for basal resistance to invasive biotrophic and hemi-biotrophic pathogens, ETI, SAR and response to photo-oxidative stress. Mutational analyses demonstrated that EDS1 is an essential component of the basal immunity to virulent biotrophic pathogens. Furthermore it plays a role in effector triggered immunity (ETI) conditioned by intracellular TIR-NB-LRR receptors recognizing specific pathogen effectors (Wiermer *et al.*, 2005 and references therein). Two recent studies revealed a direct physical interaction of EDS1 with two effectors (AvrRps4 and HopA1), and also with their corresponding TIR-NB-LRR proteins (RPS4 and RPS6) (Bhattacharjee *et al.*, 2011; Heidrich *et al.*, 2011). This suggests that EDS1 could be the target of some pathogen effectors and might be guarded by the corresponding R proteins (McDowell, 2011). A model has been proposed, whereby molecular transitions of EDS1 between complexes determine different stages of EDS1 signal relay (Rietz *et al.*, 2011). In this model, low levels of EDS1 (probably as a homodimer), and in some cases dissociated PAD4, 'kick' start the resistance response after TIR-NB-LRR receptor activation by triggering rapid, localized host cell death. In cells surrounding death foci (and in basal resistance), EDS1 and PAD4, together as a complex, serve a different function involving the transcriptional reprogramming of host cells. This enables the spread of resistance to systemic tissues and mobilization of SA-mediated and other defenses. The EDS1–SAG101 complex on the other hand acts to reinforce resistance at the edges of the local HR (Tsuda *et al.*, 2009; Rietz *et al.*, 2011). Coordination between the EDS1 cytoplasmic and nuclear pools via the nuclear pore trafficking machinery is therefore needed to condition full plant resistance (Cheng *et al.*, 2009; Garcia *et al.*, 2010). However, there is also an SA-independent EDS1 signaling pathway present in *Arabidopsis* in which FLAVIN MONOOXYGENASE (FMO1) acts as a positive regulator, whereas NUDIX HYDROLASE7 (NUDT7) acts as a negative regulator (Bartsch *et al.*, 2006; Straus *et al.*, 2010). FMO1 was also shown to be an essential component of SAR but not PTI or ETI (Mishina and Zeier, 2006). AtNUDT7 and AtNUDT6 are members of the FGFTNE clan of the Nudix hydrolases with redundant functions and exhibit ADP-ribose/NADH pyrophosphohydrolase activity *in vitro* (Ogawa *et al.*, 2005). In the *nudt6-2 nudt7* double mutants, autoimmunity is activated in an *SNC1* (*suppressor of npr1-1, constitutive1*) dependent and independent pathway, which are both temperature sensitive and dependent on *EDS1* (Wang *et al.*, 2013).

1.3.3. Phytohormone crosstalk in plant immunity

Plant hormones play important roles in regulating plant growth and defense by mediating developmental processes and signaling networks involved in plant responses to a wide range of parasitic and mutualistic biotic interactions. Salicylic acid (SA), a major player in disease resistance signaling (Vlot *et al.*, 2009), is typically but not exclusively effective against microbial biotrophic pathogens (Glazebrook, 2005). EDS1 and PAD4 act in the onset of SA biosynthesis during PTI and during TIR-NB-LRR mediated ETI (Wiermer *et al.*, 2005). As mentioned before, NPR1 is the most important signal component in response to SA. It triggers expression of *R*-genes like *PR1* or *WRKY* transcription factors in the nucleus. A similar response is often triggered in distal parts of the plant to protect undamaged tissue against subsequent pathogen invasion which is referred to as systemic acquired resistance (SAR). The second plant hormone playing a major role in pathogen response is jasmonic acid (JA), its metabolite Methyl-jasmonate (MeJA) or its conjugate with Isoleucin (JA-Ile). In unchallenged cells, JA signaling pathways are repressed by JASMONATE ZIM (JAZ) proteins through binding to positive transcriptional regulators. Together with CORONATINE INSENSITIVE1 (COI1) JAZ proteins serve as JA-Ile receptor and are targeted for proteasome turnover upon JA-Ile perception (Pauwels and Goossens, 2011). Two major signaling branches can be distinguished: the MYC branch that is controlled by MYC-type transcription factors (Fernandez-Calvo *et al.*, 2011; Niu *et al.*, 2011) and the ERF branch that is regulated by the APETALA/ETHYLENE RESPONSE FACTOR (AP2/ERF) family of transcription factors (Pré *et al.*, 2008) and includes the expression of the JA-marker gene *PLANT DEFENSIN 1.2 (PDF1.2)*. This latter pathway is associated with resistance against necrotrophic pathogens (Lorenzo *et al.*, 2003) whereas the MYC pathway is associated with the wound response and defense against insects (Kazan and Manners, 2012). The SA and JA signaling pathways are interconnected with each other in a dosage-dependent antagonistic manner (Spoel *et al.*, 2003). For example, induction of the SA pathway by avirulent *P. syringae* suppressed JA signaling and rendered infected *Arabidopsis* leaves more susceptible to the necrotrophic fungus *Alternaria brassicicola* (Spoel *et al.*, 2007). Similarly, preceding inoculation with the SA-inducing biotrophic pathogen *Hyaloperonospora arabidopsidis* suppressed JA-mediated defenses that were activated upon feeding by caterpillars of imported cabbageworm, *Pieris rapae* (Koornneef *et al.*, 2008). Additionally, both SA and JA affect the cellular redox buffer glutathione. SA increases the cellular amount as well as the ratio of reduced to oxidized glutathione, whereas JA lowers the glutathione pool (Spoel & Loake 2011). Other plant hormones modulate the balance between SA and JA signaling, for example the gaseous hormone Ethylen (ET). It potentiates the SA-responsive *PR-1* expression in *Arabidopsis* (De Vos *et al.*, 2006) and is essential for the onset of SAR in tobacco (Verbene *et al.*, 2003). When produced in combination with JA, such as upon infection by necrotrophic pathogens, ET acts

Introduction

synergistically on the expression of the ERF branch of the JA pathway, while it antagonizes the MYC branch. The result is prioritization of the immune signaling network towards JA- and ET-dependent defense signaling associated with resistance to necrotrophs (Anderson *et al.*, 2004; Lorenzo *et al.*, 2003; Pré *et al.*, 2008). Additionally, when the JA and ET pathways are fully induced prior to SA induction, the antagonistic effect of SA on the JA pathway is completely abolished. In addition to its before mentioned effects, also ABA plays a role in plant defense responses. In *Arabidopsis*, ABA and SA response mechanisms affect each other at multiple steps, from the level of biosynthesis to intermediate components of the signal transduction pathways (Yasuda *et al.*, 2008). Hence, plants seem to balance ABA-mediated abiotic stress tolerance and SA-mediated biotic stress resistance through ABA-SA crosstalk. Upon wounding or herbivory ABA is produced in combination with JA and promotes the expression of the MYC branch of the JA response pathway, while it suppresses the ERF branch (Anderson *et al.*, 2004).

The most important growth hormone auxin also plays a role during pathogen responses. Many microbes can produce auxins or manipulate auxin signaling in the host to interfere with normal growth processes (Robert-Selaniantz *et al.*, 2011a). Moreover, auxin signaling can repress SA levels and signaling (Robert-Seilaniantz *et al.*, 2011b) while in turn elevated SA levels impede auxin responses (Wang *et al.*, 2007). Gibberellins (GAs) were firmly implicated in plant immune signaling when degradation of DELLA proteins (see section 1.1.3) was shown to promote susceptibility to necrotrophs and resistance to biotrophs through modulation of JA and SA signaling (Navarro *et al.*, 2008). Recent findings have shed light on a distinct role of cytokinins in plant immune responses. Cytokinins systemically induce resistance against pathogen infection. This resistance is orchestrated by endogenous cytokinin and salicylic acid signaling (Choi *et al.*, 2011; Jiang *et al.*, 2013). Phytohormone crosstalk provides a powerful regulatory potential to finely tune defense. Nevertheless it is possible that plant attackers can manipulate the plant hormone signaling network for their own benefit. For instance, the necrotrophic fungus *Botrytis cinerea* produces an exopolysaccharide that acts as an elicitor of the SA/NPR1 pathway and thus suppresses effective JA-dependent defenses in its host, the tomato plant (*Solanum lycopersicum*) (El Oirdi *et al.*, 2011).

1.3.4. Role of polyadenylation/deadenylation proteins in plant immunity

Proteins of the 3'-end processing complex, RNA-binding proteins (RBPs) and proteins of the deadenylation machinery play an important role in plants in abiotic and biotic stress responses. For example mutant plants deficient in CPSF30 expression are more tolerant to oxidative stresses than the wild type (Zhang *et al.*, 2008). Consistent with this suggestion, the biochemical activities of the *Arabidopsis* CPSF30, which has RNA binding and endonuclease activity, are affected *in vitro* by calmodulin and sulfhydryl reagents (Delaney *et al.*, 2006; Addepalli and Hunt, 2008). In addition, one of the three zinc finger motifs of the protein is engaged in a dithiothreitol-sensitive disulfide bond (Addepalli *et al.*, 2010). These properties are suggestive of communication of the protein with calcium and redox cellular signaling pathways and provide conceptual links between these signaling pathways and alternative poly(A) site choice. Additionally, functional analysis of *Arabidopsis* cytoplasmic deadenylation factors has uncovered a link between the control of poly(A)-tail lengths and pathogen response. Mutations in *AtCAF1a* and *AtCAF1b*, the two homologues of the yeast CCR4-associated factor that is a component of the CCR4-NOT deadenylase complex, result in defective poly(A)-tail shortening of stress-associated mRNAs and in reduced expression of the *PATHOGENESIS-RELATED1 (PR1)* gene (Liang *et al.*, 2009; Walley *et al.*, 2010a; Walley *et al.*, 2010b). By contrast, overexpressing *AtCAF1a* upregulates *PR1* expression and increases pathogen resistance in the transgenic plants. Also, overexpression of the yeast poly(A)-binding protein Pab1p in tobacco or *A. thaliana* leads to a constitutive pathogen response and increased resistance (Li *et al.*, 2000). Another example is the plant RBP known as FPA, which regulates 3'-end mRNA polyadenylation and negatively regulates basal resistance to bacterial pathogen *Pseudomonas syringae* in *Arabidopsis*. A custom microarray analysis revealed that flg22, a peptide derived from bacterial flagellins, induces expression of alternatively polyadenylated isoforms of the mRNA encoding the defense-related transcriptional repressor *ETHYLENE RESPONSE FACTOR 4 (ERF4)*, which is regulated by FPA (Lyons *et al.*, 2013).

1.4. Aim of this study

To our current understanding, poly(A) polymerases play a general, essential role in the 3'-end processing in all eukaryotes. Their catalytic activity gives rise to the poly(A) tail on the 3'-end of each mRNA that has various important functions. It promotes the transport of the mRNA from the nucleus to the cytoplasm, confers mRNA stability and promotes translation. Both vertebrate and higher-plant genomes encode more than one isoform of this enzyme, and these are coexpressed in different tissues. However, in neither case is it known whether the isoforms fulfill different functions or polyadenylate distinct subsets of pre-mRNA.

An *Arabidopsis thaliana* mutant in the *poly(A) polymerase 1 (PAPS1)* gene was identified that shows bigger flowers but smaller leaves, in contrast to virtually all previously described organ-size mutants (Vi *et al.*, 2013). This effect is specific for PAPS1 since mutations in other PAPS in *Arabidopsis* (e.g. *PAPS2* or *PAPS4*) show no phenotypic effect besides late flowering.

The questions addressed in this thesis are:

How and why do the different organs in PAPS1 mutants reach their altered size?

What is the molecular basis for this effect?

Is there a functional specialization amongst the different PAPS in *Arabidopsis*?

May this support a general idea in evolution of allele specific effects?

May there be an additional level of gene regulation through poly(A) tail length or polyadenylation by different PAPS, respectively?

2. Results

2.1 Target specificity among nuclear poly(A) polymerases in plants modulates organ growth and pathogen response

The content of this chapter resembles largely the following publication:

Vi LS, Trost G, Lange P, Czesnick H, Rao N, Lieber D, Laux T, Gray WM, Manlex JL, Groth D, Kappel C, Lenhard M (2013) Target specificity among nuclear poly(A) polymerases in plants modulates organ growth and pathogen response. *Proc Natl Acad Sci USA* 110: 13994-13999.

Proceeding of the National Academy of Science of the United States of America; Vol. 110 Issue 34;
Pages: 13994-13999

doi: 10.1073/pnas.1303967110

Following Experiments and corresponding evaluation within this manuscript were done by myself:

Fig. 1E

Fig. 3B, 3C, 3D, 3E, 3F, 3G, 3H

Fig. 4B, 4C, 4D

Supplementary Fig. 3B, 3C, 3D, 3E, 3F, 3G

Supplementary Fig. 4A, 4B, 4C, 4D, 4E

Supplementary Fig. 5A

Results

Target specificity amongst canonical nuclear poly(A) polymerases in plants modulates organ growth and pathogen response.

Son Lang Vi^{1,2†}, Gerda Trost¹, Peggy Lange¹, Hjördis Czesnick¹, Nishta Rao^{3§}, Diana Lieber^{4‡}, Thomas Laux⁴, William M. Gray⁵, James L. Manley³, Detlef Groth¹, Christian Kappel¹, Michael Lenhard^{1*}

¹ Institut für Biochemie und Biologie, Universität Potsdam, Karl-Liebknecht-Str. 24-25, 14476 Potsdam, Germany.

² John Innes Centre, Cell & Developmental Biology, Colney Lane, Norwich, NR4 7UH, UK.

³ Department of Biological Sciences, Columbia University, New York, NY 10027, USA

⁴ BIOS Centre for Biological Signalling Studies, Albert-Ludwigs-Universität Freiburg, Schänzlestrasse 1, 79104 Freiburg, Germany

⁵ Department of Plant Biology, University of Minnesota, 250 Biological Sciences Center, 1445 Gortner Ave, St. Paul, MN 55108, USA

[†] present address: Cold Spring Harbor Laboratory, 1 Bungtown Road, Cold Spring Harbor, NY 11724, USA.

[§] present address: Kadmon Research Institute, 450 East 29th Street, New York, NY 10016, USA

[‡] present address: Institute of Virology, Ulm University Medical Center, Albert-Einstein-Allee 11, 89081 Ulm, Germany

* author for correspondence:

email: michael.lenhard@uni-potsdam.de

telephone: ++49-331-9775580

telefax: ++49-331-9775522

Running title: Specificity of plant canonical poly(A) polymerases

Keywords: Polyadenylation, poly(A) polymerase, leaf growth, SAUR mRNAs, pathogen response.

Author contributions:

SLV, GT, CK, ML designed research. SLV, GT, PL, HC, NR, ML performed research. DL, TL, WMG contributed new reagents. SLV, GT, HC, JLM, DG, CK, ML analysed data. SLV, ML wrote manuscript with input from all authors.

ABSTRACT

Polyadenylation of pre-mRNAs is critical for efficient nuclear export, stability and translation of the mature mRNAs, and thus for gene expression. The bulk of pre-mRNAs are processed by canonical nuclear poly(A) polymerase (PAPS). Both vertebrate and higher-plant genomes encode more than one isoform of this enzyme, and these are co-expressed in different tissues. However, in neither case is it known whether the isoforms fulfil different functions or polyadenylate distinct subsets of pre-mRNAs. Here we show that the three canonical nuclear PAPS isoforms in *Arabidopsis* are functionally specialized owing to their evolutionarily divergent C-terminal domains. A strong loss-of-function mutation in *PAPS1* causes a male gametophytic defect, whereas a weak allele leads to reduced leaf growth that results in part from a constitutive pathogen response. By contrast, plants lacking both *PAPS2* and *PAPS4* function are viable with wild-type leaf growth. Polyadenylation of *SMALL AUXIN UP RNA (SAUR)* mRNAs depends specifically on *PAPS1* function. The resulting reduction in *SAUR* activity in *paps1* mutants contributes to their reduced leaf growth, providing a causal link between polyadenylation of specific pre-mRNAs by a particular PAPS isoform and plant growth. This suggests the existence of an additional layer of regulation in plant and possibly vertebrate gene expression, where the relative activities of canonical nuclear PAPS isoforms control *de novo* synthesized poly(A)-tail length and hence expression of specific subsets of mRNAs.

INTRODUCTION

The poly(A) tail at the 3'-end is an essential feature of virtually all eukaryotic mRNAs that influences stability, nuclear export and translational efficiency of the mRNAs (1, 2). It is synthesized after RNA polymerase II has transcribed past the cleavage and polyadenylation site and associated signal sequences (3, 4). These sequences are bound by several protein complexes, including Cleavage-stimulation Factor (CstF) and Cleavage and Polyadenylation Specificity Factor (CPSF) in animals and their counterparts in yeast (5). The complexes effect the cleavage of the nascent pre-mRNA at the prospective polyadenylation site and recruit poly(A) polymerase to add the poly(A) tail. The same scenario is presumed to hold also for 3'-end processing and polyadenylation in plants, as plant genomes encode homologues to the components of these complexes in yeast and animals (2).

The poly(A) tail is synthesized by poly(A) polymerases, with the bulk of cellular pre-mRNAs being polyadenylated by canonical nuclear poly(A) polymerases (cPAPSs) (5, 6) that share substantial sequence identity with human poly(A) polymerase- α (PAPOLA), bovine poly(A) polymerase or the yeast enzyme Pap1p (7-9). While the *Saccharomyces cerevisiae* and *Drosophila melanogaster* genomes only encode one cPAPS, which is essential for growth (7, 10), three such proteins are found in humans, PAPOLA (PAP α), PAPOLB (PAP β) and PAPOLG (PAP γ) (11). Of these, PAPOLA is thought to be the main PAPS in somatic cells. PAPOLA and PAPOLG proteins contain a C-terminal regulatory region next to the highly conserved catalytic N-terminal domain and are found either in both nucleus and cytoplasm (PAPOLA) or only in the nucleus (PAPOLG) of cells throughout the human body (9, 11-14). By contrast, PAPOLB lacks the C-terminal region, is exclusively cytoplasmic, and is only found in testis cells where it is required to extend the poly(A) tail of cytoplasmic mRNAs encoding sperm-related proteins (15); as a consequence male mice mutant for *PAPOLB* are sterile.

The *Arabidopsis thaliana* genome encodes four cPAPS proteins, termed PAPS1 to PAPS4 (16, 17). PAPS3 resembles PAPOLB in lacking an extended C-terminal region, being localized in the cytoplasm and expressed mainly in the male gametophytes (the pollen). By contrast, PAPS1, PAPS2 and PAPS4 all contain an extended C-terminal region, localize exclusively to the nucleus and are expressed throughout the plant (2, 16-18). All four proteins have non-specific polyadenylation activity *in vitro*, suggesting that they represent functional cPAPSs (16, 19). Based on the failure to identify homozygous T-DNA insertion mutants for any of the three genes, it was concluded that all of them are essential for plant growth and development (17).

Gene expression can be regulated via a number of mechanisms impinging on the mRNA 3' end. The choice between alternative 3'-end cleavage sites is widely used to regulate gene expression in both animal and plant development, for example via the exclusion or inclusion of microRNA-target sites in

Results

the resulting 3'-UTRs (20-24). Also, modulating the length of the poly(A) tails on mRNAs in the cytoplasm by the opposing actions of cytoplasmic PAPS (e.g. PAPOLB) and deadenylases can be used to control the expression of the encoded proteins (1, 15). However, it is currently unclear whether polyadenylation by nuclear cPAPS can also contribute to the control of specific gene expression. In principle, this could occur in either of two ways. First, pre-mRNAs could be differentially sensitive to variations in the total cPAPS activity provided by one or more functionally interchangeable cPAPS isoforms; such a mechanism may underlie specific developmental phenotypes in weak mutants of *D. melanogaster* cPAPS (25). Second, some mRNAs may be exclusively or preferentially polyadenylated by one cPAPS in organisms with more than one isoform. Given such target specificity, modulating the balance of activities between the isoforms could then be used to alter the length of the *de novo* synthesized poly(A) tails, and hence ultimately gene expression, of subsets of mRNAs. Target specificity has at present only been observed for non-canonical PAPS (6, 26), such as Star-PAP, which is required for the cellular response to oxidative stress.

Here we provide evidence for functional specialization and target specificity amongst *A. thaliana* nuclear cPAPS isoforms. Mutations affecting different isoforms cause very different phenotypes that depend on the divergent C-terminal domains of the proteins. In particular, reduction of *PAPS1* activity disrupts polyadenylation of *SMALL AUXIN UP RNA (SAUR)* mRNAs and causes leaf growth defects due to reduced *SAUR* function and a constitutive pathogen response. We propose that this specificity of PAPS isoforms provides an additional level of regulating plant gene expression.

RESULTS AND DISCUSSION

***paps1* mutants show organ-specific effects on growth.**

From an ethyl-methanesulfonate (EMS) mutagenesis screen, we identified a novel recessive mutation causing opposite effects on the growth of leaves and flowers, termed *paps1-1* (Fig. 1A-C). While the size of *paps1-1* mutant leaves is reduced to less than one third of the wild-type value, mutant petals and other floral organs are larger than in wild type, with petals reaching almost twice the wild-type size. At the cellular level, the reduced leaf size is largely due to a defect in cell expansion (Fig. 1C). Conversely, the size of *paps1-1* mutant petal cells is only increased by 21%, indicating that the bulk of the difference in petal size is due to a higher number of cells (Fig. 1C). Thus, *PAPS1* function is required to allow normal cell expansion in leaves and to limit cell proliferation in petals.

The *paps1-1* mutation reduces the activity of PAPS1 in canonical nuclear polyadenylation of pre-mRNAs.

To determine the molecular basis of the *paps1-1* mutant phenotype, we isolated the affected gene by mapping and sequencing of candidate genes. This identified a C-to-T transition typical for EMS-induced mutations in the *At1g17980* gene coding for PAPS1 (Fig. S1A). The mutation causes an amino-acid substitution of serine for proline at position 313. The mutated proline lies in a linker peptide between the nucleotidyl-transferase domain and the RNA-binding domain within the N-terminal catalytic region of the protein and is very highly conserved in poly(A) polymerases from yeast, plants and animals (Fig. S1B). Complementation of the *paps1-1* mutant with a wild-type genomic copy of the *PAPS1* locus restored a wild-type phenotype (Fig. S1C). The *paps1-1* allele is temperature sensitive (Fig. S1D); in contrast to growth at 23°C, seedlings grown at 28°C showed a very severe phenotype with bleaching and almost complete growth inhibition, indicating that the phenotypes seen at lower temperatures result from only a moderate reduction in *PAPS1* activity (see also below).

To determine the effect of the *paps1-1* mutation on the protein's activity, we performed *in vitro* polyadenylation assays using purified recombinant protein (27). While the wild-type protein showed robust polyadenylation activity, virtually no enzymatic activity was observed when using the mutant form (Fig. 1D and Fig. S1E).

To genetically determine whether PAPS1 is indeed involved in canonical pre-mRNA processing in the nucleus, we combined the *paps1-1* allele with a mutant allele of the *CSTF64* locus encoding the sole *A. thaliana* homologue to the Cstf64 subunit of the cleavage-stimulation factor complex (28). We

Results

could not recover any double homozygous *cstf64-1 paps1-1* mutants, and the siliques from *cstf64-1/+; paps1-1/paps1-1* plants contained 25% aborted seeds (Fig. 1E and Fig. S1F), indicating that double mutant embryos are lethal. This contrasts with full seed set in either single mutant. Together, this synthetic lethality and the results of the *in vitro* assay strongly suggest that the *paps1-1* mutation affects nuclear polyadenylation of transcripts.

Figure 1: Loss of *PAPS1* function leads to altered organ growth.

(A, B) Whole-plant (A) and flower images (B) of the indicated genotypes.

(C) Quantification of organ and cell sizes from the indicated genotypes. Values are mean \pm SE from at least 5 (leaves), 20 (petals, sepals, anthers), 7 (gynoecia) or 55 (seeds) organs per genotype, normalized to the wild-type mean.

(D) Autoradiograph of *in vitro* non-specific polyadenylation assay. The indicated amounts of wild-type *PAPS1* protein (WT) or of the mutant form encoded by the *paps1-1* allele (mut) were used. Asterisk indicates the unpolyadenylated RNA substrate.

(E) Micrographs of opened siliques from the indicated genotypes. Note the aborted seeds produced by *paps1-1 cstf64-1/+* plants.

(F) Light-micrographs of openend siliques from Col-0 (left) and *paps1-3/+* heterozygous plants (right) after selfing.

(G) Transmission efficiency (TE) of the *paps1-3* mutant allele through the male and the female gametophyte. The result for the first cross is not significantly different from the expected 50:50 ratio ($p=0.10$, Chi-square test).

Scale bars are 1 cm in (A), 1 mm in (B), 500 μ m in (F).

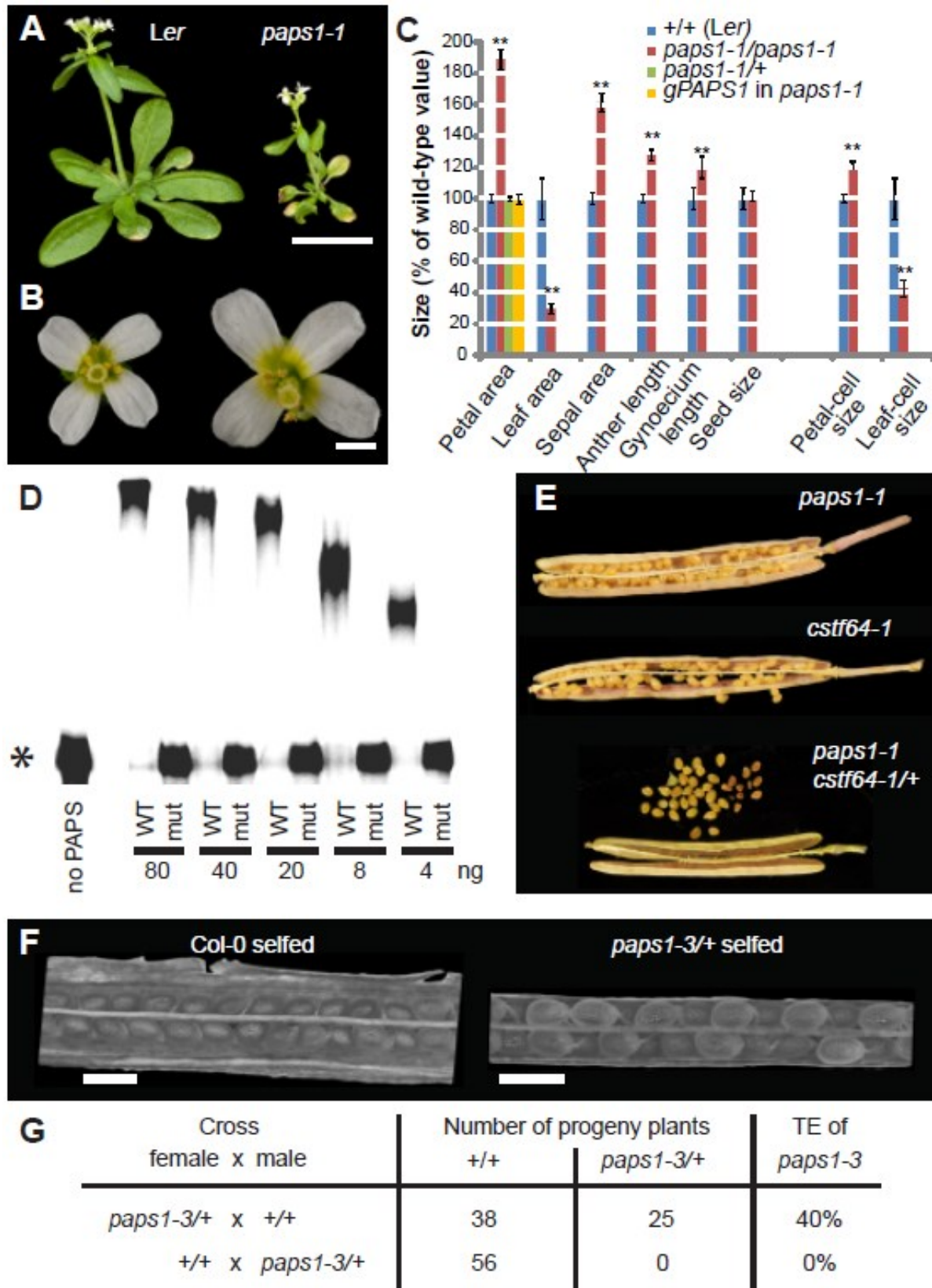


Figure 1

***PAPS1* activity is essential for male gametophyte function.**

To determine the effects of a complete loss of *PAPS1* activity, we studied a presumed null allele with a T-DNA insertion in the fifth intron within the region coding for the N-terminal catalytic protein domain (*paps1-3*; Fig. S1A). It was not possible to recover plants homozygous for the *paps1-3* allele. To determine whether this is due to embryonic lethality or to a gametophytic defect, we analysed the seeds developing on *paps1-3/+* heterozygous plants and performed reciprocal crosses. There was no evidence for either embryo lethality or a female gametophytic defect from analyzing the siliques of *paps1-3/+* plants, as we did not detect aborted seeds or unfertilized ovules (Fig. 1F). Consistent with this, the *paps1-3* mutant allele was normally transmitted through the female gametophyte (Fig. 1G). By contrast, when applying pollen from *paps1-3/+* plants to wild-type stigmas, none of the progeny carried the mutant allele (Fig. 1G), indicating that the *paps1-3* mutation causes a male-gametophytic defect. Pollen from *paps1-1* mutant plants and from *paps1-3/+* heterozygotes was morphologically normal and viable (Fig. S1G). Thus, *PAPS1* represents an essential gene for male gametophyte function, and a progressive reduction of remaining *PAPS1* activity in the diploid sporophyte causes increasingly more severe phenotypic defects as seen in the *paps1-1* allele (see above).

The three canonical nuclear poly(A) polymerases encoded by the *A. thaliana* genome are functionally specialized.

To determine the roles of the other two canonical nuclear PAPSs in *A. thaliana*, putative null alleles were isolated for *PAPS2* and *PAPS4*. In both cases the eighth exon within the region coding for the catalytic N-terminal domain was disrupted, and no full-length mRNA could be detected from the mutant alleles (Fig. S2 B, D, and E). Both single mutants and the *paps2-1 paps4-1* double mutant were viable (Fig. S2B) and showed normal leaf and petal growth (Fig. 2 A and B). To test whether the much more severe phenotypes resulting from loss of *PAPS1* function were simply due to *PAPS1* being responsible for most polyadenylation in *Arabidopsis*, we determined bulk poly(A) tail lengths in *paps1-1* mutant and wildtype seedlings. There was virtually no change in the distribution of bulk poly(A) tail lengths (Fig. S2 F and G), despite the very severe mutant phenotype under the growth conditions used (Fig. S1D). Together, these results indicate that most transcripts can be redundantly polyadenylated by either *PAPS1* or *PAPS2/PAPS4* but that a small subset of critical transcripts is exclusively or preferentially targeted by *PAPS1*.

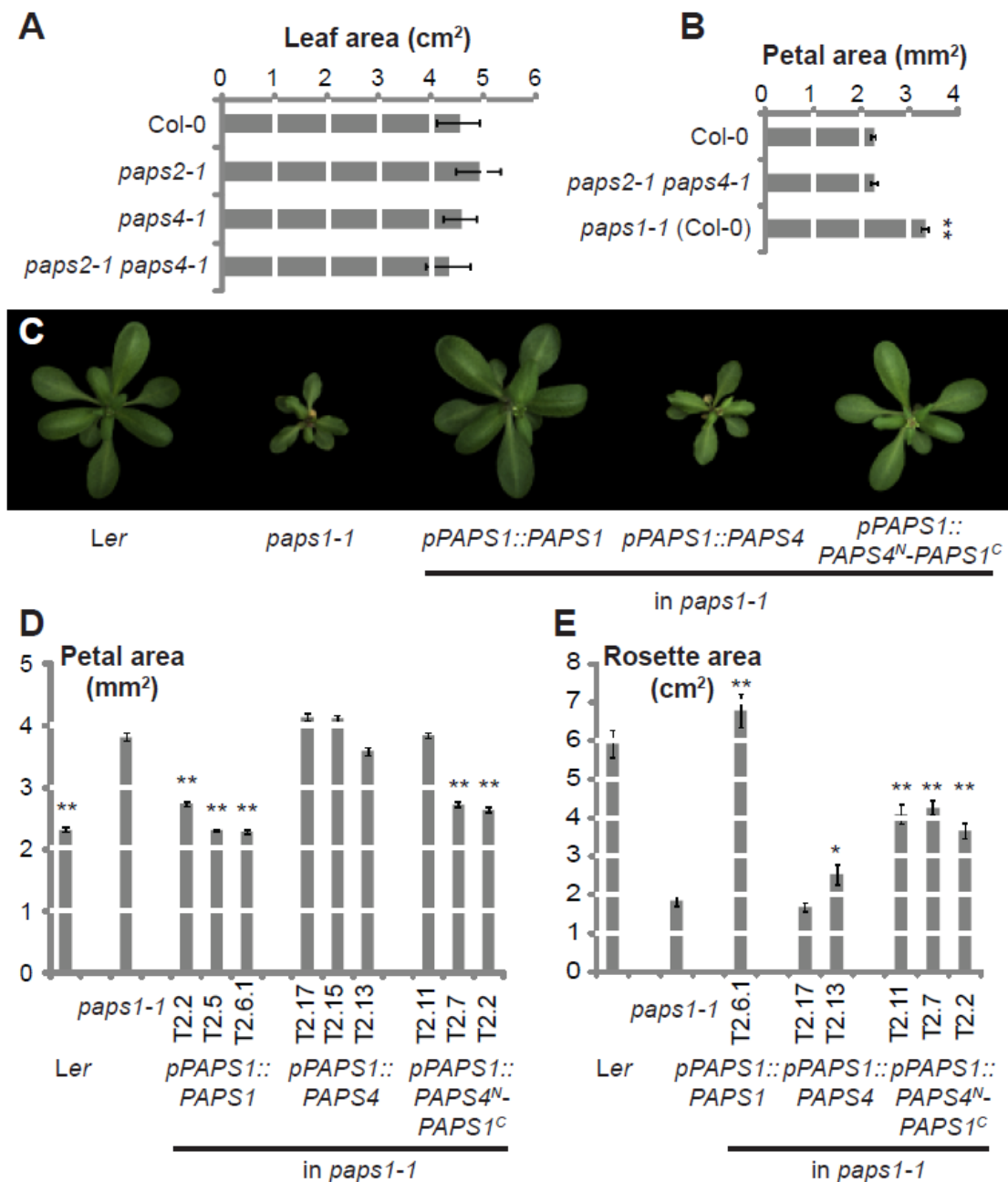


Figure 2: The three nuclear PAPS isoforms in *A. thaliana* fulfil distinct functions.

(A, B) Quantification of leaf (A) and petal size (B) in the indicated genotypes. Values are mean \pm SE from at least 5 leaves and 20 petals per genotype. **: significantly different from wild-type value at $p < 0.01$ (t-test).

(C) Top views of plants of the indicated genotypes.

(D, E) Quantification of petal (D) and rosette (E) size in the indicated genotypes. Individual bars represent independent transformant lines for the transgenic plants. Values are mean \pm SE from at least 15 petals and at least 6 rosettes per genotype. *, **: significantly different from *paps1-1* mutant value at $p < 0.05$ (*) or $p < 0.01$ (**). ** based on t-test with Bonferroni-correction.

Results

The three proteins PAPS1, PAPS2 and PAPS4 share highly conserved N-terminal catalytic regions, while the C-terminal domains are more divergent (Fig. S2A). We therefore asked whether the functional divergence apparent from the different mutant phenotypes was due to differences at the protein level. Introducing the *PAPS4* coding region under the control of the *pPAPS1* promoter (*pPAPS1::PAPS4*) into a *paps1-1* background did not complement the mutant phenotype (Fig. 2C-E; Fig. S2C). By contrast, when a chimeric protein consisting of the catalytic domain from PAPS4 and the C-terminal region from PAPS1 was expressed under the control of the *pPAPS1* promoter in *paps1-1* mutants (*pPAPS1::PAPS4^N-PAPS1^C*), it was able to substantially rescue the growth phenotype in leaves and particularly in flowers (Fig. 2C-E; Fig. S2C). Thus, divergence in the C-terminal domains of the proteins is responsible for functional specialization amongst the PAPS isoforms in *Arabidopsis thaliana*.

Polyadenylation of *SMALL AUXIN UP RNA* mRNAs is defective in *paps1* mutants.

To determine the molecular basis for the *paps1* mutant phenotypes, we compared transcript abundances in *paps1-1* mutant vs. wildtype leaves and flowers, using microarray hybridization. A total of 1,130 and 779 genes were misregulated more than twofold in *paps1-1* mutant leaves and flowers compared with wild type (Tables S1, S2). Two hundred sixty-one genes were misregulated in both organs, suggesting that despite a substantial overlap in the molecular phenotypes of mutant leaves and floral organs, many transcript changes were specific to one or the other organ type, potentially contributing to the different growth phenotypes. We found a significantly reduced hybridization signal for the family of *SAUR* mRNAs (29–31) from *paps1-1* mutants compared with wild type, particularly in seedlings (Fig. 3A, Fig. S3A; median and average fold-change of 0.72). This was not accompanied by a comparable misregulation of other auxinresponsive genes, such as *Aux/IAA* or *GH3* family members (Fig. 3A and S3A), indicating that the *paps1-1* mutation did not interfere with auxin response as such. Testing individual *SAUR* transcripts using quantitative RT-PCR (qRT-PCR) with oligo (dT) priming confirmed the reduced signal specifically from *paps1-1* mutants but not from *paps2-1 paps4-1* mutants (Fig. 3B). However, no such effect was observed when using random hexamers to prime the reverse transcription, with comparable or even higher signals in *paps1-1* mutants than in wild type (Fig. 3B). This suggests that the weaker signal on the microarrays and in the oligo(dT)-primed qRT-PCR was due to less efficient oligo (dT)-primed reverse transcription because of a shorter poly(A)tail, not due to reduced abundance of the tested *SAUR* mRNAs.

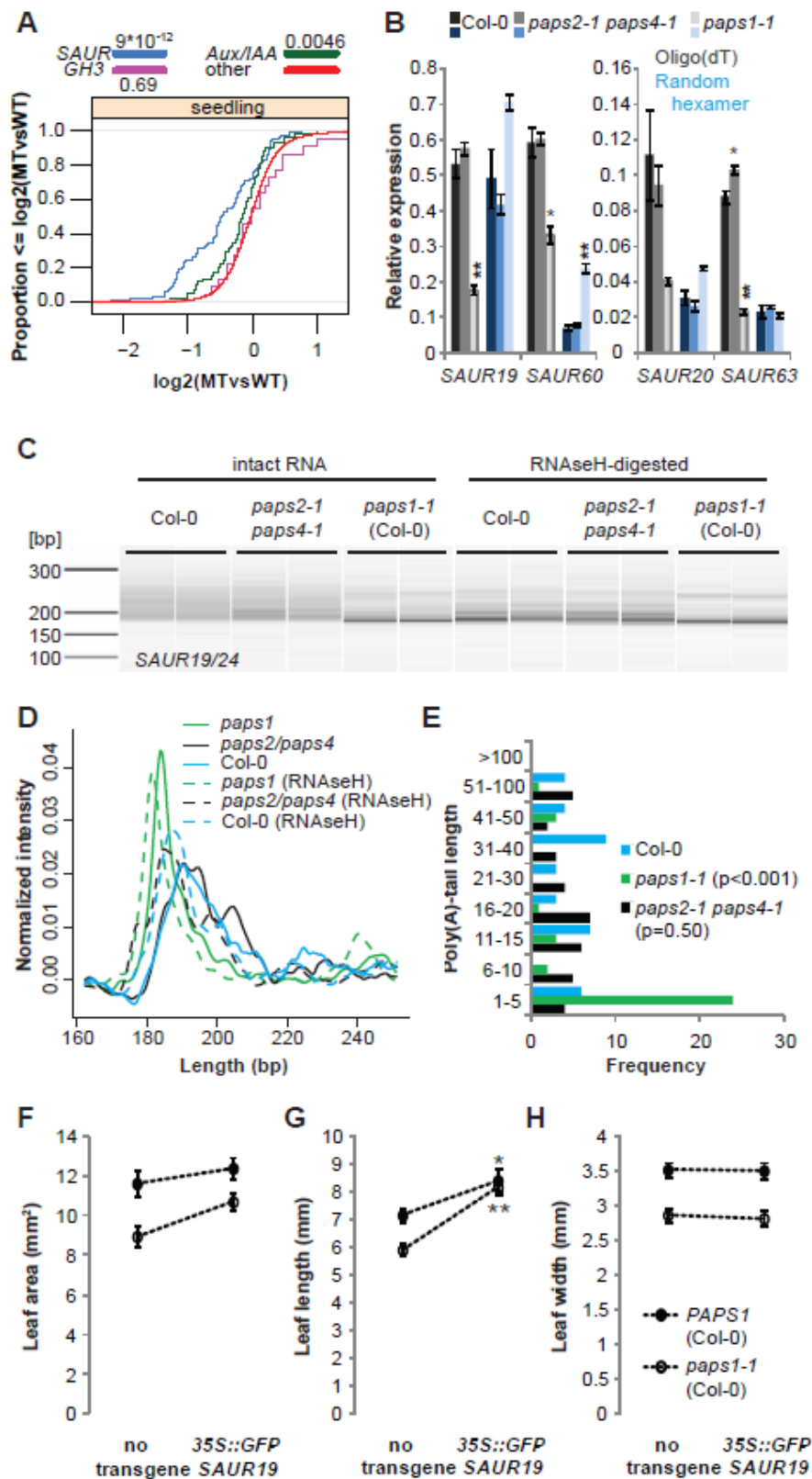


Figure 3

Results

Figure 3: Defective polyadenylation of *SAUR* mRNAs in *paps1* contributes to reduced leaf growth.

(A) Cumulative distribution plot of the expression levels of *SAUR*, *GH3* and *Aux/IAA* family members in *paps1-1* versus wild-type seedlings. Y-axis indicates the fraction of genes with a log₂-expression ratio less than or equal to the value on the X-axis. Numbers in legend are p-values of a Wilcoxon rank-sum test. "other": all remaining genes on the array.

(B) Expression of the indicated *SAUR* genes in *paps1-1* and *paps2-1 paps4-1* mutant seedlings compared to wild-type. Values from oligo(dT)-primed cDNA are shown in grey shades, those from random hexamer-primed cDNA in blue shades. Values shown are the means ±SE from three (Col-0 and *paps2-3 paps4-3*) or two (*paps1-1*) biological replicates, normalized to the constitutive reference gene *PDF2* (*AT1G13320*). Plants had been kept at 30°C for 2 h before harvesting. *: p<0.05; **: p<0.01 (Student's t-test).

(C) Bioanalyzer electropherogram of RT-PCR-amplified 3' ends of *SAUR19/24* transcripts from the indicated genotypes. Two biological replicates per genotype are shown. RNA had been left untreated (left) or poly(A)-tails had been digested with RNaseH and oligo(dT) (right) before reverse transcription.

(D) Normalized signal intensities of the PCR-products in (C). Averages of the two biological replicates per genotype are shown.

(E) Length distribution of poly(A) tails as determined by sequencing subcloned individual PCR-products from intact RNA in (C). p-values in legend are from a Wilcoxon rank-sum test.

(F-H) Leaf area (F), length (G) and width (H) of wild-type or *paps1-1* mutant plants with or without the *35S::GFP-SAUR19* transgene. *, **: significantly different from value in the absence of the transgene at p<0.05 (*) or p<0.01 (**) based on t-tests with Bonferroni correction.

To determine whether *PAPS1* activity was indeed required for polyadenylation of *SAUR* mRNAs, we compared their poly(A) tail lengths between *paps1-1* mutants and wild type using a PCR-based assay to amplify part of the coding sequence/3' UTR and the entire poly(A) tail (SI Results and Discussion). Before harvesting, seedlings were kept at 30 °C for 2 h to largely abolish the remaining activity of the temperature-sensitive mutant protein (see above). PCR products for *SAUR19/24* and *SAUR62/63/66/68* mRNAs from *paps1-1* mutants were shorter than from wild type or *paps2 paps4* double mutants (Fig. 3 C and D, Fig. S3 D and E, and SI Results and Discussion). To confirm that the different lengths of the PCR products indeed reflected a difference in poly (A) tail length and not in the choice of cleavage site, we subcloned and sequenced individual molecules. This indicated that the choice of 3' end cleavage site was not affected (Fig. S3 B and G) and confirmed the dramatic reduction in the lengths of the poly(A) tails specifically in *paps1-1* mutants but not in *paps2-1 paps4-1* plants (Fig. 3E and Fig. S3F). The median lengths of poly(A) tails determined from subcloned molecules from wildtype, *paps2-1 paps4-1*, and *paps1-1* were 22, 17, and 2 for *SAUR19/24* and 19, 20, and 2 for *SAUR62/63/66/68*, respectively. Measuring the *SAUR19/24* poly(A) tail length from nuclear RNA of wild-type and *paps1-1* inflorescences showed the same difference as seen for total RNA (Fig. S4 A–C), arguing that the shorter poly(A) tails are indeed due to defective nuclear polyadenylation, rather than faster cytoplasmic deadenylation in the mutant. The most parsimonious explanation of these results is that *SAUR* transcripts are polyadenylated directly and exclusively by the *PAPS1* isoform.

We asked whether the phenotypic rescue of the *paps1* leafgrowth defect by the chimeric *PAPS4^N-PAPS1^C* protein was mirrored at the molecular level by a rescue of the *SAUR* mRNA polyadenylation defect. The poly(A) tails on *SAUR19/24* mRNAs were longer in *paps1-1* plants expressing the chimeric

Results

PAPS4^N-PAPS1^C protein than in plants expressing PAPS4 under the control of the *pPAPS1* promoter or in nontransgenic *paps1-1* mutants, yet they did not reach the wild-type length (Fig. S4 D–F). This indicates that the divergent C-terminal domains of the PAPS proteins influence the mapping of PAPS isoforms to at least some of their presumed targets, possibly via binding to different forms of 3' end processing factors (3, 5).

Reduced SAUR activity contributes to the leaf-growth defect in *paps1* mutants.

A recent report demonstrated that the activity of the *SAUR19-24* subfamily is required for normal cell expansion in hypocotyls and leaves (31). Hypocotyls in *paps1-1* are longer than in wild type (Fig. S5A), suggesting that other expansion-promoting effects override a possibly reduced *SAUR* activity in this organ. To determine whether reduced *SAUR19-24* activity contributed to the defect in leaf growth in *paps1-1* mutants, we introduced a *35S::GFP-SAUR19* transgene with the 3' UTR of the nopaline synthase

gene (nos terminator) into the mutant background. The transgene promoted growth, especially in the leaf-length direction, in both the wild-type and the *paps1-1* mutant background; however, it had a much stronger effect in the latter, both in absolute and in relative terms (leaf length +17% in wild-type, +38% in *paps1-1* background; Fig. 3 F–H). Indeed, leaf length was indistinguishable between *35S::GFP-SAUR19* and *paps1-1; 35S::GFP-SAUR19* plants (Fig. 3G). This nonadditive effect indicates that the reduced leaf length in *paps1-1* mutants is due to lower *SAUR* activity, because otherwise the *GFP-SAUR19* transgene would be expected to have the same effect in both genetic backgrounds. The above experiment suggests that *SAUR19* protein levels are lower in *paps1-1* mutant than in wild-type leaves. However, the polyadenylation defect of *SAUR* mRNAs in *paps1* mutants does not seem to destabilize the mRNAs, as indicated by the qRT-PCR experiments on random hexamer-primed cDNA (Fig. 3B), as reported for several previous examples of stable mRNAs with very short poly(A) tails (32–34). Consistent with this, introducing the *dst2* mutant (35) into the *paps1-1* background to alleviate the inherent instability of *SAUR* mRNAs did not rescue the *paps1-1* phenotype (Fig. S5B). This suggests that in *paps1* mutants either nuclear export or translation efficiency of *SAUR* mRNAs is reduced, either of which could lead to reduced *SAUR* protein levels.

***paps1-1* mutant leaves show a constitutive pathogen response.**

To identify additional biological processes affected by the *paps1* mutation, we compared the misregulated genes to more than 600 published *A. thaliana* microarray studies using MASTA (36). This identified a strong overlap with genes affected in the *constitutive expression of pathogenesis-related genes5 (cpr5)* mutant and in response to pathogen infection and other stresses (Fig. 4A and

Results

Fig. S6A). In particular, the overlap was almost as strong with genes affected in *cpr5* vs. wild type as with genes affected in *cpr5 npr1* vs. *npr1*. This suggests that the constitutive pathogen response in *paps1-1* is independent of *NON-EXPRESSOR OF PR1 (NPR1)*, a master regulator of the SA-mediated pathogen response (Fig. 4A) (37). This in turn suggests the activation of the *ENHANCED DISEASE SUSCEPTIBILITY1 (EDS1)/PHYTOALEXIN DEFICIENT 4 (PAD4)*-dependent pathogen response in *paps1-1*, which forms part of the *cpr5* phenotype (38). The signature of a constitutive pathogen response was also evident at the single-gene level, with several classic marker genes specifically up-regulated in *paps1-1* mutant vs. wild-type leaves but not in *paps2-1 paps4-1* plants (e.g., *PR1*, *PR2*, *SID2*, and the defensins *PDF1.2b*, *PDF1.2c*, and *PDF1.4*) (Fig. 4B and Table S1).

Constitutive activation of the pathogen response results in reduced leaf growth due to reduced cell expansion (39). We therefore tested whether an *EDS1/PAD4*-dependent constitutive pathogen response contributes to the *paps1-1* phenotype. Indeed, leaf growth in the *eds1-2 paps1-1* and the *pad4-1 paps1-1* double mutants was substantially rescued (Fig. 4 C and D and Fig. S6 B and C). However, petal overgrowth was not rescued (Fig. S6D). Thus, an *EDS1/PAD4*-dependent constitutive pathogen response contributes to the reduced leaf growth but not to the petal overgrowth in *paps1* mutants. This indicates that *PAPS1*, but not *PAPS2* or *PAPS4*, negatively modulates the plant pathogen response. However, none of several pathogen-response associated genes tested (e.g., *EDS1*, *NPR1*, *PR1*, *PR2*, *SID2*, *SIZ1*, *WRKY18*), some of which are affected in the microarray analysis, showed a robust change in the lengths of their poly(A) tails.

Figure 4: Reduced leaf growth in *paps1* is partly due to an *EDS1*-dependent pathogen response.

(A) Overlap of genes misregulated in leaves of *paps1-1* mutants versus wild-type with genes misregulated in the experiments indicated. See Table S3 for an explanation of the abbreviations used.

(B) Expression of the indicated genes in *paps1-1* mutant seedlings compared to wild-type, using oligo(dT)-primed (grey shades) or random hexamer-primed cDNA (blue shades). Values shown are the means \pm SE from three biological replicates, normalized to the constitutive reference gene *PDF2 (AT1G13320)*.

(C) Quantification of leaf area in the indicated genotypes. Values shown are means \pm SE from at least three plants per genotype.

(D) Whole-plant phenotypes of the indicated genotypes.

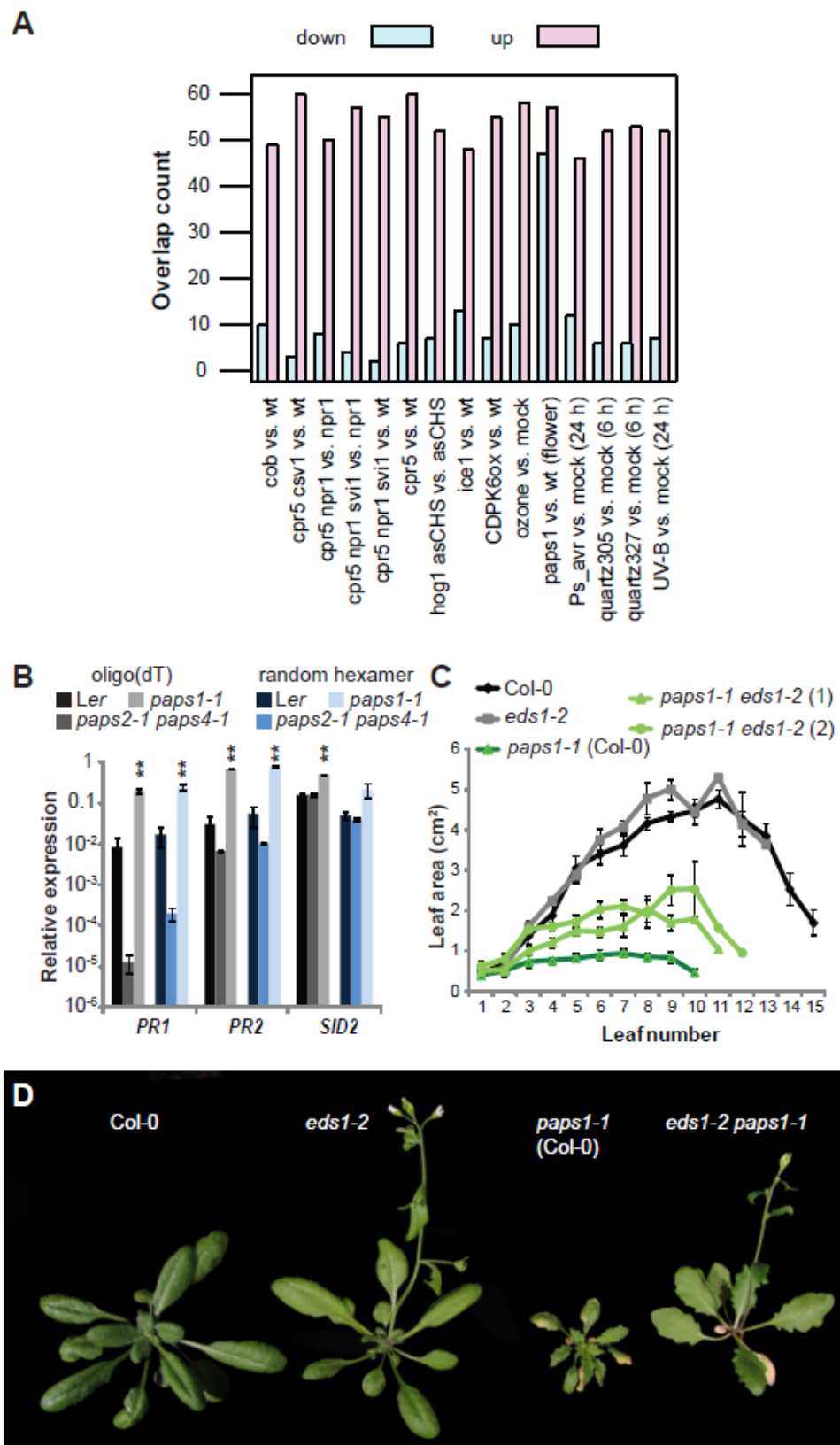


Figure 4

Functional specialization amongst PAPS isoforms provides an additional level of gene regulation

Our results demonstrate that the three canonical nuclear poly(A) polymerases in *Arabidopsis* fulfil different functions due to their divergent C-terminal domains. The very different mutant phenotypes, the results of analyzing bulk poly(A)-tail length, and the defects in polyadenylation of *SAUR* mRNAs in *paps1*, but not *paps2 paps4* mutants strongly suggest that a fraction of mRNAs is exclusively or preferentially targeted by PAPS1. As outlined in the introduction, such target specificity provides an opportunity for regulating gene expression by modulating the balance of activities amongst the PAPS isoforms. PAPS1 is phosphorylated on several residues in its C-terminal domain (<http://phosphat.mpimp-golm.mpg.de>; (40)), suggesting posttranslational modification as one way of altering PAPS1 activity. Reduced PAPS1 activity causes a constitutive pathogen response via an EDS1/PAD4-dependent mechanism. Thus, it is tempting to speculate that response to pathogen infection may be a scenario in which modulation of PAPS1 activity is used to alter the mRNA polyadenylation status and thus expression of a subset of pathogen-response factors. A genome-wide approach to determine poly(A)-tail lengths will be required to identify the pathogen-response genes whose polyadenylation depends on PAPS1 in order to conclusively test this notion. Finally, we note that as homologues to *PAPS1* and *PAPS2/PAPS4* are found throughout higher plants in phylogenetically well-supported clades (17), this mode of regulation may function broadly in higher plants.

Materials and Methods

Plant Materials and Growth Conditions. The *paps1-1* mutation was identified in an EMS-mutagenesis screen in the Landsberg erecta (Ler) background and back-crossed three times to Ler before analysis. For comparison with mutants in the Col-0 background, the *paps1-1* mutation was introgressed into Col-0 by three rounds of back-crossing. Details of T-DNA insertion lines and other mutants used can be found in SI Materials and Methods. Plant growth conditions were as described previously (41). All measurements were done with plants grown at 23 °C, unless otherwise stated. For the experiment involving the 35S::GFP-SAUR19 transgene plants were grown on 1/2 MS plates including 1% sucrose at 21 °C (day) and 14 °C (night).

Genotyping Mutant Alleles. For genotyping the *paps1-1* allele, a dCAPS marker (oSV126 and oSV166) was used. The PCR product (210 bp) from the mutated allele is cut by EcoRI. For genotyping of T-DNA insertion alleles, gene-specific primers (called LP and RP primer) that flank the T-DNA insertion site, and a T-DNA right border primer (BP) were used. These are listed in SI Materials and Methods.

Phenotypic Analysis, Measurements of Organ and Cell Sizes. Dissected organs were scanned, and their size was measured using ImageJ software (<http://rsbweb.nih.gov/ij/>). Petal-cell size was determined essentially as described previously (42). For determining cell size in leaves, leaves were fixed in FAA solution [10% (wt/vol) formaldehyde, 5% (vol/vol) acetic acid, 50% (vol/vol) ethanol], cleared with chloral hydrate, and observed using differential phase contrast. Further details can be found in SI Materials and Methods.

In Vitro Polyadenylation Assay and Measurement of Bulk Poly(A) Tail Length. Nonspecific polyadenylation assays were performed essentially as described previously (27), as was the measurement of bulk poly(A) tail lengths (43). Further details can be found in SI Materials and Methods.

Microarray Analysis. Transcriptomes of *paps1-1* mutant and wild-type seedlings and flowers (details in SI Materials and Methods) were compared using the Agilent Arabidopsis 4 × 44K oligo microarray. Two-color microarrays were normalized using the loess method (44). Differentially expressed genes were identified using the R/Bioconductor package Limma (45).

qRT-PCR and Measurements of Poly(A) Tail Length. Total RNA was prepared by the hot phenol method (46), DNase-digested, and reverse-transcribed using oligo(dT)17 or random-hexamer primers. Expression levels were analysed using a Roche LightCycler 480. Poly(A) tail length was determined using the Affymetrix Poly(A) Tail-Length Assay Kit. Details and primers used are described in SI Materials and Methods. Molecular Cloning and Plant Transformation. The floral dip

Results

transformation protocol was carried out as described previously (47). Details of molecular cloning can be found in SI Materials and Methods.

ACKNOWLEDGMENTS. We thank Isabel Bäurle, Cyril Zipfel, and members of the Lenhard laboratory for discussion; Timothy Wells, Christiane Schmidt, and Doreen Mäker for excellent plant care; and Jane Parker and Pamela Green for seeds. S.L.V was supported by the Rotation PhD program from the John Innes Centre. Work in the M.L. laboratory was supported by Deutsche Forschungsgemeinschaft Grant Le1412/3-1. D.L. and T.L. were supported by Deutsche Forschungsgemeinschaft Grant La606/13-1 and the EUINTEREG IV Upper Rhine program. W.M.G. was supported by National Institutes of Health (NIH) Grant GM067203 and National Science Foundation Grant MCB-0817205. N.R. and J.L.M. were supported by NIH Grant GM28983.

References

1. Eckmann CR, Rammelt C, & Wahle E (2011) Control of poly(A) tail length. *Wiley Interdiscip Rev RNA* 2(3):348-361.
2. Hunt AG (2008) Messenger RNA 3' end formation in plants. *Curr Top Microbiol Immunol* 326:151-177.
3. Millevoi S & Vagner S (2010) Molecular mechanisms of eukaryotic pre-mRNA 3' end processing regulation. *Nucleic Acids Res* 38(9):2757-2774.
4. Proudfoot NJ (2011) Ending the message: poly(A) signals then and now. *Genes Dev* 25(17):1770-1782.
5. Mandel CR, Bai Y, & Tong L (2008) Protein factors in pre-mRNA 3'-end processing. *Cell Mol Life Sci* 65(7-8):1099-1122.
6. Schmidt MJ & Norbury CJ (2010) Polyadenylation and beyond: emerging roles for noncanonical poly(A) polymerases. *Wiley Interdiscip Rev RNA* 1(1):142-151.
7. Lingner J, Kellermann J, & Keller W (1991) Cloning and expression of the essential gene for poly(A) polymerase from *S. cerevisiae*. *Nature* 354(6353):496-498.
8. Raabe T, Bollum FJ, & Manley JL (1991) Primary structure and expression of bovine poly(A) polymerase. *Nature* 353(6341):229-234.
9. Thuresson AC, Astrom J, Astrom A, Gronvik KO, & Virtanen A (1994) Multiple forms of poly(A) polymerases in human cells. *Proc Natl Acad Sci U S A* 91(3):979-983.
10. Juge F, Zaessinger S, Temme C, Wahle E, & Simonelig M (2002) Control of poly(A) polymerase level is essential to cytoplasmic polyadenylation and early development in *Drosophila*. *Embo J* 21(23):6603-6613.
11. Martin G & Keller W (2007) RNA-specific ribonucleotidyl transferases. *RNA* 13(11):1834-1849.
12. Topalian SL, *et al.* (2001) Identification and functional characterization of neo-poly(A) polymerase, an RNA processing enzyme overexpressed in human tumors. *Mol Cell Biol* 21(16):5614-5623.
13. Kyriakopoulou CB, Nordvang H, & Virtanen A (2001) A novel nuclear human poly(A) polymerase (PAP), PAP gamma. *J Biol Chem* 276(36):33504-33511.
14. Zhao W & Manley JL (1996) Complex alternative RNA processing generates an unexpected diversity of poly(A) polymerase isoforms. *Mol Cell Biol* 16(5):2378-2386.
15. Kashiwabara S, *et al.* (2002) Regulation of spermatogenesis by testis-specific, cytoplasmic poly(A) polymerase TPAP. *Science* 298(5600):1999-2002.

Results

16. Addepalli B, Meeks LR, Forbes KP, & Hunt AG (2004) Novel alternative splicing of mRNAs encoding poly(A) polymerases in Arabidopsis. *Biochim Biophys Acta* 1679(2):117-128.
17. Meeks LR, Addepalli B, & Hunt AG (2009) Characterization of genes encoding poly(A) polymerases in plants: evidence for duplication and functional specialization. *PLoS One* 4(11):e8082.
18. Hunt AG, *et al.* (2008) Arabidopsis mRNA polyadenylation machinery: comprehensive analysis of protein-protein interactions and gene expression profiling. *BMC Genomics* 9:220.
19. Hunt AG, Meeks LR, Forbes KP, Das Gupta J, & Mogen BD (2000) Nuclear and chloroplast poly(A) polymerases from plants share a novel biochemical property. *Biochem Biophys Res Commun* 272(1):174-181.
20. Di Giammartino DC, Nishida K, & Manley JL (2011) Mechanisms and consequences of alternative polyadenylation. *Mol Cell* 43(6):853-866.
21. Ji Z, Lee JY, Pan Z, Jiang B, & Tian B (2009) Progressive lengthening of 3' untranslated regions of mRNAs by alternative polyadenylation during mouse embryonic development. *Proc Natl Acad Sci U S A* 106(17):7028-7033.
22. Sandberg R, Neilson JR, Sarma A, Sharp PA, & Burge CB (2008) Proliferating cells express mRNAs with shortened 3' untranslated regions and fewer microRNA target sites. *Science* 320(5883):1643-1647.
23. Sherstnev A, *et al.* (2012) Direct sequencing of Arabidopsis thaliana RNA reveals patterns of cleavage and polyadenylation. *Nat Struct Mol Biol* 19(8):845-852.
24. Wu X, *et al.* (2011) Genome-wide landscape of polyadenylation in Arabidopsis provides evidence for extensive alternative polyadenylation. *Proc Natl Acad Sci U S A* 108(30):12533-12538.
25. Murata T, *et al.* (2001) The hiiragi gene encodes a poly(A) polymerase, which controls the formation of the wing margin in *Drosophila melanogaster*. *Dev Biol* 233(1):137-147.
26. Mellman DL, *et al.* (2008) A PtdIns4,5P2-regulated nuclear poly(A) polymerase controls expression of select mRNAs. *Nature* 451(7181):1013-1017.
27. Takagaki Y, Ryner LC, & Manley JL (1988) Separation and characterization of a poly(A) polymerase and a cleavage/specificity factor required for pre-mRNA polyadenylation. *Cell* 52(5):731-742.
28. Liu F, Marquardt S, Lister C, Swiezewski S, & Dean C (2010) Targeted 3' processing of antisense transcripts triggers Arabidopsis FLC chromatin silencing. *Science* 327(5961):94-97.
29. Chae K, *et al.* (2012) Arabidopsis SMALL AUXIN UP RNA63 promotes hypocotyl and stamen filament elongation. *Plant J* 71:684-697.
30. Hagen G & Guilfoyle T (2002) Auxin-responsive gene expression: genes, promoters and regulatory factors. *Plant Mol Biol* 49(3-4):373-385.
31. Spartz AK, *et al.* (2012) The SAUR19 subfamily of SMALL AUXIN UP RNA genes promote cell expansion. *Plant Journal* 70(6):978-990.
32. Meijer HA, *et al.* (2007) A novel method for poly(A) fractionation reveals a large population of mRNAs with a short poly(A) tail in mammalian cells. *Nucleic Acids Res* 35(19):e132.
33. Gu H, Das Gupta J, & Schoenberg DR (1999) The poly(A)-limiting element is a conserved cis-acting sequence that regulates poly(A) tail length on nuclear pre-mRNAs. *Proc Natl Acad Sci U S A* 96(16):8943-8948.
34. Peng J & Schoenberg DR (2005) mRNA with a <20-nt poly(A) tail imparted by the poly(A)-limiting element is translated as efficiently in vivo as long poly(A) mRNA. *RNA* 11(7):1131-1140.
35. Johnson MA, Perez-Amador MA, Lidder P, Green PJ (2000) Mutants of Arabidopsis defective in a sequence-specific mRNA degradation pathway. *Proc Natl Acad Sci USA* 97(25):13991-13996.
36. Reina-Pinto JJ, Voisin D, Teodor R, & Yephremov A (2010) Probing differentially expressed genes against a microarray database for in silico suppressor/enhancer and inhibitor/activator screens. *Plant J* 61(1):166-175.
37. Dong X (2004) NPR1, all things considered. *Curr Opin Plant Biol* 7(5):547-552.

Results

38. Clarke JD, Aarts N, Feys BJ, Dong X, & Parker JE (2001) Constitutive disease resistance requires EDS1 in the Arabidopsis mutants cpr1 and cpr6 and is partially EDS1-dependent in cpr5. *Plant J* 26(4):409-420.
39. Bowling SA, *et al.* (1994) A mutation in Arabidopsis that leads to constitutive expression of systemic acquired resistance. *Plant Cell* 6(12):1845-1857.
40. Durek P, *et al.* (2010) PhosPhAt: the Arabidopsis thaliana phosphorylation site database. An update. *Nucleic Acids Res* 38(Database issue):D828-834.
41. Disch S, *et al.* (2006) The E3 ubiquitin ligase BIG BROTHER controls Arabidopsis organ size in a dosage-dependent manner. *Curr Biol* 16(3):272-279.
42. Horiguchi G, Fujikura U, Ferjani A, Ishikawa N, & Tsukaya H (2006) Large-scale histological analysis of leaf mutants using two simple leaf observation methods: identification of novel genetic pathways governing the size and shape of leaves. *Plant J* 48(4):638-644.
43. Preker PJ, Lingner J, Minvielle-Sebastia L, & Keller W (1995) The FIP1 gene encodes a component of a yeast pre-mRNA polyadenylation factor that directly interacts with poly(A) polymerase. *Cell* 81(3):379-389.
44. Smyth GK & Speed T (2003) Normalization of cDNA microarray data. *Methods* 31(4):265-273.
45. Smyth GK (2004) Linear models and empirical Bayes methods for assessing differential expression in microarray experiments. *Statistical Applications in Genetics and Molecular Biology* 3(1):Article 3.
46. Box MS, Coustham V, Dean C, & Mylne JS (2011) Protocol: A simple phenol-based method for 96-well extraction of high quality RNA from Arabidopsis. *Plant Methods* 7:7.
47. Clough SJ & Bent AF (1998) Floral dip: a simplified method for Agrobacterium-mediated transformation of Arabidopsis thaliana. *Plant J* 16(6):735-743.
48. Johnson MA, Perez-Amador MA, Lidder P, Green PJ (2000) Mutants of Arabidopsis defective in a sequence-specific mRNA degradation pathway. *Proc Natl Acad Sci USA* 97(25):13991-13996.

SUPPORTING INFORMATION

Vi *et al.* 10.1073/pnas.1303967110

SI Figures

Figure S1: Molecular characterization of PAPS1 and transgenic complementation of the *paps1-1* mutant.

(A) Schematic representation of PAPS1 gene structure and the position of mutant alleles. The promoter is shown as a light blue arrow, 5' and 3' untranslated regions as blue rectangles, exons as beige pointed rectangles, and introns as thin black lines. The red ellipse marks the boundary between the region coding for the N-terminal catalytic domain and that coding for the C-terminal domain. The position of the *paps1-1* point mutation is indicated by the red asterisk.

(B) Multiple sequence alignment of canonical poly(A) polymerases from the indicated organisms surrounding the proline (highlighted) that is mutated in the *paps1-1* allele.

(C) Whole-plant images of the indicated genotypes demonstrating rescue of the *paps1-1* phenotype by a wild-type genomic PAPS1 fragment. (Scale bar, 2 cm.)

(D) Seedling phenotypes of the indicated genotypes grown at 23 °C or 28 °C.

(E) Coomassie-stained SDS/PAGE of purified recombinant wild-type PAPS1 protein (WT) or mutant protein encoded by the *paps1-1* allele (mut). Asterisk indicates the position of the full-length protein. Marker sizes are in kDa.

(F) Genetic interaction between *paps1-1* and *cstf64-1*. The numbers and proportions of aborted seeds are shown for the indicated genotypes.

(G) Photographs of Alexander-stained mature pollen from Ler wild-type and *paps1-1* mutant plants, as well as from a *paps1-3/+* heterozygous plant.

Results

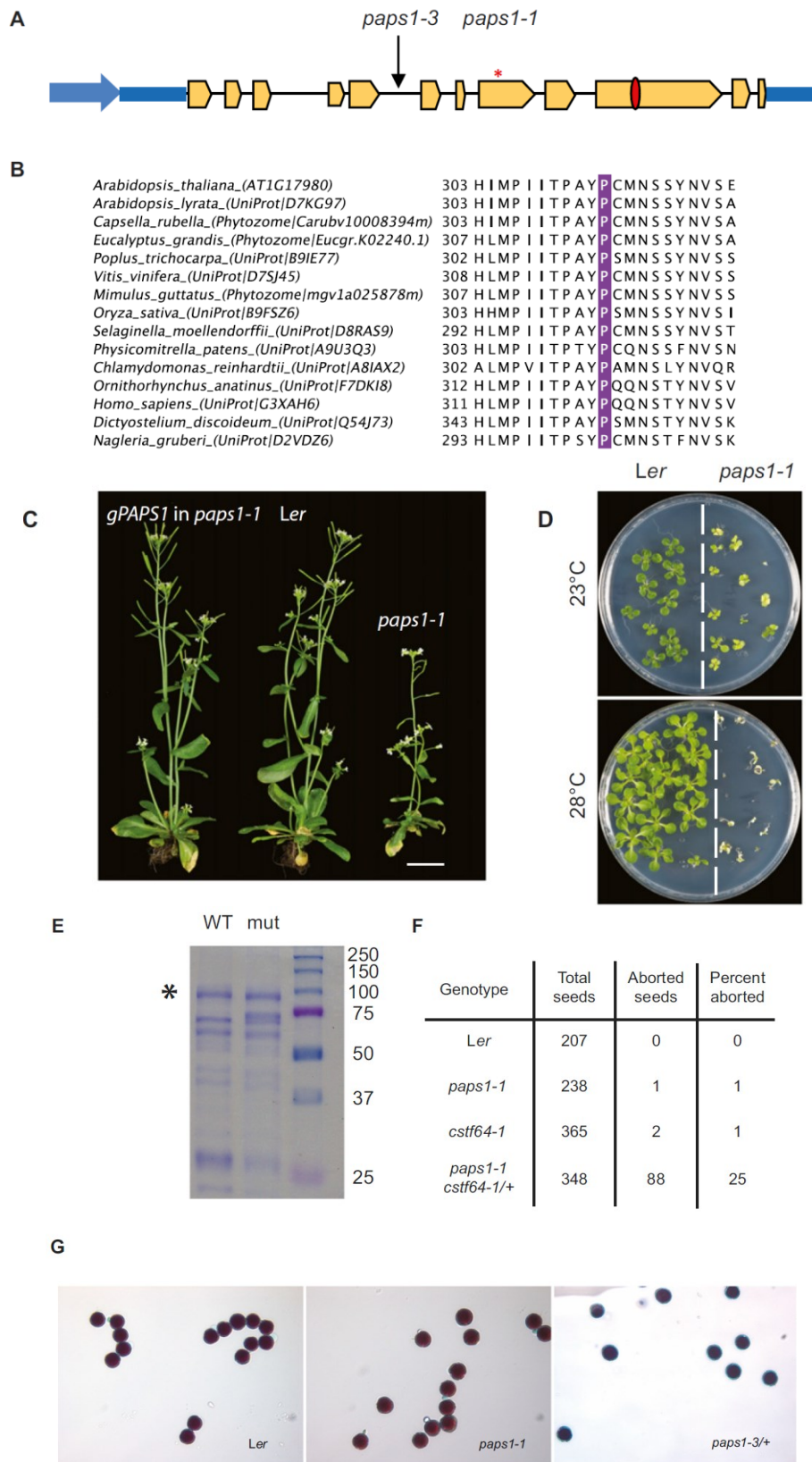


Figure S1

Results

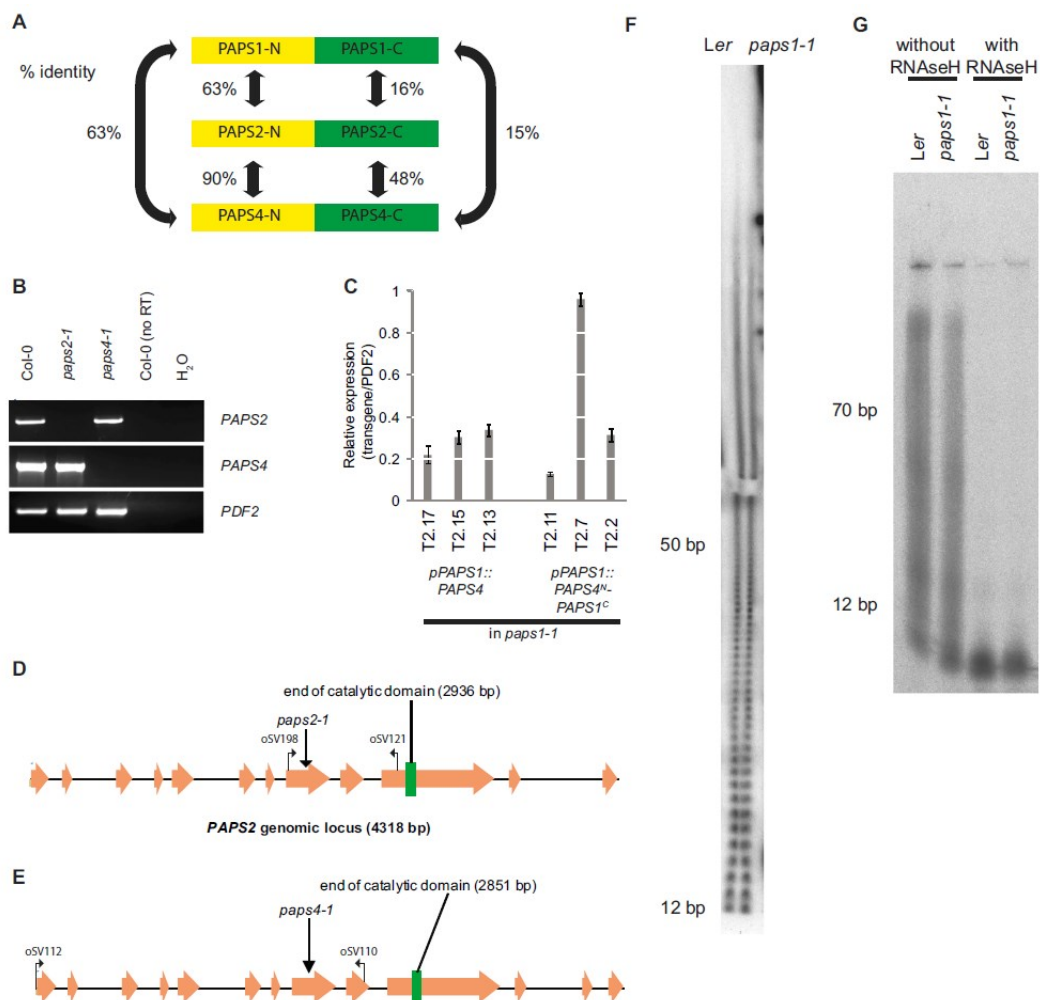


Figure S2: Molecular characterization of PAPS isoforms in *Arabidopsis thaliana*.

(A) Sequence comparison of the three nuclear PAPS proteins. Values shown are amino acid identities between the indicated protein domains.

(B) Agarose-gel electrophoresis of RT-PCR products on RNA from the indicated genotypes using primers directed against the target transcripts shown on the right.

(C) Expression of the indicated PAPS chimeric transgenes as determined by quantitative RT-PCR on RNA from three independent lines each. Primers used amplify only the chimeric transcripts which contain the 5' UTR from PAPS1 and the region coding for the N-terminal protein domain from PAPS4. Expression was normalized to that of the constitutive control gene *PDF2* (*AT1G13320*). Values shown are the means \pm SE from three technical replicates on one biological replicate of pooled inflorescences.

(D and E) Schematic representation of *PAPS2* (D) and *PAPS4* (E) gene structure and the position of mutant alleles. Beige arrows represent exons, black lines show introns. The position of primers used for the RT-PCR in B is indicated (oSV198, oSV121 for *PAPS2*; oSV110, oSV112 for *PAPS4*).

(F) Autoradiogram of radioactively labeled bulk poly(A) tails from Ler (Left) and *paps1-1* mutant seedlings (Right) grown for 11 d at 28 °C. Poly(A) tails were separated on an 8.3 M urea/10% polyacrylamide gel. Fig. S1D shows phenotypes of *paps1-1* mutant seedlings grown at 28 °C. The discontinuity at around 70 bp is due to a tear in the gel. (G) Same as F, but including control reactions treated with RNaseH/oligo(dT) before cordycepin labeling to demonstrate that the observed labeled products indeed represent poly(A) tails.

Results

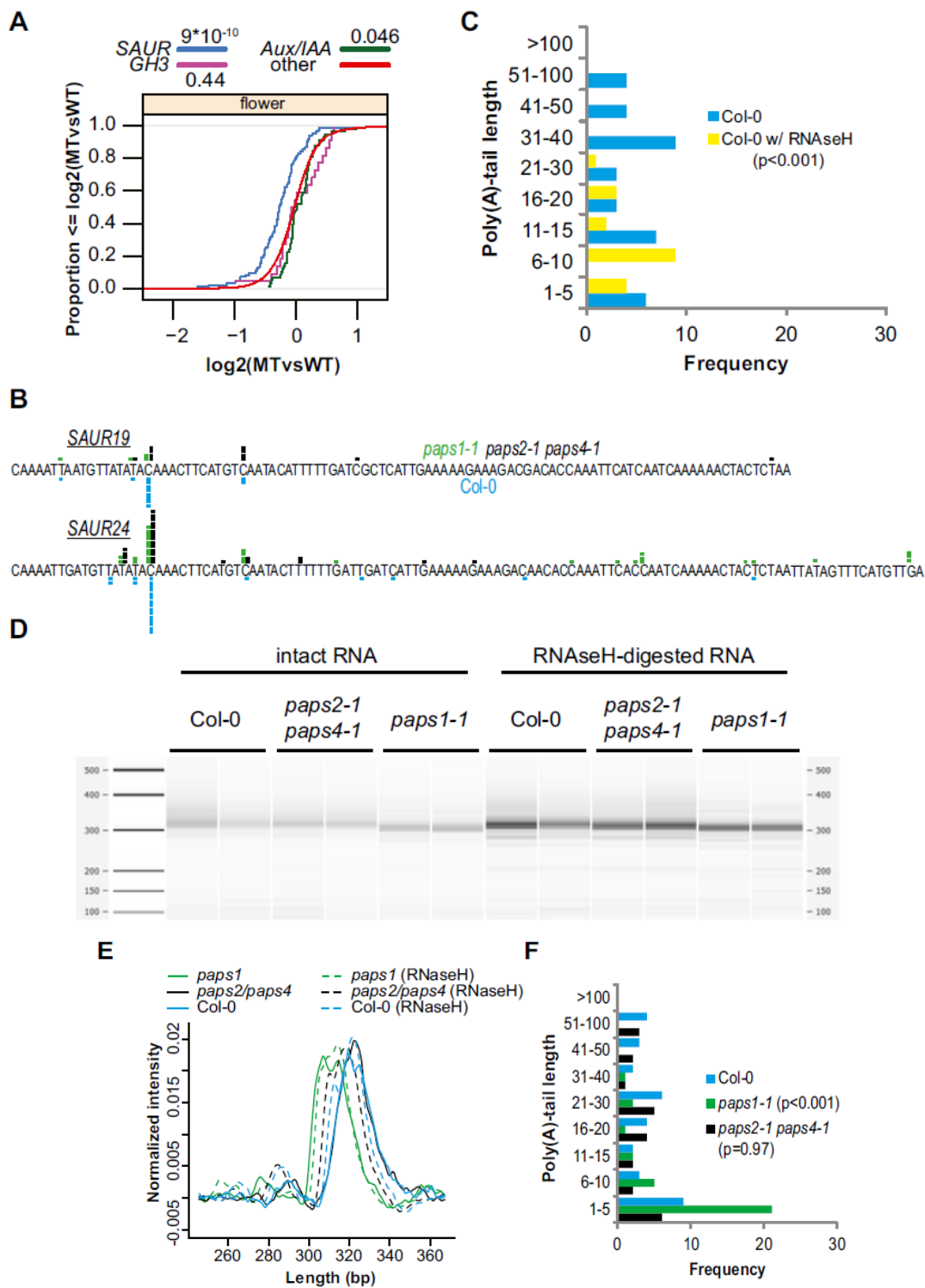


Figure S3

Figure S3 continues on the next page

Results

G

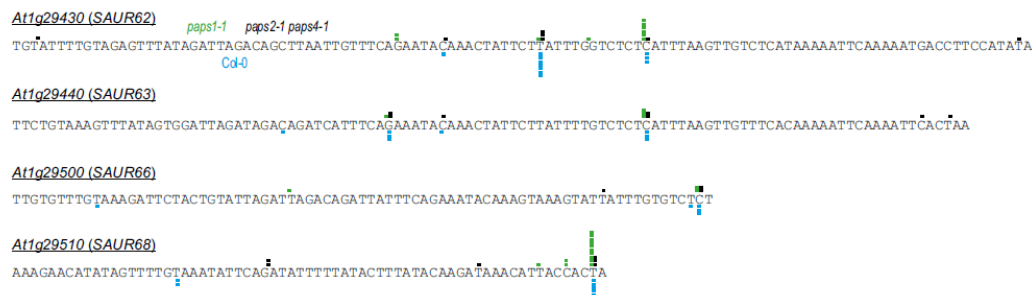


Figure S3: Polyadenylation, but not 3'-end cleavage of SAUR mRNAs, is affected in *paps1* mutants.

(A) Cumulative distribution plot of the expression levels of SAUR, GH3, and Aux/IAA family members in *paps1-1* vs. wild-type inflorescences. The y axis indicates the fraction of genes with a log₂-expression ratio less than or equal to the value on the x axis. Numbers in legends are P values of a Wilcoxon rank-sum test. "other," all remaining genes on the array.

(B) Determination of 3'-end cleavage sites of SAUR19 and SAUR24 mRNAs as determined by sequencing subcloned individual PCR products from intact RNA in Fig. 3C.

(C) Length distribution of poly(A) tails as determined by sequencing subcloned individual molecules of SAUR19/24 PCR products from intact RNA or from RNaseH/oligo (dT)-treated RNA from wild type. Data for intact RNA are the same as in Fig. 3E. The P value in the legend is from a Wilcoxon rank-sum test.

(D) Bioanalyzer electropherogram of RT-PCR-amplified 3' ends of *At1g29430/SAUR62*, *At1g29440/SAUR63*, *At1g29500/SAUR66*, and *At1g29510/SAUR68* transcripts from the indicated genotypes. Two biological replicates per genotype are shown. RNA had been left untreated (Left) or poly(A) tails had been digested with RNaseH and oligo(dT) (Right) before reverse transcription.

(E) Normalized signal intensities of the PCR products in D. Averages of the two biological replicates per genotype are shown.

(F and G) Length distribution of poly(A) tails (F) and 3'-end cleavage sites (G) as determined by sequencing subcloned individual molecules from intact RNA in D. P values in legend to F are from a Wilcoxon rank-sum test. Distance to the primer-binding site is the same for all four sequences shown in G.

Figure S4: Nuclear polyadenylation of SAUR transcripts is defective in *paps1-1* mutants, but polyadenylation is partially rescued in plants expressing the chimeric PAPS4^N-PAPS1^C protein.

(A) Bioanalyzer electropherogram of RT-PCR products against the constitutive-control gene *PDF2* on oligo(dT)-primed cDNA from nuclear RNA (Left) or total cellular RNA (Right). The primers used span two introns, and "s" indicates completely spliced products, whereas "u" marks unspliced or partially spliced products. Quantification of peak intensities shows that the ratio of unspliced/partially spliced transcript to completely spliced transcript is more than 14-fold higher in the nuclear relative to the total-RNA sample. RT, reverse transcriptase.

(B) Bioanalyzer electropherogram of RT-PCR-amplified 3' ends of SAUR19/24 transcripts from the indicated genotypes. Two biological replicates per genotype are shown. RNA had been isolated from purified nuclei (Left) or from total cellular extract (Center). (Right) Total RNA digested with RNaseH and oligo(dT) before reverse transcription was used for these reactions.

(C) Normalized signal intensities of the PCR products in B, each panel corresponding to the electropherogram shown above.

(D) Bioanalyzer electropherogram of RT-PCR-amplified 3' ends of SAUR19/24 transcripts from the indicated genotypes. Two biological replicates per genotype are shown. RNA had been left untreated (Left) or poly(A) tails had been digested with RNaseH and oligo(dT) (Right) before reverse transcription.

(E and F) Normalized signal intensities of the PCR-products in D, with intact-RNA samples in E and oligo(dT)/RNaseH-digested RNA samples in F. Averages of the two biological replicates per genotype are shown.

Results

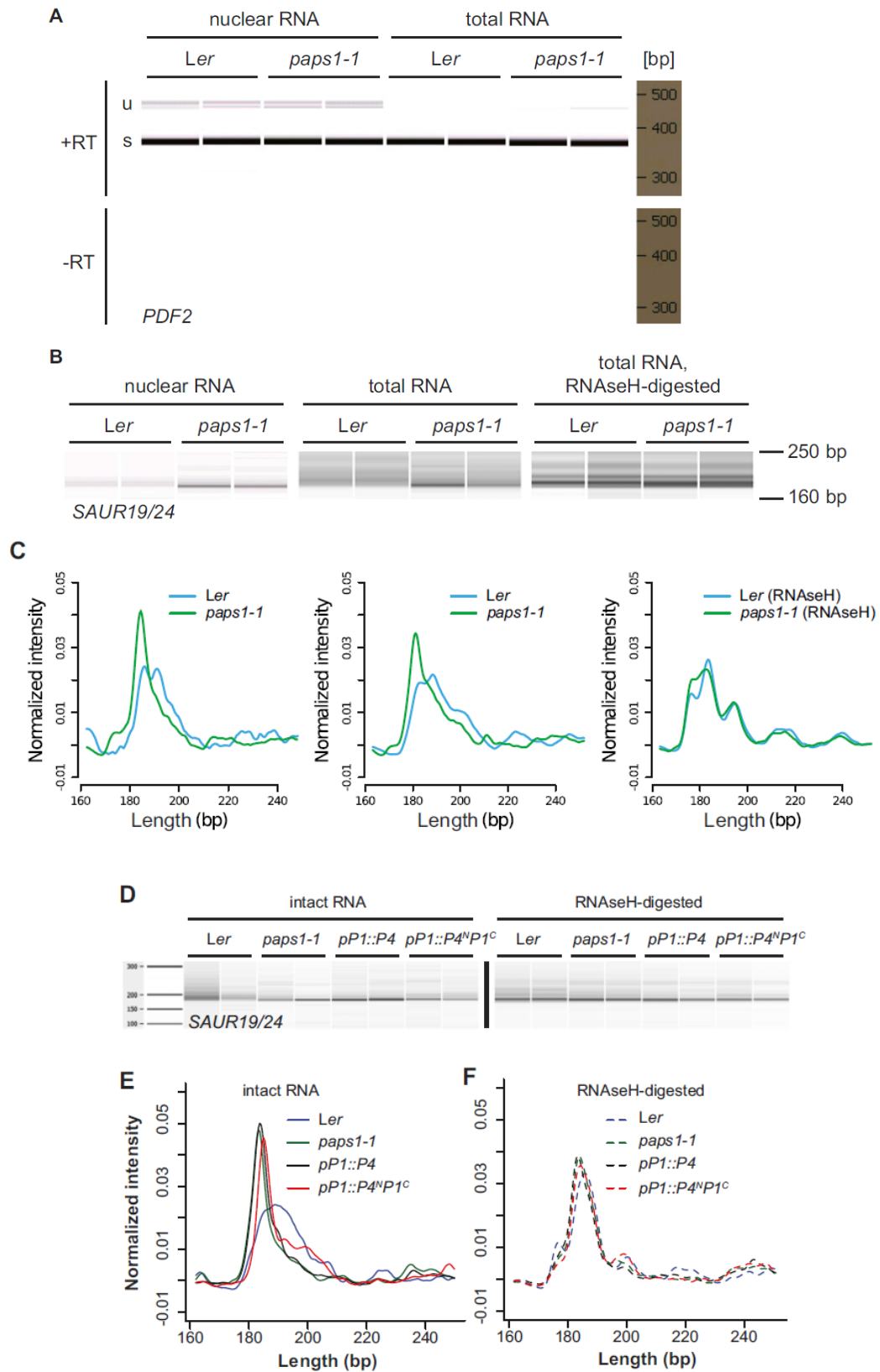


Figure S4

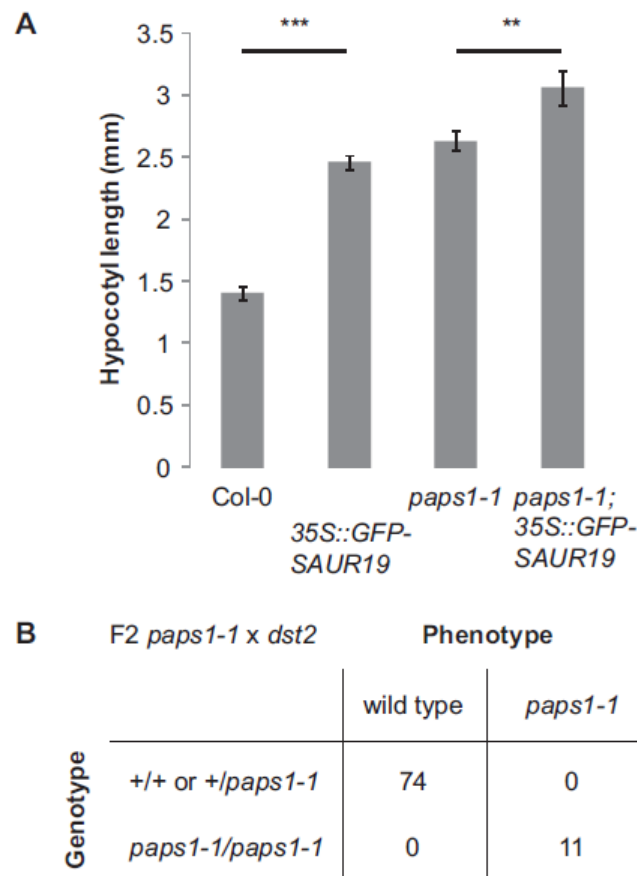


Figure S5: Interaction between PAPS1, SAUR19, and DST2.

(A) Hypocotyl lengths of light-grown seedlings from the indicated genotypes. At least 17 seedlings were measured per genotype. Asterisks (**, ***) indicate significant differences at $P < 0.01$ (**) or $P < 0.001$ (***) as determined by Student t test.

(B) Distribution of genotypes and phenotypes observed in an F2 population of a *dst2* × *paps1-1* cross. Note that no *paps1-1* homozygous mutants with a modified or rescued phenotype were found. The overrepresentation of wild-type plants at the expense of *paps1-1* mutant plants reflects bias in the selection of plants to be genotyped, based on the assumption that the double mutant might have a (partially) rescued phenotype. Genotyping for the *dst2* allele is not possible, because the gene has not been identified. Performing this analysis with *dst1* is not feasible, because *dst1* appears to be closely linked to *paps1* on chromosome I (6).

Figure S6: The constitutive pathogen response in *paps1-1* mutant leaves depends on *PAD4* activity.

(A) Overlap of genes misregulated in flowers of *paps1-1* mutants vs. wild-type with genes misregulated in the experiments indicated. Table S3 defines the abbreviations used.

(B) Whole-plant phenotypes of the indicated genotypes.

(C) Leaf area throughout the rosette from the indicated genotypes. Values shown are mean ± SE from four plants each.

(D) Petal area of the indicated genotypes. Values shown are mean ± SE from at least 22 petals from four different plants each.

Results

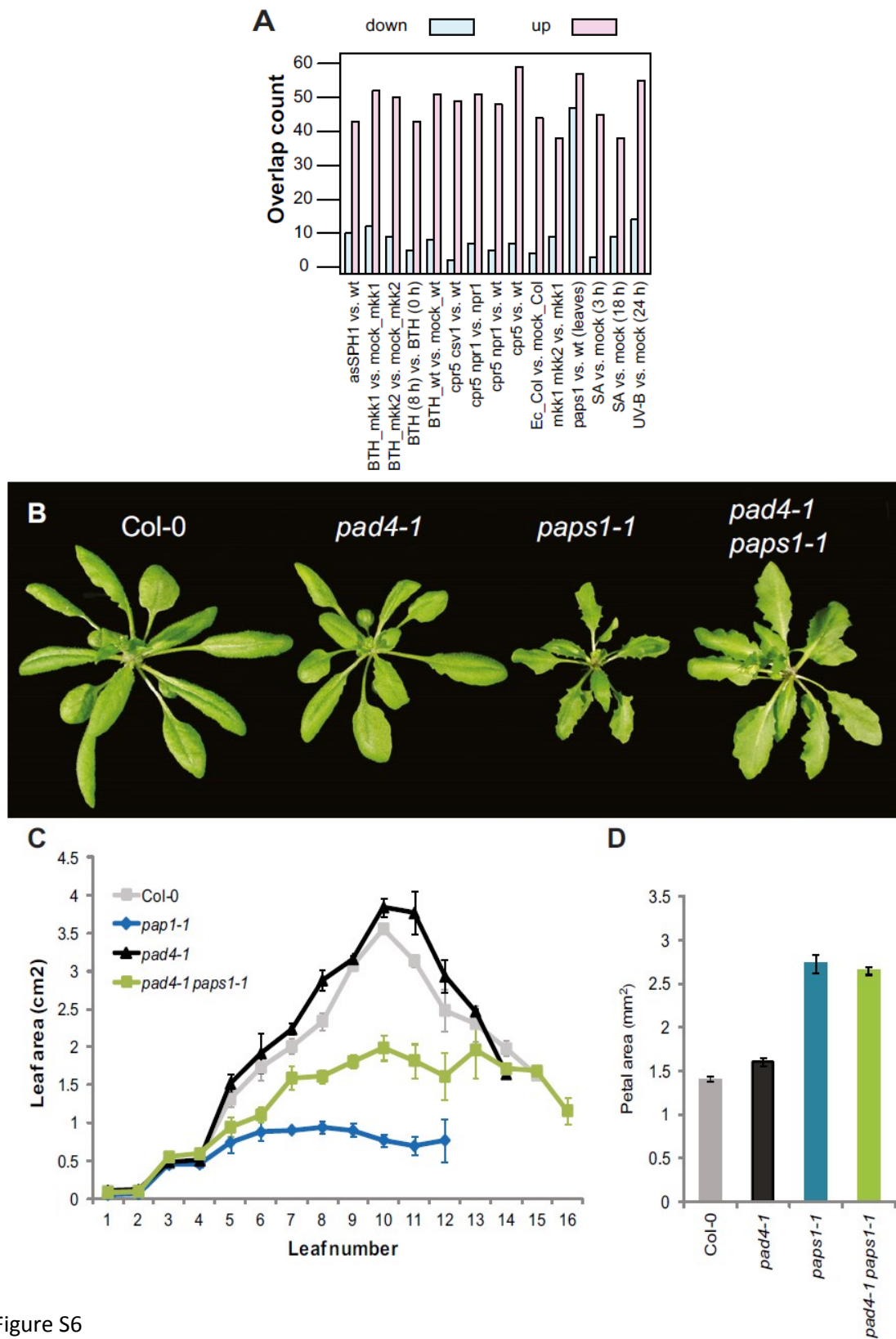


Figure S6

SI Results and Discussion

The following comments relate to the poly(A)-tail length assay. Because of the high sequence similarity between different members of the *SMALL AUXIN UP RNA (SAUR)* gene family, it was not possible to design primers that gave both efficient PCR amplification when used with the universal reverse primer from the Affymetrix poly(A) tail-length assay kit and that were able to discriminate between closely related SAUR genes. As a result, the PCR products shown in Fig. 3C and Figs. S3D and S4 B and D represent mixtures of products derived from two or four individual SAUR transcripts. When comparing the normalized-intensity profiles in Fig. 3C and Fig. S3D, it appears that even after RNaseH digestion there is still a difference between the products from the *paps1-1* mutants and the other two genotypes. This might indicate a difference in the choice of cleavage site, with a bias toward more distal sites in wild type and *paps2 paps4* mutants. However, the sequencing results shown in Fig. S3B and Fig. S3G rule out this explanation; if anything, distal sites seem to be used more frequently in *paps1-1* mutants. In addition, subcloning and sequencing individual molecules from the *SAUR19/24* PCR products on RNaseH-treated wild-type RNA indeed detected short remaining poly(A) tails (Fig. S3C). Thus, the difference seen in the RNaseH-digested samples results from incomplete digestion of the poly(A) tails by RNaseH.

SI Materials and Methods

Plant Materials. Transfer DNA (T-DNA) insertion mutants are in Col-0 background including *paps1-3* (T-DNA line WiscDsLox413-416L14), *paps2-1* (T-DNA line SALK_126395), and *paps4-1* (T-DNA line SALK_007979), and therefore Col-0 was used as wild-type control for these plants. SALK and WiscDsLox collections of T-DNA insertion mutants have been described previously (1, 2). T-DNA insertion mutants were obtained from the Nottingham *Arabidopsis* Stock Centre. For comparison with mutants in Col-0 background, the *paps1-1* allele was introgressed into the Col-0 background by three rounds of back-crossing. The *cstf64-1* mutant, the *eds1-2* mutant, the *pad4-1* mutant, and the *dst2* mutant have been described previously (3-6), as has the *35S::GFP-SAUR19* transgene (7).

Genetic Mapping and Mutant Identification. The *paps1-1* mutant in Ler background was crossed to wild-type Col-0, and a segregating F2 population was established. This was used for genetic mapping as previously described (8).

Results

Genotyping mutant alleles

The following primers were used:

Oligonucleotide name	Sequence	Description
oSV166	TAATGCCCATCATTACTCCTGCGAAT	genotype <i>paps1-1</i>
oSV126	GCTTTGTTTGATTCCATAGC	genotype <i>paps1-1</i>
oSV126	GCTTTGTTTGATTCCATAGC	genotype <i>paps1-3</i> LP primer
oSV78	TGGGACCTAGACATGCAACTAG	genotype <i>paps1-3</i> RP primer
oSV120	ACATGGAGATGTTGAACTGCC	genotype <i>paps2-3</i> LP primer
oSV121	CCACTGTTCCACGTATATCAAAC	genotype <i>paps2-3</i> RP primer
oSV110	TGCATCTGCTGCCACTATATC	genotype <i>paps4-3</i> LP primer
oSV111	TTGCTGAAGCTGTAGGGTCTG	genotype <i>paps4-3</i> RP primer
ML437	TGGTTCACGTAGTGGGCCATCG	BP primer for SALK-TDNA
oSV139	AACGTCCGCAATGTGTTATTAAGTTGTC	BP primer for Ws-TDNA

Primers used for determining gene expression in T-DNA insertion mutants were:

Oligonucleotide name	Sequence	Description
oSV198	CCTAGTATGTTGGTTTCTCGA	RT-PCR PAPS2
oSV121	CCACTGTTCCACGTATATCAAAC	RT-PCR PAPS2
oSV110	TGCATCTGCTGCCACTATATC	RT-PCR PAPS4
oSV112	CAATCGTGCCATGGTGGTGGTACTCAAAATTTAGG	RT-PCR PAPS4

Phenotypic Analysis, Measurements of Organ and Cell Sizes.

Petals were dissected from the 6th to 15th flowers and used for measurements. For leaves, the fourth and fifth leaves of plants at the bolting stage or the entire rosette were taken for measurements in all experiments except the one involving the 35S::GFPSAUR19 transgene. For the latter the first two true leaves were collected. For measuring petal-cell size, a drop of 2% (wt/vol) low-melt agarose containing 0.01% bromophenol blue prewarmed at 50 °C was placed on a prewarmed glass slide. The droplet was spread by a pipette tip to get a thin layer of agarose. A petal was immediately gently placed on it. Once the gel solidified, the petal was carefully peeled off, and the remaining gel cast was left to dry for approximately 10 min. The gel cast was then observed without a cover glass under a differential phase contrast microscope. For determining cell size in leaves, leaves were fixed in FAA solution [10% (wt/vol) formaldehyde, 5% (vol/vol) acetic acid, and 50% (vol/vol) ethanol]. The FAA solution was then replaced with chloral hydrate solution (200 g chloral hydrate, 20 g glycerol, and 50 mL distilled water), and the tube was incubated overnight.

Results

Samples were mounted on a glass slide and observed under a differential phase contrast microscope.

Alexander Staining of Pollen. Mature pollen was mounted in Alexander's stain (9) and observed under a light microscope with 20× magnification after incubating for 15 min.

In Vitro Polyadenylation Assay. Reaction mixtures contained 2.5% (wt/vol) polyvinyl alcohol, 1 mM MnCl₂, 100 ng BSA, 1 mM ATP, 0.5 U RNasin, 10 mM Hepes (pH 7.9), 25 mM NH₄(SO₄)₂, 0.2 mM PMSF, and 0.2 mM DTT, and the indicated amounts of protein (wild type or mutant). Reaction mixtures were incubated for 30 min at room temperature, followed by proteinase K treatment, phenol/chloroform extraction, ethanol precipitation, and separation on 6% (wt/vol) urea-acrylamide gels. The constructs pSV11b (pET28a-PAPS1cDNA-wt) and pSV11d (pET28a_cDNAPAPS1-P313S-mutated; see below) were used for expressing the proteins. These were purified using Ni-NTA agarose.

Measurement of Bulk Poly(A) Tail Length. The protocol was adapted from ref. 10. RNA samples [2 µg, either untreated or digested with RNaseH/oligo(dT); see below] were 3'-end-labeled with 10 µCi ³²P-cordycepin using 5 U of yeast poly(A) polymerase. The reaction (10 µL) was incubated at 37 °C for 20 min, followed by heat inactivation at 70 °C for 10 min. The sample was then subjected to RNase treatment in a volume of 80 µL consisting of 10 mM Tris-HCl (pH 8), 300 mM NaCl, 5 µg RNaseA, and 125 U RNase T1 for 60 min at 37 °C. The RNase treatment was stopped in a volume of 100 µL consisting of 100 µg Proteinase K, 0.5% SDS, and 10 mM EDTA and incubated for 30 min at 37 °C. The reaction volume was then adjusted to 200 µL with the addition of 52 µg tRNA, 125 µg glycogen, ammonium acetate (to a final concentration of 2.5 M), and magnesium chloride (to a final concentration of 15 mM) and water. The RNA [poly(A) tails] were precipitated by adding 2.5 volumes of ice-cold ethanol and centrifuging for 1 h at 13,000 × g at 8 °C. The pellet was washed with ice-cold 80% (vol/vol) ethanol and allowed to dry at room temperature. The dried pellet was resuspended in 10 µL of loading buffer [94% (vol/vol) formamide, 20 mM EDTA, 0.2% bromophenol blue, and 0.2% xylene cyanol]. The poly(A) tails were then separated by electrophoresis on a 8.3 M urea/10% (wt/vol) polyacrylamide gel and visualized using autoradiography on a Typhoon phosphorimager.

Microarray Analysis. All plants were grown at 21 °C. For inflorescence collection, main inflorescences excluding the open flowers/buds were collected from 30-d-old plants grown on soil. Plants at the stage of harvest had approximately 7–12 siliques (wild type) or 2–5 siliques (mutant). Plants were grown in long day conditions, and material was collected at 5–7 h after the light period starts. Whole seedlings including roots were harvested from 11-d-old (mutant) or 9-d-old (wild type) plants grown on MS plates. The different ages were used to ensure that the first true leaves were at a comparable developmental stage. Plants were grown in long day conditions, and material was

Results

collected at 5–7 h after the light period starts. Total RNA was prepared by the hot phenol method (11) and cleaned up with the Qiagen RNeasy Kit, digested with TURBO Dnase (Ambion). Subsequent labeling and array hybridization were carried out by CRX Biosciences Ltd. A two-color array platform was used: Agilent Arabidopsis 4 × 44K oligo microarray and Agilent 4 × 44K gasket slides. One microgram of total RNA samples was used for labeling with the Quick Amp Labeling Kit–Two Color using the manufacturer’s protocols. Differentially expressed genes were identified using the R/Bioconductor package Limma (12). Background correction was done by subtracting background intensities and then setting zero or negative intensities to half the minimum of the positive ones. Two-color microarrays were normalized using the loess method (13).

qRT-PCR and measurements of polyA-tail length

Primers used for qRT-PCR are listed below.

Gene name	AGI code	Primer sequences	
SAUR19	AT5G18010	fw	ATTTGGTGCCGCTCTCATAC
		rev	TTCATTGGAGCCGAGAAGTC
SAUR20	AT5G18020	fw	CCAAAAGGGTTTCTTGCACT
		rev	CATCGTTGGAACCGAGAAGT
SAUR60	AT4G38860	fw	GTGCAAGCCACCACTTATCA
		rev	CGGACTAAAACCTGTAAGATCCA
SAUR63	AT1G29440	fw	AGATTTCCGGTCTCCCAACG
		rev	TGGTTGAAAAGAGCATCTAGCA
PDF2	At1g13320	fw	GCATTTCACTCCTCTGGCTAAG
		rev	GGCACTTGGGTATGCAATATG
PR1	AT2G14610	fw	TGTGCCAAAGTGAGGTGTAAC
		rev	TGATGCTCCTTATTGAAATACTGATAC
PR2	AT3G57260	fw	GGTGTCCGAGACCGGTTGGC
		rev	CCCTGGCCTTCTCGGTGATCCA
SID2	AT1G74710	fw	TGAAGCAACAACATCTCTACAGGCG
		rev	CCCGAAAAGGCTCGGCCCAT

For poly(A) tail measurement, RNAs were isolated as described before. To eliminate the activity of the temperature-sensitive protein encoded by the *paps1-1* allele as far as possible, plants were shifted to 30 °C for 2 h before harvesting. Poly(A) tail length was determined using the Affymetrix Poly(A) Tail- Length Assay Kit according to the manufacturer’s instructions, using primers detailed below. PCR products from the poly(A) tail-length assays were analysed on an Agilent 2100 Bioanalyzer. PCR products of *SAUR19/24* and *SAUR62/63/66/68* were subcloned and Sanger-sequenced. Obtained sequencing results were compared with the Arabidopsis genome. Oligod(T)17/RNaseH digestion was performed as follows: 20 µg of DNase-digested RNA was mixed with 3.2 µL oligod (T)17, 10 µL 10× RNaseH buffer, 0.4 µL RNaseH (NEB), and 79.4 µL water and incubated for 1 h at 37 °C. Before G/I Tailing, RNA was precipitated adding 0.1 vol 3 M NaAc, 1 vol Isopropanol, incubated at –20 °C for a

Results

minimum of 30 min, centrifuged, washed with 70% (vol/vol) ethanol, dried, and dissolved in 10–15 μ L water. The following primers were used for poly(A) tail (PAT) tests. As discussed above, these primers amplify two to four very closely related transcripts when used in PAT assays.

At1g29440 (SAUR63)	AACGGAAGGACCAATCACATT
At5g18010 (SAUR19)	GGCTCCAATGAAGATGATCCAACATTT

Nuclei Isolation. Nuclei were isolated from Ler wild-type and *paps1-1* mutant inflorescences that had been treated at 30 °C for 2 h, following the procedure from ref. 14. Enrichment of nuclei was determined by RT-PCR against PDF2, using the above primers that span two introns. As seen in Fig. S4A, there is a strong enrichment of unspliced or partially spliced transcripts in the nuclear RNA compared with total RNA. When quantified using the Bioanalyzer, the ratio of unspliced/partially spliced to completely spliced transcripts is more than 14-fold higher in the nuclear RNA sample than in total RNA.

Molecular Cloning. Complementation of *paps1-1* mutants. A genomic fragment of PAPS1 (5,877 bp) was isolated from a TAC clone and ligated into the binary vector for plant transformation. TAC JAtY72B09 (15) containing the PAPS1 locus was digested with XbaI, and the fragment around 5.8 kb was gel-purified and ligated into ML939 (a modified form of pBluescript) using the XbaI site to create plasmid pSV1. All plasmids were verified by partial sequencing and restriction enzyme digestion. The PAPS1 locus was released from pSV1 by digesting with AscI and ligated into binary vector ML1297 [a derivative of pGPTV-BAR (16)] using the AscI site. The resulting plasmid (pSV2) was transformed into *Agrobacterium* strain GV3101, which was used to transform *paps1-1* mutants.

Promoter swap pPAPS1::genomicPAPS4 experiment. The genomic PAPS4 fragment was isolated from TAC clone JAt49G10 by NcoI digestion and gel-purification of the 9,906-bp fragment. The fragment was ligated into ML939 using the NcoI site to create pSV5a (ML939-NcoI_gPAPS4_NcoI). An NcoI site was introduced at the ATG start codon of gPAPS4 by overlap PCR using primer oSV106, oSV107, oSV112, and oSV113. The PCR product was ligated into pSV5a using PmeI and XhoI sites to create pSV5b (ML939_SDM_NcoI at ATG_gPAPS4_NcoI). An NcoI site was introduced at the ATG start codon of gPAPS1 in pSV1 by overlap PCR using primer oSV104, oSV105, oSV91, and oSV101. The PCR product was ligated into pSV1 using ClaI and BstEII sites to create pSV5c (pSV1_SDM_NcoI at ATG_gPAPS1). The genomic PAPS4 fragment starting at the ATG start codon was released from pSV5b by digesting with NcoI and ligated into pSV5c digested with NcoI to give pSV5d (ML939-pPAPS1:: ATGgPAPS4-PAPS4UTR3'). The pPAPS1::genomicPAPS4 fragment was released from pSV5d by digesting with AscI and ligated into the AscI site of pBarMAP [a derivative of pGPTV-BAR (16)] to

Results

create pSV5e (pBarMAP/Ascl/pPAPS1UTR5::ATGgPAPS4-PAPS4UTR3'). This plasmid pSV5e was used to transform *paps1-1* mutants.

Chimeric construct pPAPS1::NPAPS4::CPAPS1. A *StuI* site was introduced into the genomic PAPS1 fragment in pSV5c at the nucleotide that encodes the start of the C-terminal domain of the PAPS1 protein by overlap PCR using primer oSV202, oSV203, oSV102, and oSV103. The PCR product was ligated into pSV5c (pSV1_SDM_NcoI at ATG_gPAPS1) using *PmeI* and *Bsp1407I* sites to create pSV12 (pSV1_SDM_NcoI at ATG_gNPAPS1-*StuI*-gCPAPS1). The *StuI/PstI* fragment from pSV12 (containing the C-terminal coding region of the PAPS1 protein) was ligated into the *StuI/PstI*-digested vector pSV5d (containing the pPAPS1::gPAPS4-N-terminal coding region) to create pSV14 (pPAPS1::UTR5PAPS1:: NPAPS4::CtermPAPS1). The fragment containing the chimeric construct was released from pSV14 by digesting with *Ascl* and was ligated into the *Ascl* site of pBarMAP to create pSV15 pBarMAP/Ascl/pPAPS1::UTR5PAPS1::ATGNPAPS4-CtermPAPS1 (all genomic)]. This plasmid pSV15 was used to transform *paps1-1* mutants. With this cloning procedure, the amino acid sequence at the junction between the N and C terminus of the resulting chimeric protein was FVFPNGYRRPSHT, whereas the original sequence at corresponding position for PAPS1 is FVFPNGYRRPSHT and for PAPS4 is FVFPNGYRRPRQSRH.

Constructs for expression of PAPS1 proteins in Escherichia coli. The fulllength PAPS1 coding region, amplified from cDNA of either wild-type or mutated *paps1-1* plants, were subcloned into pET28a (Novagen) between *NdeI* and *EcoRI* site. This results in a translational fusion of the His-tag to the N terminus of PAPS1. The resulting plasmids pSV11b (pET28a-PAPS1cDNA-wt) and pSV11d (pET28a_cDNAPAPS1-P313S-mutated) were verified by DNA sequencing. Primers used for cloning:

Primer	Name	Sequence
oSV102	At1g17980_exon10R	ACTGCTTCATAAGGGAAAGGAG
oSV103	At1g17980_exon10F	GCAGAAGGCGAGCAATTCGA
oSV106	At4g32850_1R	CACACAAAGTATCAATGTCAG
oSV107	At4g32850_2F	GTCAAGCTAATGTATAGATCG
oSV112	At4g32850_ATGNcoIF	CAATCGTGCCATGGTGGTGGGTA CTCAA AATTTAGG
oSV113	At4g32850_AtGNcoIR	GTACCCACCACCATGGCAGCATTGATAATCCTAAGC
oSV202	<i>StuI</i> _PAP1_F	GAGTTAGACCTAGGCCTTACATACCTCTAAAGGAACATG
oSV203	<i>StuI</i> _PAP1_R	AGAGGTATGTGAAGGCCTAGGTCTAACTCCACCAGGAAAC

Table S1 is attached as electronic file on a CD.

Table S2 is attached as electronic file on a CD.

Table S3 is attached as electronic file on a CD.

Results

1. Alonso JM, et al. (2003) Genome-wide insertional mutagenesis of *Arabidopsis thaliana*. *Science* 301(5633):653–657.
2. Woody ST, Austin-Phillips S, Amasino RM, Krysan PJ (2007) The WiscDsLox T-DNA collection: An *Arabidopsis* community resource generated by using an improved highthroughput T-DNA sequencing pipeline. *J Plant Res* 120(1):157–165.
3. Liu F, Marquardt S, Lister C, Swiezewski S, Dean C (2010) Targeted 3' processing of antisense transcripts triggers *Arabidopsis* FLC chromatin silencing. *Science* 327(5961):94–97.
4. Aarts N, et al. (1998) Different requirements for EDS1 and NDR1 by disease resistance genes define at least two R gene-mediated signaling pathways in *Arabidopsis*. *Proc Natl Acad Sci USA* 95(17):10306–10311.
5. Glazebrook J, Rogers EE, Ausubel FM (1996) Isolation of *Arabidopsis* mutants with enhanced disease susceptibility by direct screening. *Genetics* 143(2):973–982.
6. Johnson MA, Perez-Amador MA, Lidder P, Green PJ (2000) Mutants of *Arabidopsis* defective in a sequence-specific mRNA degradation pathway. *Proc Natl Acad Sci USA* 97(25):13991–13996.
7. Spartz AK, et al. (2012) The SAUR19 subfamily of SMALL AUXIN UP RNA genes promote cell expansion. *Plant J* 70(6):978–990.
8. Disch S, et al. (2006) The E3 ubiquitin ligase BIG BROTHER controls *Arabidopsis* organ size in a dosage-dependent manner. *Curr Biol* 16(3):272–279.
9. Alexander MP (1969) Differential staining of aborted and nonaborted pollen. *Stain Technol* 44(3):117–122.
10. Preker PJ, Lingner J, Minvielle-Sebastia L, Keller W (1995) The FIP1 gene encodes a component of a yeast pre-mRNA polyadenylation factor that directly interacts with poly(A) polymerase. *Cell* 81(3):379–389.
11. Box MS, Coustham V, Dean C, Mylne JS (2011) Protocol: A simple phenol-based method for 96-well extraction of high quality RNA from *Arabidopsis*. *Plant Methods* 7:7.
12. Smyth GK (2004) Linear models and empirical Bayes methods for assessing differential expression in microarray experiments. *Stat Appl Genet Mol Biol* 3(1):Article 3.
13. Smyth GK, Speed T (2003) Normalization of cDNA microarray data. *Methods* 31(4):265–273.
14. Park MY, Wu G, Gonzalez-Sulser A, Vaucheret H, Poethig RS (2005) Nuclear processing and export of microRNAs in *Arabidopsis*. *Proc Natl Acad Sci USA* 102(10):3691–3696.
15. Knee EM, Rivero L, Crist D, Grotewold E, Scholl R (2011) Germplasm and Molecular Resources. *Genetics and Genomics of the Brassicaceae, Plant Genetics and Genomics: Crops and Models*, eds Schmidt R, Bancroft I (Springer, New York), pp 437–468.
16. Becker D, Kemper E, Schell J, Masterson R (1992) New plant binary vectors with selectable markers located proximal to the left T-DNA border. *Plant Mol Biol* 20(6):1195–1197.

2.2. Arabidopsis poly(A) polymerase PAPS1 limits founder-cell recruitment to organ primordia and suppresses the salicylic acid-independent pathogen response downstream of EDS1/PAD4

The content of this chapter resembles largely the following publication:

Trost G, Vi LS, Czesnick H, Lange P, Holton N, Giavalisco P, Zipfel C, Kappel C, Lenhard M (2013) Arabidopsis poly(A) polymerase PAPS1 limits founder-cell recruitment to organ primordia and suppresses the salicylic acid-independent immune response downstream of EDS1/PAD4. *Plant J Early View* (Online Version of Record published before inclusion in an issue)

The Plant Journal; Vol.77 Issue 5; Pages: 688-699

doi: 10.1111/tpj.12421

Following Experiments and corresponding evaluation within this manuscript were done by myself:

Fig. 2B, 2C, 2D

Fig. 4C

Fig. 5A, 5B, 5C, 5D

Fig. 6A, 6B, 6C, 6D

Fig. 7B

Fig. S2

Fig. S3

The manuscript was written by myself.

Results

Arabidopsis poly(A) polymerase PAPS1 limits founder-cell recruitment to organ primordia and suppresses the salicylic acid-independent immune response downstream of EDS1/PAD4

Gerda Trost¹, Son Lang Vi^{1,2,†}, Hjördis Czesnick¹, Peggy Lange¹, Nick Holton³, Patrick Gialvalisco⁴, Cyril Zipfel³, Christian Kappel¹ and Michael Lenhard^{1,#}

¹ Institut für Biochemie und Biologie, Universität Potsdam, Karl-Liebknecht-Str. 24-25, 14476 Potsdam, Germany.

² John Innes Centre, Cell & Developmental Biology, Norwich Research Park, Norwich, NR4 7UH, UK.

³ The Sainsbury Laboratory, Norwich Research Park, Norwich, NR4 7UH, UK.

⁴ Max Planck Institut für molekulare Pflanzenphysiologie (MPI-MP), Wissenschaftspark Golm, Am Mühlenberg 1, 14476 Potsdam

[†] present address: Cold Spring Harbor Laboratory, 1 Bungtown Road, Cold Spring Harbor, NY 11724, USA.

author for correspondence:

telephone: +49-331-9775580

telefax: +49-331-9775522

email: michael.lenhard@uni-potsdam.de

Running title: *PAPS1* function in development and immune response

Keywords: Polyadenylation, poly(A) polymerase, organ growth, founder-cell recruitment, clonal analysis, immune response, salicylic acid, *Arabidopsis thaliana*

Results

Summary

Polyadenylation of pre-mRNAs by poly(A) polymerase (PAPS) is a critical process in eukaryotic gene expression. Like in vertebrates, plant genomes encode several isoforms of canonical nuclear PAPS enzymes. In *Arabidopsis thaliana* these isoforms are functionally specialized, with *PAPS1* affecting both organ growth and immune response, at least in part by the preferential polyadenylation of subsets of pre-mRNAs. Here, we demonstrate that the opposite effects of *PAPS1* on leaf and flower growth reflect the different identities of these organs, identifying a role for *PAPS1* in the elusive connection between organ-identity control and growth regulation. The overgrowth of *paps1* mutant petals is due to increased recruitment of founder cells into early organ primordia, suggesting that *PAPS1* activity plays unique roles influencing organ growth. By contrast, the leaf phenotype of *paps1* mutants is dominated by a constitutive immune response that leads to increased resistance to the biotrophic oomycete *Hyaloperonospora arabidopsidis* and reflects activation of the salicylic acid-independent signalling pathway downstream of ENHANCED DISEASE SUSCEPTIBILITY1 (EDS1)/PHYTOALEXIN DEFICIENT4 (PAD4). These findings provide insight into the developmental and physiological basis of the functional specialization amongst plant PAPS isoforms.

Introduction

The poly(A) tail at the 3' end is an essential feature of virtually all eukaryotic mRNAs that has various important biological functions, including the export of the mRNA from the nucleus, protection from degradation in the cytoplasm and efficient initiation of translation (Hunt 2008, Eckmann *et al.*, 2011). After transcription by polymerase II the addition of the poly(A) tail is catalyzed by the multienzymatic 3'-end processing complex. Because of its general importance, 3' end processing has been studied extensively in yeast, animals and plants (for a detailed review on eukaryotic pre-mRNA 3'-end processing see (Millevoi and Vagner 2010)). After cleavage by other subunits of the complex, the actual addition of the poly(A) tail is catalyzed by canonical poly(A) polymerases (cPAPS) (Mandel *et al.*, 2008; Schmidt and Norbury 2010). Some of the components of the 3'-end processing complex are encoded by small gene families, while others are present as single-copy genes. Strong loss-of-function mutations of 3'-end processing factors in *A. thaliana* are frequently lethal, especially when the factor in question is only encoded by one gene (Hunt 2008; Tsukaya *et al.*, 2013). However, there are also examples of weak mutations or ones disrupting only one member of a small gene family that lead to viable plants with more or less pleiotropic phenotypes (Simpson *et al.*, 2003; Herr *et al.*, 2006; Zhang *et al.*, 2008); these phenotypes likely reflect the aberrant 3'-end processing of critical, dosage-sensitive mRNAs, such as the one coding for the central floral repressor *FLOWERING LOCUS C* (Liu *et al.*, 2010). In the model plant *Arabidopsis thaliana* (*Arabidopsis* hereafter), three canonical nuclear poly(A) polymerases are encoded in the genome that share a highly conserved N-terminal catalytic domain, but differ in their C-terminal domains (Addepalli *et al.*, 2004; Meeks *et al.*, 2009). Mutant analysis has recently uncovered functional specificity amongst these three poly(A) polymerases PAPS1, PAPS2 and PAPS4 (Vi *et al.*, 2013). While *paps2 paps4* double mutants are viable with normal leaf and flower growth, a strong loss-of-function mutation in *PAPS1* leads to non-functional male gametophytes, and a weak allele displays reduced leaf, but enhanced flower size. PAPS1 is specifically required for normal polyadenylation of *SMALL AUXIN UP RNA (SAUR)* mRNAs, and reduced *SAUR* activity contributes to the reduced cell expansion and leaf growth in *paps1* mutants. Thus, there appears to be a subpopulation of pre-mRNAs in *Arabidopsis* that is only efficiently polyadenylated by PAPS1, and defective processing of these transcripts likely causes the phenotypes seen in the mutants. Such target specificity can introduce an additional layer of regulation in plant gene expression. The growth phenotype of *paps1* mutants with its opposite changes to leaf and floral-organ growth touches on a central, yet poorly understood problem in plant developmental biology, the link between organ identity and growth control. Mutant analysis has indicated that a common set of regulators controls the growth of leaves and floral organs (Johnson and Lenhard 2011; Powell and Lenhard 2012), yet the final size and shape of leaves, sepals

Results

and petals is clearly distinct due to different growth patterns (Sauret-Gueto *et al.*, 2013). This suggests that organ-identity modulates the activity of a basic growth machinery to achieve these specific morphologies (Dornelas *et al.*, 2010). However, how this occurs remains largely unknown.

The reduced leaf-cell expansion in weak *paps1* mutants is partly due to a constitutive immune response as detected by transcriptomic analysis (Vi *et al.*, 2013). Plant immunity is constituted of two levels. Pathogen-associated molecular patterns (PAMPs) are recognized by the host cell via pattern recognition receptors on the cell surface that trigger cellular immune signaling to restrict pathogen growth. PAMPs are important components of a whole class of pathogens (e.g. flagellin) (for review see (Dodds and Rathjen 2010)), and this first layer of immunity is called PAMP-triggered immunity (PTI). Specialized pathogens can in turn suppress the host's immune response through deployment of effector proteins. In resistant plants, these effectors are recognized by intracellular immune receptor containing nucleotide-binding and leucine-rich repeat domains leading to effector-triggered immunity (ETI). Different phytohormones and proteins create a complex network to enable the plant to act and react against pathogens via PTI and ETI (for review see (Pieterse *et al.*, 2009; Dodds and Rathjen 2010)). In particular, the two lipase-like proteins ENHANCED DISEASE SUSCEPTIBILITY 1 (EDS1) and PHYTOALEXIN DEFICIENT 4 (PAD4) act together in both PTI and ETI. Their activation triggers the accumulation of salicylic acid (SA) and presumably other signalling compounds, thus setting off both an SA-dependent and an SA-independent immune response (Zhou *et al.*, 1998; Jirage *et al.*, 1999; Feys *et al.*, 2001; Bartsch *et al.*, 2006). The SA-dependent response is mediated primarily by the transcriptional co-regulator NON-EXPRESSOR OF PR GENES1 (NPR1). Following an SA-induced change in the cellular redox potential, NPR1 protein is converted from an inactive multimer in the cytoplasm to an active monomer that can enter the nucleus and modulate gene expression (Mou *et al.*, 2003). The constitutive pathogen-response in *paps1-1* mutants involves ectopic activation of the EDS1/PAD4 pathway (Vi *et al.*, 2013).

Here we address the developmental and physiological basis of the *paps1* mutant growth phenotypes. We find that the different effects on leaf and floral-organ growth depend on the organs' identity. The enlarged size of *paps1* mutant petals is accompanied by the incorporation of more founder cells into the earliest petal primordium and reflects *PAPS1* function directly in the petals. In leaves the constitutive immune response that contributes to reduced leaf expansion also leads to higher pathogen resistance. This constitutive immune response is mediated by the EDS1/PAD4 pathway via an SA-independent route. Together, these findings provide detailed insight into the developmental and physiological basis of the functional specialization amongst canonical nuclear PAPS isoforms in *Arabidopsis*.

Results

Results

An allelic series of *PAPS1* alleles indicates different requirements of pre-mRNAs for polyadenylation by PAPS1

To obtain a more comprehensive picture of *PAPS1* function, we isolated additional mutant alleles carrying transferred-DNA (T-DNA) insertions (Fig. S1A). The *paps1-2* allele harbours an insertion in the 5' untranslated region (UTR), and in the *paps1-4* allele the T-DNA disrupts the tenth exon coding for the evolutionarily less conserved C-terminal domain of the protein. Reverse-transcription PCR (RT-PCR) analysis indicated that very little full-length *PAPS1* transcript is present in *paps1-2* mutants, while no full-length transcript was detected in *paps1-4* plants (Fig. S1B). This suggests the formation of a C-terminally truncated protein in *paps1-4* mutants and potentially defects in protein translation in *paps1-2* mutants. Phenotypically, homozygous *paps1-4* mutants show similar, albeit somewhat weaker defects than *paps1-1* plants, with smaller leaves and enlarged floral organs (Fig. 1A). By contrast, the flowers of *paps1-2* plants appear deformed with strongly reduced petals (Fig. 1A), while their leaves resemble those of *paps1-4* mutants, being smaller than in wild type.

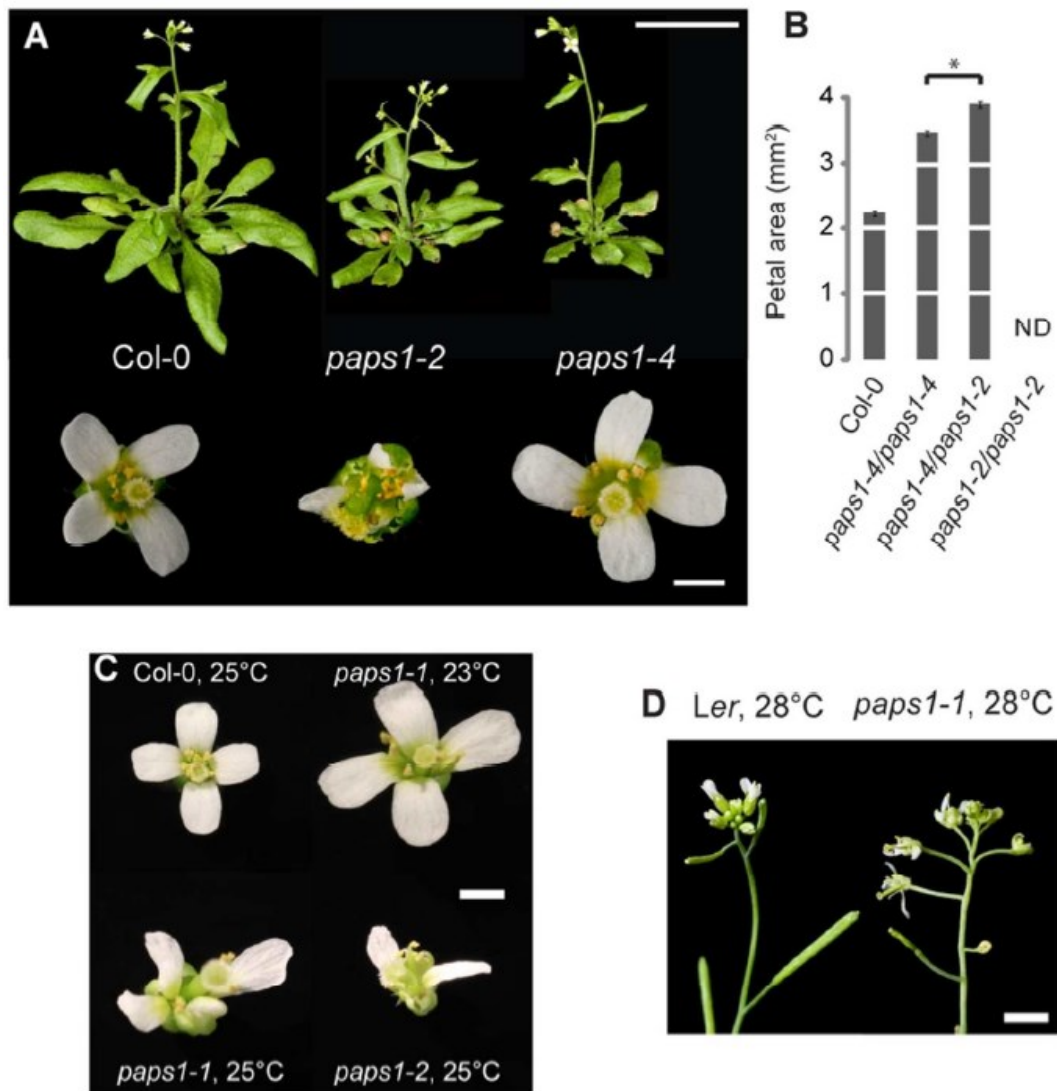


Figure 1: An allelic series of *paps1* mutations

(A) Whole plant and flower images of the indicated genotypes.

(B) Petal area of the indicated genotypes. Values are mean \pm SE of at least 18 petals from at least five individual plants. Asterisk indicates significant difference at $p < 0.01$ (t-test).

(C) Flowers of Col-0, *paps1-1* and *paps1-2* mutant plants grown at 23°C or 25 °C. *paps1-1* flowers are deformed when grown at 25 °C.

(D) Inflorescences of Ler and *paps1-1* plants grown at 28 °C

Scale bars are 1 cm (A, top row), 2 mm (A, bottom row; C) and 5 mm (D).

Results

We hypothesized that the different phenotypes observed in flowers of *paps1-1*, *paps1-2* and *paps1-4* mutants reflect a progressive reduction in the remaining PAPS1 activity according to the following series: *paps1-4* > *paps1-1* > *paps1-2*. This notion is supported by two lines of evidence.

Firstly, transheterozygous *paps1-2/paps1-4* plants form larger petals than either of the homozygous mutants, similar in size to *paps1-1* mutant petals (Fig. 1B), suggesting that combining a weaker and a stronger allele results in an intermediate level of remaining PAPS1 activity as in *paps1-1* mutants. Secondly, as described before (Vi *et al.*, 2013), in contrast to the T-DNA insertion allele *paps1-2* (Figure S1C) the *paps1-1* allele is temperature-sensitive; when grown at higher temperatures (25°C or 28°C versus 23°C), *paps1-1* plants form similarly disorganized flowers and inflorescences as the *paps1-2* mutant (Fig. 1C,D). Thus, the progressively more severe phenotypes in this allelic series suggest the existence of transcript classes with different sensitivities to reduced PAPS1 activity: While in *paps1-4* and *paps1-1* mutants (grown at low temperature) only very sensitive transcripts are affected in their polyadenylation, including ones coding for inhibitors of petal growth, the stronger reduction in remaining PAPS1 activity in *paps1-2* mutants and in *paps1-1* grown at high temperatures appears to cause defective polyadenylation of a larger range of transcripts and consequently more severe and pleiotropic phenotypes.

The effect of the *paps1-1* mutation on growth depends on organ identity and is organ-autonomous.

As mentioned above, the *paps1-1* mutant grown at low temperatures forms enlarged floral organs by up to two-fold, whereas the size of rosette leaves is decreased to about one third (Vi *et al.*, 2013). By contrast, virtually all previously described mutants that affect organ size (except for *cincinnata* in *Antirrhinum majus*) either do so in the same manner in leaves and floral organs, or they only affect one type of organ, but not the other (Johnson and Lenhard 2011, Powell and Lenhard 2012). The opposite effects of the *paps1-1* mutation could be due to the identity (leaf versus flower) or the position of the organs on the plant (in the basal rosette or elevated on the inflorescence stem). To distinguish between these possibilities, we separated organ position and organ identity, using the floral homoeotic mutation *apetala2-1* (*ap2-1*) (Bowman *et al.*, 1989). In *ap2-1* mutants, sepals are converted into ectopic leaves, allowing us to ask whether these ectopic leaves would respond to reduced PAPS1 function according to their identity or their position. While reducing PAPS1 function in an otherwise wild-type background increased sepal size by 36%, reducing PAPS1 function in an *ap2-1* mutant background halved the size of the ectopic leaves in the first whorl of the mutant flowers (Fig. 2A,B). The expression of two sepal marker genes that are strongly downregulated in

Results

ap2-1 mutant first-whorl organs compared to wild-type sepals were equally downregulated in the first whorl of *ap2-1 paps1-1* plants compared to *paps1-1* sepals, confirming the altered identity of these organs (Fig. 2D). Thus, the effect of the *paps1-1* mutation on organ size does not depend on the position of the organs on the plant, but is rather modulated by organ identity.

It has been reported that the *PAPS1* transcript is alternatively spliced between leaves and flowers, with flower cells retaining the sixth intron leading to a form of the mRNA that can only be translated into a putatively non-functional, truncated protein (Addepalli et al., 2004). It is conceivable that such alternative splicing underlies the different effects of the *paps1* mutations in leaves versus flowers. However, using the same primers as Addepalli *et al.*, we could not detect any evidence for retention of the sixth intron of *PAPS1* in flowers (Fig. 2C), suggesting that alternative splicing is not the reason for the organ-specific effects

Figure 2: PAPS1 activity is modulated by organ-identity

(A) Flowers and dissected first-whorl organs of the indicated genotypes.

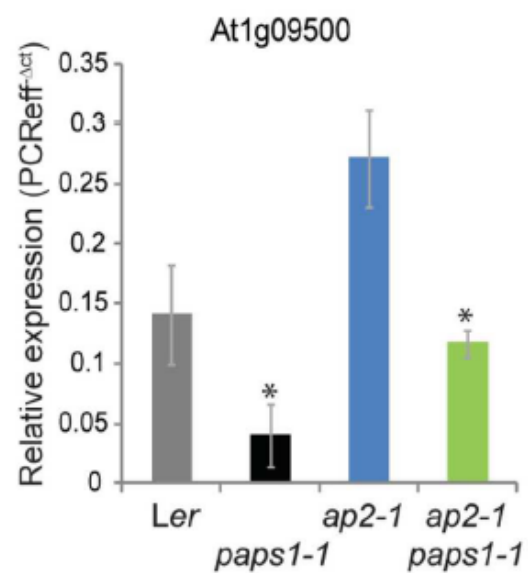
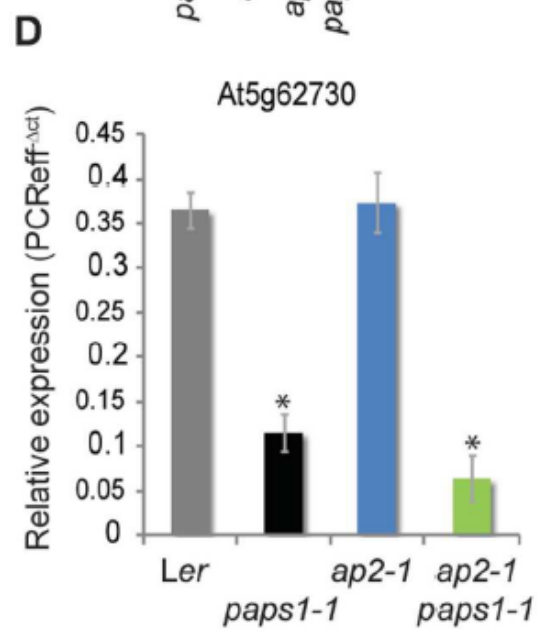
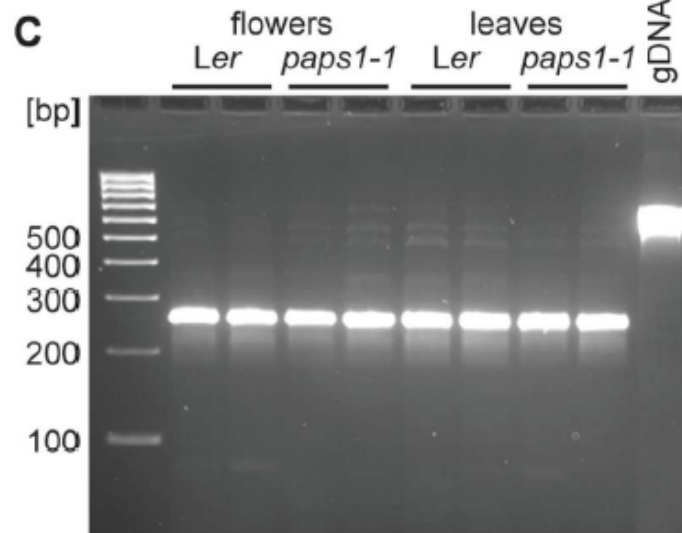
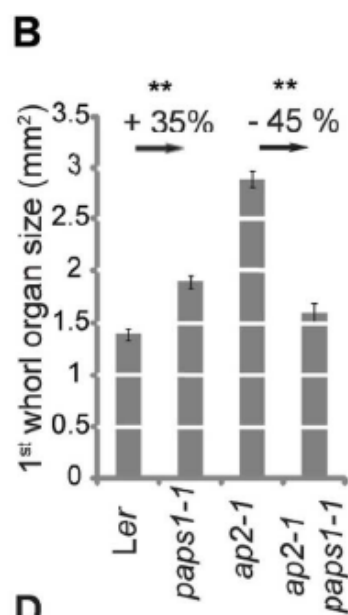
(B) Quantification of first-whorl organ size for the genotypes shown in (A). Values shown are mean \pm SE from at least 11 organs per genotype. Scale bar is 2 mm.

** : difference is significant at $p < 0.01$ (t-test).

(C) RT-PCR products for *PAPS1* from Ler wild-type and *paps1-1* mutant leaves and flowers, using primers that span the sixth intron. gDNA: genomic DNA as template

(D) Expression levels of two sepal-specific marker genes in the indicated genotypes as assessed by qRT-PCR. Values shown are mean \pm SE from three biological replicates.

* : difference to the corresponding *AP2* genotype is significant at $p < 0.05$ (t-test)



Results

To further characterize the role of *PAPS1* in floral-organ growth, we asked whether the petal overgrowth in the mutant reflects a function of *PAPS1* directly in the floral meristem and/or the petal primordium, or whether it results non-autonomously from the constitutive immune response in the earlier formed rosette leaves (see below). To address this, we made use of a Cre/*loxP*-based system for generating chimaeric plants in which Cre-mediated excision converts YFP-expressing complemented cells into CFP-expressing homozygous mutant cells (Adamski *et al.*, 2009). Cre expression is restricted to the stem cells of the shoot apical meristem and can be temporally controlled by induction with ethanol. Using this approach, we generated plants that formed a complemented, phenotypically wild-type rosette, but whose inflorescence was composed of homozygous *paps1-1* mutant next to complemented flowers (Fig. 3A,B). Measuring the size of complemented and mutant petals developing side by side in the same inflorescence indicated that *paps1-1* mutant petals were almost twice as large as the complemented petals (Fig. 3C,D). This is the same ratio as in *paps1-1* mutant compared to wild-type flowers from different plants (Vi *et al.*, 2013). Thus, we conclude that the strong overgrowth seen in *paps1-1* mutant organs even when developing on a largely wild-type plant reflects a direct, autonomous role for *PAPS1* in the flowers to limit organ growth.

Increased founder-cell recruitment contributes to the petal overgrowth in *paps1-1* mutants.

In *paps1-1* mutant petals cell size is increased by 21%, yet overall the petals are almost two-fold larger than wild type, indicating that the bulk of the difference in petal size is due to a higher cell number (Vi *et al.*, 2013). To trace the developmental basis for this effect, we followed the growth of petal primordia over time. While the rate of petal growth was essentially unchanged in the *paps1-1* mutant relative to wild type, mutant petals continued growing for a longer period of time than wild-type primordia, suggesting that *PAPS1* acts to limit the duration of petal growth (Fig. 4A). Proliferation in *paps1-1* mutant petals as monitored by the mitotic reporter gene *pAtCycB1;1::CDBGUS* similarly continued for longer than in wild-type: While almost no dividing cells were observed in wild-type petals larger than 0.2 mm², a large proportion of the area of corresponding mutant petals was still dividing (Fig. 4B).

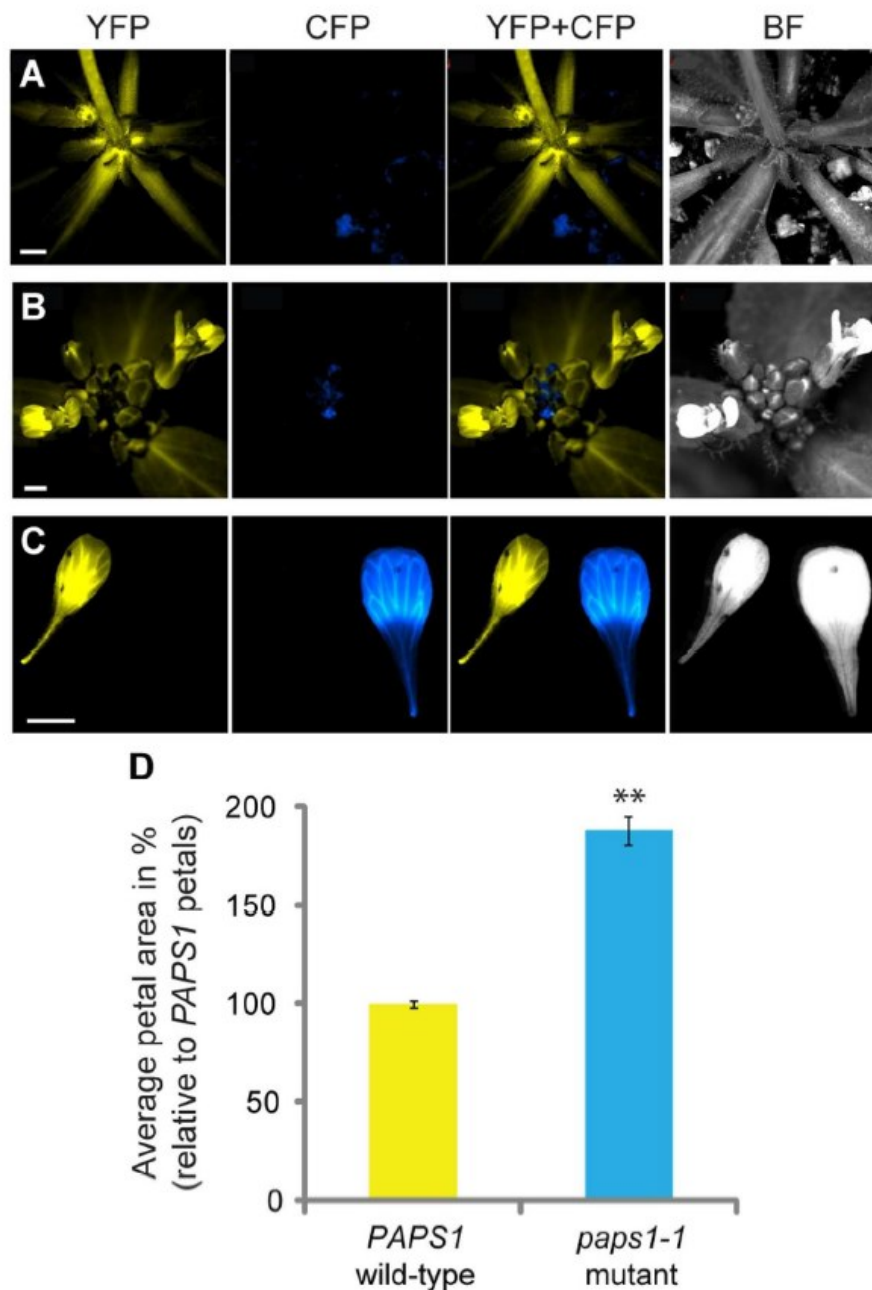


Figure 3: *PAPS1* acts autonomously at the level of individual organs.

(A-C) Fluorescence and bright field micrographs of the rosette (A) and the inflorescence (B) from one chimaeric plant, as well as two petals from one chimaeric flower (C). YFP-fluorescence indicates *PAPS1* wild-type tissue, while CFP fluorescence marks *paps1-1* mutant tissue.

(D) Quantification of *PAPS1* wild-type and *paps1-1* mutant petal size from chimaeric inflorescences as shown in (B). Completely *PAPS1* wild-type and *paps1-1* mutant petals developing in the same main inflorescence were collected from three individual plants. The size of wild-type and mutant petals from one inflorescence was normalized to the average size of wild-type petals from that inflorescence. Values shown are the mean \pm SE of these normalized sizes. We measured 26 *PAPS1* wild-type and 9 *paps1-1* mutant petals.

** : difference is significant at $p < 0.01$ (t-test). Scale bars are 5 mm in A and B, 1 mm in C

Results

The above approach is based on dissecting petals from closed flowers. It is therefore unable to investigate the very early stage of petal development. This can be done by inducing marked stem-cell clones in the shoot apical meristem and using the boundary between marked and unmarked clones to dissect the number of founder cells in the earliest petal primordium (Bossinger and Smyth 1996, Jenik and Irish 2000, Stransfeld *et al.*, 2010). In wild-type, such clone boundaries only ever split petals in half, either in the epidermis or in the subepidermal tissue, indicating that the earliest petal primordium is made up of two epidermal and two subepidermal cells (Bossinger and Smyth 1996; Jenik and Irish 2000; Stransfeld *et al.*, 2010). We have previously confirmed this result using a *Cre/loxP* system for generating YFP-expressing clones by the excision of a spacer fragment from a non-functional reporter gene (Eriksson *et al.*, 2010; Stransfeld *et al.*, 2010). As above, *Cre* expression can be induced by EtOH treatment and is restricted to the stem cells of the shoot and floral meristems. To determine the size of the early petal primordium in *paps1-1* mutants, *Cre* expression was induced at seven days after germination, long before the switch to flowering occurred. This ensures that all clones originate outside of the flower meristems. We found that only 58% (15 of 26) of *paps1-1* mutant petals are split along the midvein. The remaining 42% showed sector patterns indicative of three to four founder cells per tissue layer, i.e. roughly two-thirds or three-quarters of the petal were taken up by the marked or the unmarked sector (Fig. 4C). Thus, already the size of the early primordium and the number of founder cells appears to be increased in *paps1-1* mutants.

Results

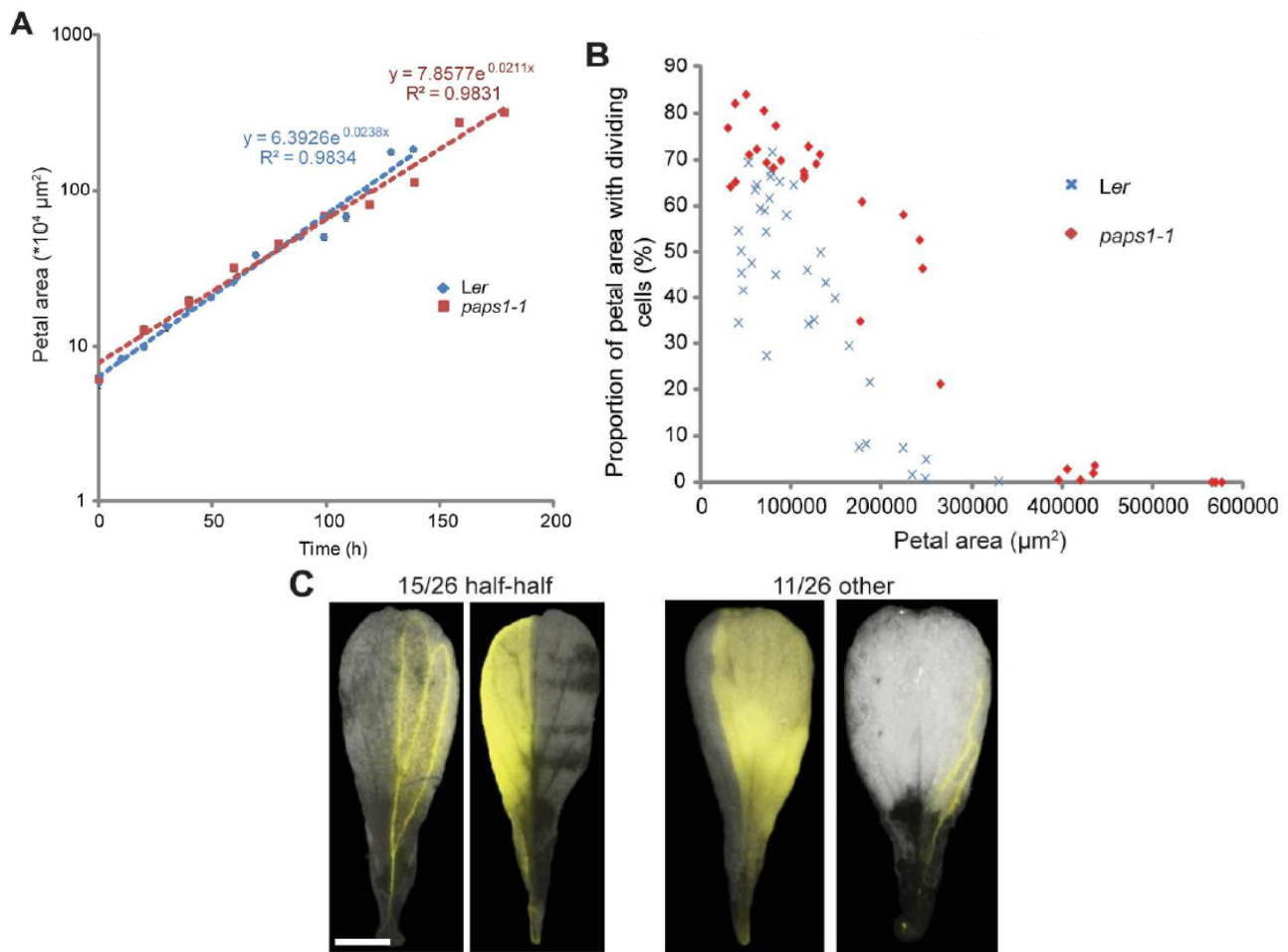


Figure 4: More founder cells contribute to *paps1-1* mutant than to wild-type petal primordia

(A) Quantification of petal growth in *paps1-1* mutants compared to *Ler* wild type. Values are means \pm SE from at least 10 petal primordia from six (*paps1-1*) or four (*Ler*) plants. Regression lines for exponential growth are shown. The last two data points for each series are from open flowers.

(B) Dynamics of cell proliferation in *paps1-1* mutant compared to *Ler* wild-type petals. The relative petal area with dividing cells as indicated by staining for *pAtCycB1;1::CDBGUS* reporter activity is plotted relative to the total size for individual primordia.

(C) Representative petals from *paps1-1* mutants with YFP-marked sectors originating in the stem cells of the shoot apical meristem. The frequencies of petals split by the clonal boundary along the midvein and of petals showing different arrangements of marked and unmarked cells are given. Scale bar is 2 mm

***paps1* mutants show increased pathogen resistance.**

We next turned to the basis for the reduced growth seen in *paps1* mutant leaves. Transcriptomic and double mutant analyses had indicated that *paps1-1* mutant leaves show a constitutive immune response (Vi *et al.*, 2013). In particular, the reduced leaf growth was substantially rescued by introducing the *eds1-2* or *pad4-1* mutations, indicating that this constitutive immune response partly underlies the growth defect. To determine whether this is reflected in an enhanced pathogen resistance in the *paps1* mutants, we performed infection assays with the biotrophic oomycete *Hyaloperonospora arabidopsidis* strain Emco5, which is virulent on Col-0 (Fig. 5A). Indeed, both *paps1-1* and *paps1-4* mutants supported significantly less conidiospore formation than wild-type plants. The increased pathogen resistance of *paps1* was abolished in *eds1 paps1* and *pad4 paps1* double mutants, in line with the phenotypic suppression at the level of leaf growth. This suppression of the constitutive immune response of *paps1* plants by *pad4* loss of function was further confirmed at the molecular level by examining the expression of several marker genes (Fig. 5B). *PR1*, *PR2* and *PR5* expression were all reduced in *pad4 paps1* double mutants compared to *paps1* plants, whereas for *SID2* the suppression in the double mutant was not significant.

In contrast to *paps1* mutants, *paps2 paps4* double mutants (Vi *et al.*, 2013) were as susceptible to *H. arabidopsidis* as the wild type, confirming the functional specificity of the different PAPS isoforms. Domain-swap experiments had suggested that this specificity is encoded by the C-terminal protein domains that are divergent between PAPS1 and PAPS2/4. To confirm this at the molecular level, we assayed the expression of *PR1*, *PR2* and *SID2* in *paps1-1* mutants expressing either the *PAPS4* coding sequence or a fusion of the N-terminal domain of PAPS4 and the C-terminal domain of PAPS1 under the control of the *pPAPS1* promoter. Both *PR1* and *PR2* were still overexpressed in *pPAPS1::PAPS4* expressing *paps1-1* mutants compared to wild-type, but their expression was rescued to wild-type levels in the *pPAPS1::PAPS4^N-PAPS1^C* expressing *paps1-1* mutants (Fig. 5C). By contrast, *SID2* expression was indistinguishable from wild type in either transgenic line. Thus, the C-terminal domains of the PAPS isoforms influence their specific functions in the immune response.

To further characterize the constitutive immune response at the physiological and cellular levels, we tested for two hallmarks of the plant hypersensitive response to pathogens, the occurrence of ectopic cell death and the accumulation of H₂O₂ (Thordal-Christensen *et al.*, 1997; Mur *et al.*, 2008). Trypan Blue staining did not detect any ectopic cell death in the leaves of 9- or 12-day old *paps1-1* mutants or wild-type plants. Only six weeks after germination, when senescence becomes phenotypically visible in *paps1-1* plants, dead cells were detected in the mutant leaves. These were visible as randomly distributed spots, whereas still none were observed in wild type *Ler* leaves (Fig.

Results

5D, arrows). Thus, the constitutive immune response in *paps1-1* mutants does not include ectopic cell death.

Reactive oxygen species (ROS) in general and hydrogen peroxide (H₂O₂) in particular are well known signalling components in response to pathogens, elicitors, wounding or heat (Slesak *et al.*, 2007). To test for H₂O₂ accumulation in *paps1-1* mutants, we made use of 3'3' Diaminobenzidine (DAB) staining. DAB captures H₂O₂ when peroxidase activity is present and is converted into a brown polymer (Thordal-Christensen *et al.*, 1997). We could not detect a stronger accumulation of H₂O₂ in *paps1-1* leaves that could contribute to the ectopic immune response (Fig.S2).

Figure 5: *paps1* mutants are more resistant to the biotrophic oomycete *Hyaloperonospora arabidopsidis*

(A) Quantification of conidiospore formation as a measure for *Hyaloperonospora arabidopsidis* (strain Emco5) growth on the indicated genotypes. Values are mean \pm SE of six biological replicates, representing 60 seedlings.

*: difference is significant at $p < 0.01$ (t-test).

(B, C) *PR*-gene expression in the indicated genotypes as assessed by qRT-PCR. Values are means \pm SE from three biological replicates. Difference to wild type is significant at *: $p < 0.05$, ***: $p < 0.001$ (t-test).

(D) Trypan Blue staining of *Ler* and *paps1-1* leaves from 9 and 12 day-old seedlings and mature leaves. Scale bar is 1 mm; DAG: days after germination. A senescent wild-type leaf was used as control.

Results

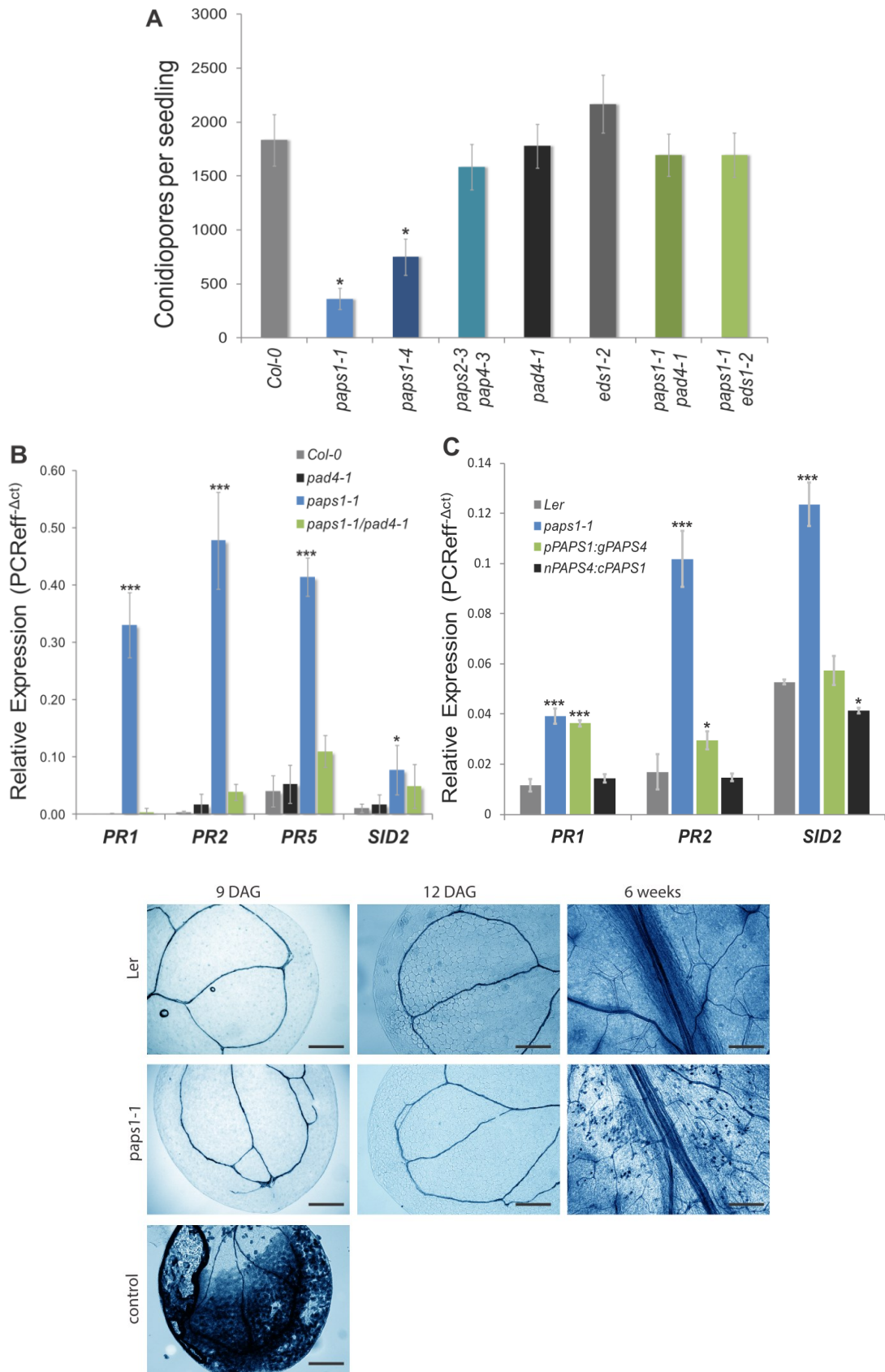


Figure 5

The SA-independent branch of the EDS1/PAD4-triggered immune response is active in *paps1* mutants.

As described above, activation of EDS1/PAD4 stimulates both an SA-dependent and an SA-independent branch of the immune response (Bartsch *et al.*, 2006). To determine whether the EDS1/PAD4-dependent constitutive pathogen response in *paps1-1* mutants is mediated via the SA-dependent pathway, we generated *npr1-1 paps1-1* double mutants. In contrast to the *eds1 paps1* or the *pad4 paps1* double mutants, there was no phenotypic rescue of the *paps1* leaf growth defect in the *npr1-1 paps1-1* double mutant (Fig. 6A,B), and these were indistinguishable from *paps1-1* single mutants at the rosette stage. In flowers, the double mutant showed an additive phenotype, with a 17% reduction in petal area compared to *paps1-1*, which is also seen when comparing Col-0 to *npr1* single mutants (Fig. 6C). Thus, *NPR1* is not required for the constitutive immune response in *paps1* mutant leaves. To further confirm this result, we also generated the *npr1-1 pad4-1 paps1-1* triple mutant, asking whether the additional loss of *NPR1* function could enhance the partial rescue of the *paps1* mutant leaf-growth defect by the *pad4* mutation. Leaf growth was indistinguishable between *pad4-1 paps1-1* and the triple mutant, supporting our conclusion that *NPR1* is not ectopically activated in *paps1* mutant leaves.

To further define the genetic requirements for the constitutive immune response in *paps1* mutant leaves, we analysed double mutants between *jar1-1* and *paps1-1*. The *jar1-1* mutation shows a reduced sensitivity to jasmonic acid and is required for expression of the *NPR1*-independent constitutive immune response in *cpr5* mutants (Clarke *et al.*, 2000), whose transcriptome changes strongly overlap with those seen in *paps1-1* mutants (Vi *et al.*, 2013). The *jar1-1 paps1-1* double mutant was indistinguishable from the *paps1-1* single mutant (Fig. S3). In addition, as the cytochrome P450 *PHYTOALEXIN DEFICIENT3* (*PAD3*; (Zhou *et al.*, 1999)) was the fourth most strongly upregulated gene in *paps1-1* mutant leaves based on microarray analysis, we asked whether increased formation of phytoalexins contributed to the reduced leaf growth. As for *jar1*, the *pad3 paps1-1* double mutant was indistinguishable from the *paps1-1* single mutant (Fig. S3). Thus, neither jasmonic-acid signalling nor phytoalexin biosynthesis appear to be required for the constitutive immune response in *paps1* mutants.

Results

SA levels are not altered in *paps1* mutants.

To directly test our hypothesis that the constitutive immune response in *paps1-1* mutants is SA-independent and to assess the potential contribution of other stress- and immune response-related hormones, we determined the levels of SA, jasmonates, the auxin indole-acetic acid (IAA) and abscisic acid (ABA) (Fig. 7A). As expected, free SA levels were indistinguishable between wild type and *paps1-1* mutants, as were IAA levels. By contrast, concentrations of both ABA and the jasmonates JA and JA-Isoleucine (JA-Ile) were significantly reduced in *paps1-1* mutants, while the JA precursor OPDA was present at wild-type levels. The conclusion that accumulation of SA does not trigger the constitutive immune response was further supported by introducing a *35S::NahG* transgene into the *paps1-1* mutant background. *NahG* encodes salicylate hydroxylase, an SA-degrading enzyme whose overexpression lowers SA levels (Lawton *et al.*, 1995). However, the *35S::NahG* transgene had no effect on the *paps1-1* mutant phenotype (Fig. 7B). Thus, constitutive SA accumulation does not underlie the immune-response phenotype of *paps1* mutants.

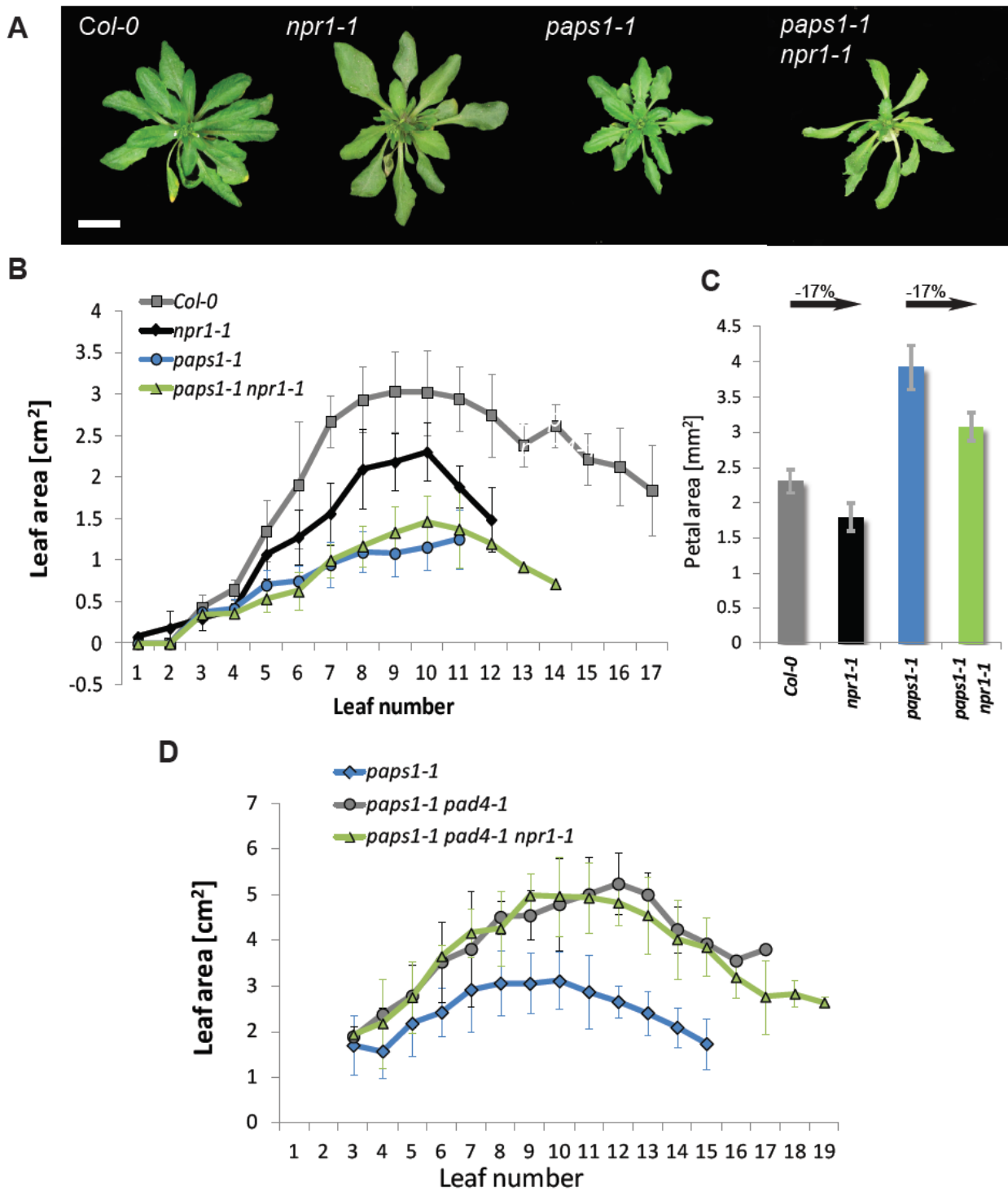
Figure 6: The constitutive immune response in *paps1* mutants depends on *EDS1/PAD4* but not on *NPR1*

(A) Whole-plant images of the indicated genotypes. Scale bar is 1 cm.

(B) Quantification of leaf area in the indicated genotypes. Values are means \pm SE from at least three plants per genotype.

(C) Quantification of petal area in the indicated genotypes. Values are means \pm SE from at least 12 petals from at least three individual plants per genotype.

(D) Quantification of leaf area in the indicated genotypes. Values are means \pm SE from at least three plants per genotype.



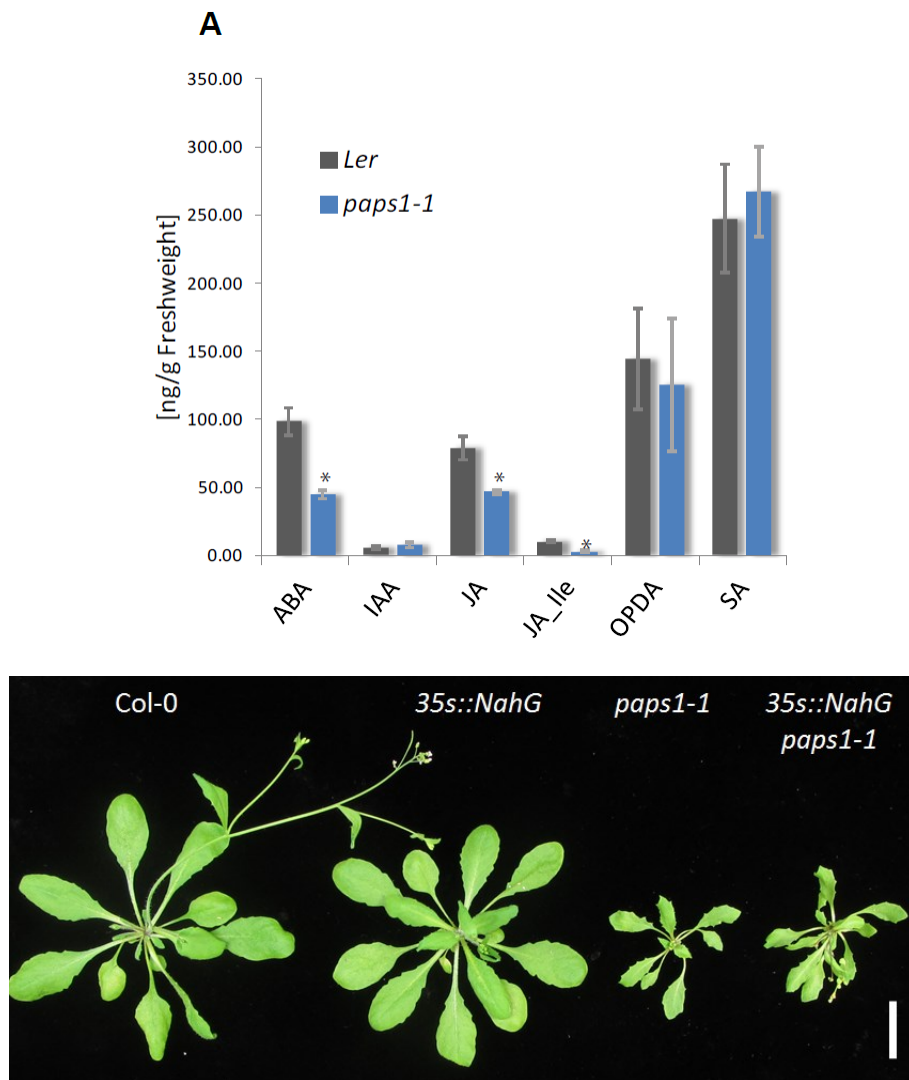


Figure 7: SA levels are unaltered in *paps1* mutants

(A) Phytohormone levels in *Ler* and *paps1-1* seedlings. Values are means \pm SE of five independent biological samples.

*difference is significant at $p < 0.001$ (t-test).

(B) Whole-plant images of the indicated genotypes. Scale bar is 1cm.

Discussion

Organ identity modulates the function of *PAPS1* in growth control and immune response.

The *paps1* mutation shows opposite effects on the growth of leaves and floral organs, in contrast to virtually all previously described organ-size mutants (Vi *et al.*, 2013). Here we have demonstrated that these different effects indeed depend on the different identities of the organs, rather than their position on the plant, and that the effect on floral organs reflects the action of PAPS1 in the flowers themselves. These findings make *PAPS1* a promising starting point to study the important, yet poorly understood functional connection between organ identity and growth control. How could this modulation by organ identity be achieved? Both *PAPS1* transcript accumulation (Hunt *et al.*, 2008) and splicing do not show marked differences between leaves and flowers, arguing that differences in *PAPS1* expression are unlikely to account for the different effects. Alternatively, it is conceivable that PAPS1 protein is subject to different post-translational modifications in leaves versus flowers that alter its activity level or its preference for certain sets of pre-mRNAs. However, at least for *SAUR19/24* transcripts defective polyadenylation was equally seen in leaves and flowers, arguing against wide-spread differences in isoform-target relations (Vi *et al.*, 2013). Thus, the most plausible hypothesis at the moment appears to be that identity-dependent changes in transcript patterns between leaves and flowers underlie the different outcomes of reducing *PAPS1* activity. In this view, flowers would express certain pre-mRNAs that need to be polyadenylated by PAPS1 and that are not expressed in leaves. Defective processing of these flower-specific transcripts in *paps1* mutants would then ultimately result in the observed overgrowth in contrast to the reduced size of leaves.

Amongst the transcripts that are affected by reduced *PAPS1* activity in flowers, there seem to be differences in their requirement for *PAPS1* activity. This conclusion is based on the different phenotypes observed in the allelic series of *paps1* mutations. Weak to moderate reduction in *PAPS1* activity in *paps1-4* or *paps1-1* mutants grown at low temperatures appears to result in defective polyadenylation of only those pre-mRNAs with the highest specificity for PAPS1, some of which encode for negative regulators of founder-cell recruitment and/or organ growth (see below). A more severe reduction in *PAPS1* activity as in *paps1-2* or *paps1-1* mutants grown at high temperature causes polyadenylation defects of a larger number of transcripts, resulting in more pleiotropic effects with disorganized flowers.

One of the consequences of these polyadenylation defects in the mutant flowers appears to be the incorporation of more founder cells than the usual four into the petal primordia, as demonstrated by our sector analysis of *paps1-1* mutant petals. It will be interesting to test whether this is reflected in a larger expression domain of the petal-anlagen marker *DORNRÖSCHEN-LIKE* (Chandler *et al.*, 2011)

Results

and whether it results from an overall increase in floral-meristem size. To our knowledge, increased floral-organ size resulting from an increase in the founder cell population has not been demonstrated before. How can this observation be reconciled with our result that cell proliferation in and growth of petal primordia appears to occur for a longer period of time in *paps1-1* mutants? The latter conclusion is based on the manual dissection of petal primordia from flower buds, while the clonal analysis relates to the petal primordium at the time of its inception at the floral meristem. Thus, there is a period in petal growth to which both of these analyses are blind: the time from primordium initiation to the earliest stage when petals can be manually dissected. Being larger from the outset, the mutant petals most likely require less time to reach the stage where they can be manually dissected, suggesting that the duration of petal growth and also of petal-cell proliferation is in fact similar in mutant and wild-type plants, yet a larger fraction of this time is visible to our dissection-based approach. Thus, along with the somewhat increased cell size in *paps1-1* mutant petals (Vi *et al.*, 2013) it appears that the mutant petals become larger, because they already start out larger.

The constitutive immune response of *paps1* mutants is triggered by an SA-independent, but EDS1/PAD4-dependent pathway.

In contrast to flowers, the *paps1* mutant phenotype in leaves is dominated by a constitutive immune response, resulting in reduced cell expansion and thus smaller leaves. This constitutive immune response is not only apparent at the transcriptomic level, but is manifested in increased resistance to the biotrophic oomycete *H. arabidopsidis*. Similar to the reduced leaf growth, the increased resistance can be suppressed by *eds1* and *pad4* mutations, indicating that the EDS1/PAD4-dependent signalling pathway is constitutively active in *paps1* mutants. Our further analyses indicate that it is more specifically the SA-independent branch of the EDS1/PAD4-signalling pathway that is involved. This conclusion is based on three lines of evidence: (1) Loss of *npr1* function, a major downstream component of SA-dependent EDS1/PAD4-signalling, does not suppress the constitutive immune response in *paps1*. (2) SA levels are not increased in *paps1* mutants relative to wild type. (3) Reducing SA levels by overexpressing the SA-degrading enzyme NahG does not rescue the *paps1* mutant leaf phenotype. While overall little is known about the SA-independent functions of EDS1/PAD4, two important modulators of this process have been identified, the flavin-containing monooxygenase FMO1 and the Nudix hydrolase NUDT7 (Bartsch *et al.*, 2006). Consistent with our above interpretation, the expression of *FMO1*, which positively regulates the EDS1 pathway, is strongly upregulated in *paps1-1* mutant leaves (Vi *et al.*, 2013).

Results

A functional link between the control of poly(A)-tail lengths and immune response is supported by the analysis of several other mutant and transgenic plant lines. Mutations in *AtCAF1a* and *AtCAF1b*, the two homologues of the yeast CCR4-associated factor that is a component of the CCR4-NOT deadenylase complex, result in defective poly(A)-tail shortening of stress-associated mRNAs and in reduced expression of the *PATHOGENESIS-RELATED1 (PR1)* gene (Liang *et al.*, 2009). By contrast, overexpressing *AtCAF1a* upregulates *PR1* expression and increases pathogen resistance. Similarly, overexpression of the yeast poly(A)-binding protein Pab1p in tobacco or *A. thaliana* leads to a constitutive immune response and increased resistance (Li *et al.*, 2000). The functional link between polyadenylation or poly(A)-tail length control and immune response extends beyond plants. Blocking polyadenylation by cordycepin treatment inhibits the induction of inflammatory mRNAs by cytokines in human airway smooth muscle cells (Kondrashov *et al.*, 2012). However, critical immune response-related molecular targets for poly(A)-tail length control have not been defined yet.

In conclusion, the results presented here support and refine our model of the functional specialization amongst *Arabidopsis* canonical nuclear poly(A) polymerases. While most pre-mRNAs can be efficiently polyadenylated by either isoform (Vi *et al.*, 2013), other sets of transcripts have an increasingly higher requirement for polyadenylation specifically by PAPS1. In flowers, transcripts encoding negative regulators of founder-cell recruitment are amongst the transcripts with the highest requirement for PAPS1, while other transcripts are only mis-polyadenylated after more pronounced reduction in PAPS1 activity. By contrast, in leaves the mis-polyadenylated transcripts ultimately trigger the SA-independent branch of the EDS1/PAD4-signalling pathway, causing increased pathogen resistance at the expense of reduced growth. These different effects depend on the identity of the organ, suggesting that some of the highly PAPS1-dependent transcripts are only expressed in leaves, but not in flowers and vice versa. Identifying these organ-specific critical targets will be required to validate this notion.

EXPERIMENTAL PROCEDURES

Plant lines and growth conditions *A. thaliana* plants were grown in a plant growth chamber with 21 °C during the 16 h light period and 16 ° during the 8 h dark period if not stated differently. Plants used here include the Columbia-0 (Col-0) and Landsberg erecta (*Ler*) wildtypes as well as the *paps1-1* (Vi *et al.*, 2013), *ap2-1* (Bowman *et al.*, 1989), *npr1-1* (Cao *et al.*, 1997), *pad4-1* (Jirage *et al.*, 1999), *jar1-1* (Staswick *et al.*, 2002) *pAtCycB1;1::CDBGUS* line (de Almeida Engler *et al.*, 1999), *eds1-2* (Falk *et al.*, 1999) mutants and the *35S::NahG* transgenic line (Lawton *et al.*, 1995). T-DNA insertion lines were obtained from the Nottingham Arabidopsis Stock Centre. These are in Col-0 background including *paps1-2* (T-DNA line SAIL_172_F11), *paps1-4* (T-DNA line WiscDsLox441G5), *pad3* (SALK_026585), *paps2-3* (SALK_126395), and *paps4-3* (SALK_007979) (Vi *et al.*, 2013) lines.

Genotyping Mutant Alleles or genotyping the *paps1-1* allele, a dCAPS marker (oSV126 and oSV166) was used (Vi *et al.*, 2013). For genotyping of T-DNA insertion alleles, gene-specific primers (called LP and RP primer) that flank the T-DNA insertion site, and a T-DNA right border primer (LBP) were used. These are listed in Supporting Information.

Phenotypic analysis of leaf and petal growth Petal and leaf sizes, as well as cell sizes were essentially measured as described (Vi *et al.*, 2013), with petals taken from flowers 6 to 15. Further details are given in Supporting Information. The developmental series of petal growth and cell proliferation was determined as described before (Disch *et al.*, 2006).

qRT-PCR Measurements Total RNA was prepared by the hot phenol method (Box *et al.*, 2011), DNase-digested, and reverse-transcribed using oligo(dT)17 or random-hexamer primers. Expression levels were analysed using a Roche LightCycler 480. Details and primers used are described in Supporting Information.

Molecular cloning and plant transformation To generate the *loxP*-flanked *PAPS1* rescue construct for clonal analysis, a genomic *PAPS1* fragment of 5.8 kb was excised by *Ascl* from plasmid pSV1 (Vi *et al.*, 2013) and cloned into the destination vector ML1297 (pBI101:*p35S::loxP-vYFPer:nos-Ascl-loxP:CFPer:pA*) to generate plasmid pSV2. Plant transformation was performed by floral dip (Clough and Bent 1998).

Clonal analysis To generate YFP-marked clones for dissecting early petal primordia, *pCLV3::AlcR-AlcA::Cre* or *p35S::loxP-2xnos-SUG-loxP:vYFPer:pA* transgenes (Strasfeld *et al.*, 2010) were introduced into the *paps1-1* mutant background by crossing. Homozygous *paps1-1* mutants carrying one copy each of the two transgenes were produced by intercrossing. To generate *paps1-1* loss-of-function chimaeras, homozygous *paps1-1* plants carrying *pCLV3::AlcR-AlcA::Cre* were crossed with homozygous *paps1-1* plants carrying pSV2, and F1 plants were used for EtOH induction. Induction

Results

was done using EtOH-vapour for 20-30 min at 7 days after germination (for dissecting the petal primordia) and at 10-12 days after germination for *paps1-1* loss-of-function chimaeras.

Pathogen infection assay *Hyaloperonospora arabidopsidis* inoculations were performed as described (Tor *et al.*, 2002). Emco5 infection was determined by vortexing infected seedlings in water and counting conidiospores using a hemocytometer.

Staining for cell death and H₂O₂ accumulation Trypan blue staining was done as described (Koch and Slusarenko 1990). DAB staining was done as described (Thordal-Christensen *et al.*, 1997).

Phytohormone measurements *Extraction* 250 mg of rosette leaves of *Arabidopsis thaliana* were ground to a fine powder using a mortar and a pestle and the powder was transferred to 15 mL tube. The first extraction was performed at 4°C for 30 min in 12 mL 2% (v/v) formic acid in water. The supernatant was separated from the plant debris by a 5 min centrifugation at 3000 g. The procedure was repeated twice to yield a final combined extract volume of 24 mL. This pooled supernatant was subjected to a reversed phase (C18) solid phase extraction (Strata X 33µm particles in a 10mg bed, Phenomenex, Aschaffenburg, Germany). After having washed the SPE columns once with 2 mL methanol and an equilibration step using 2 mL of 2% (v/v) formic acid in water, the 24 mL extract were loaded onto the solid phase cartridge, Residual salts were then washed off with two times using 1 mL 2% formic acid (v/v). Finally the phytohormones were eluted using two times 0.5 mL methanol and the eluate was evaporated to dryness using a speed vacuum concentrator.

LC MS measurement The MS-based analysis was performed on a triple quadrupole mass spectrometer (ABI 3000, Applied Biosystems, Foster City, CA) connected to an Acquity ultra performance liquid chromatography (UPLC, Waters, Milford, USA). The UPLC was equipped with a BEH C18 reversed-phase column (100 x 2.1 mm i.d., 1.8-µm particle size; Waters), which was operated at a flow rate of 400 µL min⁻¹. Solvent A consisted of 0.1% formic acid in water and solvent B consisted of 0.1% formic acid in methanol. The gradient started at 62 % A followed by a 7-min linear gradient to 10 % A. The column was re-equilibrated for 3 min at 62% A for 3 min. The eluate was continuously monitored in negative ion mode using MRM (multiple reaction monitoring). Each compound (indole-3-acetic acid (IAA), jasmonic acid (JA), JA conjugated with isoleucine (JA-Ile), 12-oxo-phytodienoic acid (OPDA), salicylic acid (SA), and cis-abscisic acid (ABA)) was identified and quantified based on two fragments (SA 137 m/z to 93 m/z and 85 m/z; JA 209 m/z to 15 m/z and 59 m/z; JA-Ile 322 m/z to 130 m/z and 128 m/z; ABA 23 m/z to 219 m/z and 153 m/z; IAA 174 m/z to 130 m/z and 128 m/z and OPDA 291 m/z to 15 m/z and 247 m/z). The parameters of the mass spectrometer for the analysis were set to -4.5 kV electro spray voltage at a temperature of 350°C. The dwell time was set to 50 msec and pause between mass ranges was set to 5 msec. The collision energy was determined for each compound using authentic reference compounds, which were obtained from OIChem

Results

(Olomouc, Czech Republic). The standards were run in parallel. The quantities of phytohormones in the crude plant extracts were calculated from calibration curves obtained from dilution series of the authentic standards.

ACKNOWLEDGEMENTS

We thank Christiane Schmidt and Doreen Mäker for excellent plant care, and members of the Lenhard group for helpful discussion and comments. We are grateful to Jane Parker, Erich Glawischnig and the Nottingham Arabidopsis Stock Centre for providing seeds. This work was supported by funding from the Deutsche Forschungsgemeinschaft (Le1412/3-1) to M.L., by a Rotation Programme PhD Fellowship from the John Innes Centre to L.S.V., and by funding from the Gatsby Charitable Foundation to C.Z..

References

- Adamski, N.M., Anastasiou, E., Eriksson, S., O'Neill, C.M. and Lenhard, M.** (2009) Local maternal control of seed size by KLUH/CYP78A5-dependent growth signalling. *Proc Natl Acad Sci U S A*, **106**, 20115-20120.
- Addepalli, B., Meeks, L.R., Forbes, K.P. and Hunt, A.G.** (2004) Novel alternative splicing of mRNAs encoding poly(A) polymerases in Arabidopsis. *Biochim Biophys Acta*, **1679**, 117-128.
- Bartsch, M., Gobbato, E., Bednarek, P., Debey, S., Schultze, J.L., Bautor, J. and Parker, J.E.** (2006) Salicylic acid-independent ENHANCED DISEASE SUSCEPTIBILITY1 signaling in Arabidopsis immunity and cell death is regulated by the monooxygenase FMO1 and the Nudix hydrolase NUDT7. *Plant Cell*, **18**, 1038-1051.
- Bossinger, G. and Smyth, D.R.** (1996) Initiation patterns of flower and floral organ development in Arabidopsis thaliana. *Development*, **122**, 1093-1102.
- Bowman, J.L., Smyth, D.R. and Meyerowitz, E.M.** (1989) Genes directing flower development in Arabidopsis. *Plant Cell*, **1**, 37-52.
- Box, M.S., Coustham, V., Dean, C. and Mylne, J.S.** (2011) Protocol: A simple phenol-based method for 96-well extraction of high quality RNA from Arabidopsis. *Plant Methods*, **7**, 7.
- Cao, H., Glazebrook, J., Clarke, J.D., Volko, S. and Dong, X.** (1997) The Arabidopsis NPR1 gene that controls systemic acquired resistance encodes a novel protein containing ankyrin repeats. *Cell*, **88**, 57-63.
- Chandler, J.W., Jacobs, B., Cole, M., Comelli, P. and Werr, W.** (2011) DORNROSCHE-LIKE expression marks Arabidopsis floral organ founder cells and precedes auxin response maxima. *Plant Molecular Biology*, **76**, 171-185.
- Clarke, J.D., Volko, S.M., Ledford, H., Ausubel, F.M. and Dong, X.** (2000) Roles of salicylic acid, jasmonic acid, and ethylene in cpr-induced resistance in Arabidopsis. *Plant Cell*, **12**, 2175-2190.
- Clough, S.J. and Bent, A.F.** (1998) Floral dip: a simplified method for Agrobacterium-mediated transformation of Arabidopsis thaliana. *Plant J*, **16**, 735-743.
- de Almeida Engler, J., De Vleeschauwer, V., Bursens, S., Celenza, J.L., Jr., Inze, D., Van Montagu, M., Engler, G. and Gheysen, G.** (1999) Molecular Markers and Cell Cycle Inhibitors Show the

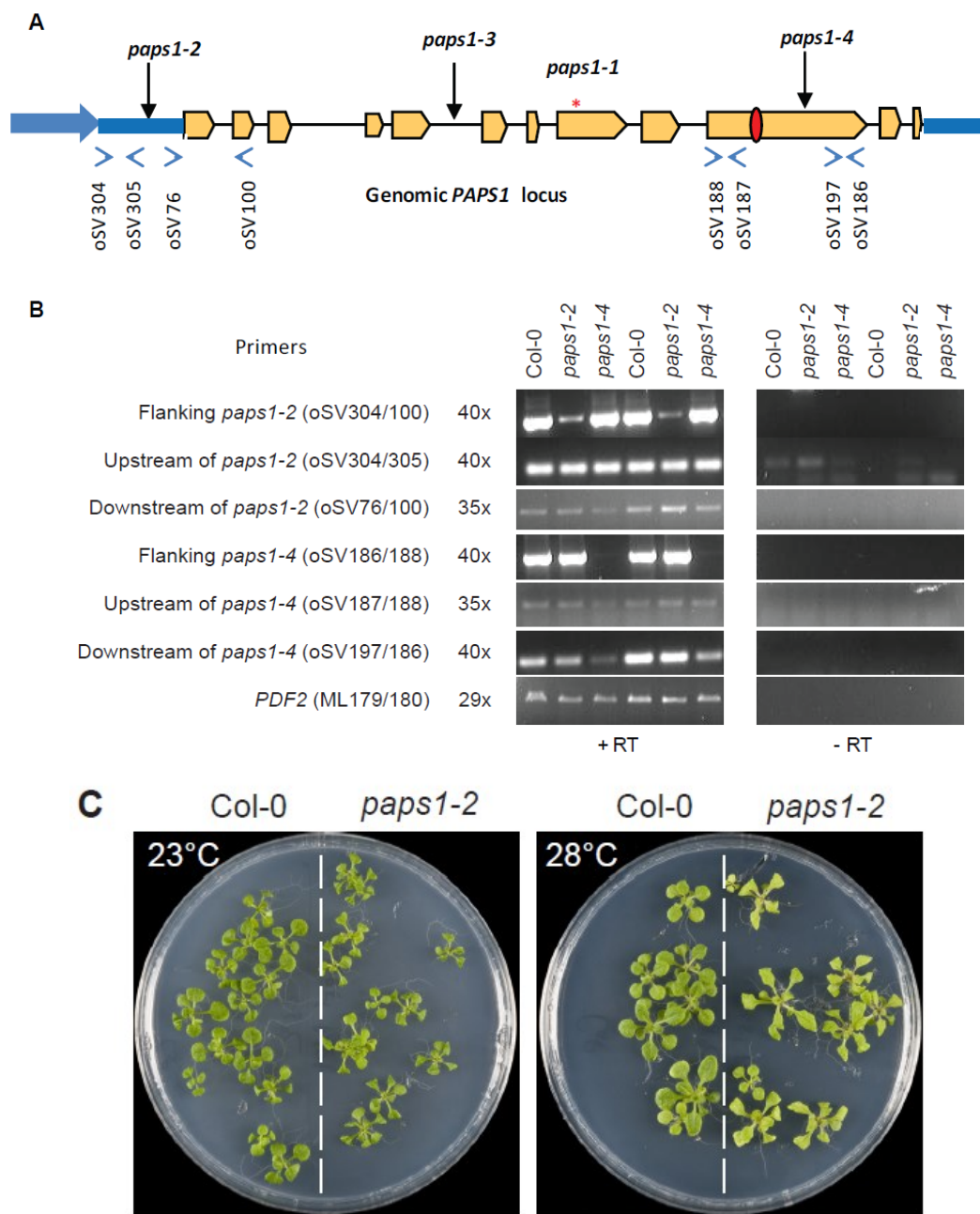
Results

- Importance of Cell Cycle Progression in Nematode-Induced Galls and Syncytia. *Plant Cell*, **11**, 793-808.
- Disch, S., Anastasiou, E., Sharma, V.K., Laux, T., Fletcher, J.C. and Lenhard, M.** (2006) The E3 ubiquitin ligase BIG BROTHER controls Arabidopsis organ size in a dosage-dependent manner. *Curr Biol*, **16**, 272-279.
- Dodds, P.N. and Rathjen, J.P.** (2010) Plant immunity: towards an integrated view of plant-pathogen interactions. *Nat Rev Genet*, **11**, 539-548.
- Dornelas, M.C., Patreze, C.M., Angenent, G.C. and Immink, R.G.** (2010) MADS: the missing link between identity and growth? *Trends Plant Sci*.
- Eckmann, C.R., Rammelt, C. and Wahle, E.** (2011) Control of poly(A) tail length. *Wiley Interdiscip Rev RNA*, **2**, 348-361.
- Eriksson, S., Stransfeld, L., Adamski, N.M., Breuninger, H. and Lenhard, M.** (2010) KLUH/CYP78A5-dependent growth signaling coordinates floral organ growth in Arabidopsis. *Curr Biol*, **20**, 527-532.
- Falk, A., Feys, B.J., Frost, L.N., Jones, J.D.G., Daniels, M.J. and Parker, J.E.** (1999) EDS1, an essential component of R gene-mediated disease resistance in Arabidopsis has homology to eukaryotic lipases. *P Natl Acad Sci USA*, **96**, 3292-3297.
- Feys, B.J., Moisan, L.J., Newman, M.A. and Parker, J.E.** (2001) Direct interaction between the Arabidopsis disease resistance signaling proteins, EDS1 and PAD4. *Embo J*, **20**, 5400-5411.
- Herr, A.J., Molnar, A., Jones, A. and Baulcombe, D.C.** (2006) Defective RNA processing enhances RNA silencing and influences flowering of Arabidopsis. *Proc Natl Acad Sci U S A*, **103**, 14994-15001.
- Hunt, A.G.** (2008) Messenger RNA 3' end formation in plants. *Curr Top Microbiol Immunol*, **326**, 151-177.
- Hunt, A.G., Xu, R., Addepalli, B., Rao, S., Forbes, K.P., Meeks, L.R., Xing, D., Mo, M., Zhao, H., Bandyopadhyay, A., Dampanaboina, L., Marion, A., Von Lanken, C. and Li, Q.Q.** (2008) Arabidopsis mRNA polyadenylation machinery: comprehensive analysis of protein-protein interactions and gene expression profiling. *BMC Genomics*, **9**, 220.
- Jenik, P.D. and Irish, V.F.** (2000) Regulation of cell proliferation patterns by homeotic genes during Arabidopsis floral development. *Development*, **127**, 1267-1276.
- Jirage, D., Tootle, T.L., Reuber, T.L., Frost, L.N., Feys, B.J., Parker, J.E., Ausubel, F.M. and Glazebrook, J.** (1999) Arabidopsis thaliana PAD4 encodes a lipase-like gene that is important for salicylic acid signaling. *Proc Natl Acad Sci U S A*, **96**, 13583-13588.
- Johnson, K. and Lenhard, M.** (2011) Genetic control of plant organ growth. *New Phytol*, **191**, 319-333.
- Koch, E. and Slusarenko, A.** (1990) Arabidopsis is susceptible to infection by a downy mildew fungus. *Plant Cell*, **2**, 437-445.
- Kondrashov, A., Meijer, H.A., Barthet-Barateig, A., Parker, H.N., Khurshid, A., Tessier, S., Sicard, M., Knox, A.J., Pang, L. and De Moor, C.H.** (2012) Inhibition of polyadenylation reduces inflammatory gene induction. *RNA*, **18**, 2236-2250.
- Lawton, K., Weymann, K., Friedrich, L., Vernooij, B., Uknes, S. and Ryals, J.** (1995) Systemic acquired resistance in Arabidopsis requires salicylic acid but not ethylene. *Mol Plant Microbe Interact*, **8**, 863-870.
- Li, Q., Von Lanken, C., Yang, J., Lawrence, C.B. and Hunt, A.G.** (2000) The yeast polyadenylate-binding protein (PAB1) gene acts as a disease lesion mimic gene when expressed in plants. *Plant Mol Biol*, **42**, 335-344.
- Liang, W., Li, C., Liu, F., Jiang, H., Li, S., Sun, J. and Wu, X.** (2009) The Arabidopsis homologs of CCR4-associated factor 1 show mRNA deadenylation activity and play a role in plant defence responses. *Cell Res*, **19**, 307-316.
- Liu, F., Marquardt, S., Lister, C., Swiezewski, S. and Dean, C.** (2010) Targeted 3' processing of antisense transcripts triggers Arabidopsis FLC chromatin silencing. *Science*, **327**, 94-97.
- Mandel, C.R., Bai, Y. and Tong, L.** (2008) Protein factors in pre-mRNA 3'-end processing. *Cell Mol Life Sci*, **65**, 1099-1122.

- Meeks, L.R., Addepalli, B. and Hunt, A.G.** (2009) Characterization of genes encoding poly(A) polymerases in plants: evidence for duplication and functional specialization. *PLoS One*, **4**, e8082.
- Millevoi, S. and Vagner, S.** (2010) Molecular mechanisms of eukaryotic pre-mRNA 3' end processing regulation. *Nucleic Acids Res*, **38**, 2757-2774.
- Mou, Z., Fan, W. and Dong, X.** (2003) Inducers of plant systemic acquired resistance regulate NPR1 function through redox changes. *Cell*, **113**, 935-944.
- Mur, L.A., Kenton, P., Lloyd, A.J., Ougham, H. and Prats, E.** (2008) The hypersensitive response; the centenary is upon us but how much do we know? *J Exp Bot*, **59**, 501-520.
- Pieterse, C.M., Leon-Reyes, A., Van der Ent, S. and Van Wees, S.C.** (2009) Networking by small-molecule hormones in plant immunity. *Nat Chem Biol*, **5**, 308-316.
- Powell, A.E. and Lenhard, M.** (2012) Control of organ size in plants. *Curr Biol*, **22**, R360-367.
- Sauret-Gueto, S., Schiessl, K., Bangham, A., Sablowski, R. and Coen, E.** (2013) JAGGED controls Arabidopsis petal growth and shape by interacting with a divergent polarity field. *PLoS Biol*, **11**, e1001550.
- Schmidt, M.J. and Norbury, C.J.** (2010) Polyadenylation and beyond: emerging roles for noncanonical poly(A) polymerases. *Wiley Interdiscip Rev RNA*, **1**, 142-151.
- Simpson, G.G., Dijkwel, P.P., Quesada, V., Henderson, I. and Dean, C.** (2003) FY is an RNA 3' end-processing factor that interacts with FCA to control the Arabidopsis floral transition. *Cell*, **113**, 777-787.
- Slesak, I., Libik, M., Karpinska, B., Karpinski, S. and Miszalski, Z.** (2007) The role of hydrogen peroxide in regulation of plant metabolism and cellular signalling in response to environmental stresses. *Acta Biochim Pol*, **54**, 39-50.
- Staswick, P.E., Tiryaki, I. and Rowe, M.L.** (2002) Jasmonate response locus JAR1 and several related Arabidopsis genes encode enzymes of the firefly luciferase superfamily that show activity on jasmonic, salicylic, and indole-3-acetic acids in an assay for adenylation. *Plant Cell*, **14**, 1405-1415.
- Stransfeld, L., Eriksson, S., Adamski, N.M., Breuninger, H. and Lenhard, M.** (2010) KLUH/CYP78A5 promotes organ growth without affecting the size of the early primordium. *Plant Signal Behav*, **5**, 982-984.
- Thordal-Christensen, H., Zhang, Z., Wei, Y. and Collinge, D.B.** (1997) Subcellular localization of H₂O₂ in plants. H₂O₂ accumulation in papillae and hypersensitive response during the barley—powdery mildew interaction. *Plant J*, **11**, 1187–1194.
- Tor, M., Gordon, P., Cuzick, A., Eulgem, T., Sinapidou, E., Mert-Turk, F., Can, C., Dangl, J.L. and Holub, E.B.** (2002) Arabidopsis SGT1b is required for defense signaling conferred by several downy mildew resistance genes. *Plant Cell*, **14**, 993-1003.
- Tsukaya, H., Byrne, M.E., Horiguchi, G., Sugiyama, M., Van Lijsebettens, M. and Lenhard, M.** (2013) How do 'housekeeping' genes control organogenesis?-unexpected new findings on the role of housekeeping genes in cell and organ differentiation. *J Plant Res*, **126**, 3-15.
- Vi, S.L., Trost, G., Lange, P., Czesnick, H., Rao, N., Lieber, D., Laux, T., Gray, W.M., Manley, J.L., Groth, D., Kappel, C. and Lenhard, M.** (2013) Target specificity among canonical nuclear poly(A) polymerases in plants modulates organ growth and pathogen response. *Proc Natl Acad Sci U S A*, **110**, 13994-13999.
- Zhang, J., Addepalli, B., Yun, K.Y., Hunt, A.G., Xu, R., Rao, S., Li, Q.Q. and Falcone, D.L.** (2008) A polyadenylation factor subunit implicated in regulating oxidative signaling in Arabidopsis thaliana. *PLoS One*, **3**, e2410.
- Zhou, N., Tootle, T.L. and Glazebrook, J.** (1999) Arabidopsis PAD3, a gene required for camalexin biosynthesis, encodes a putative cytochrome P450 monooxygenase. *Plant Cell*, **11**, 2419-2428.
- Zhou, N., Tootle, T.L., Tsui, F., Klessig, D.F. and Glazebrook, J.** (1998) PAD4 functions upstream from salicylic acid to control defense responses in Arabidopsis. *Plant Cell*, **10**, 1021-1030.

Supporting Information

Supporting Figures

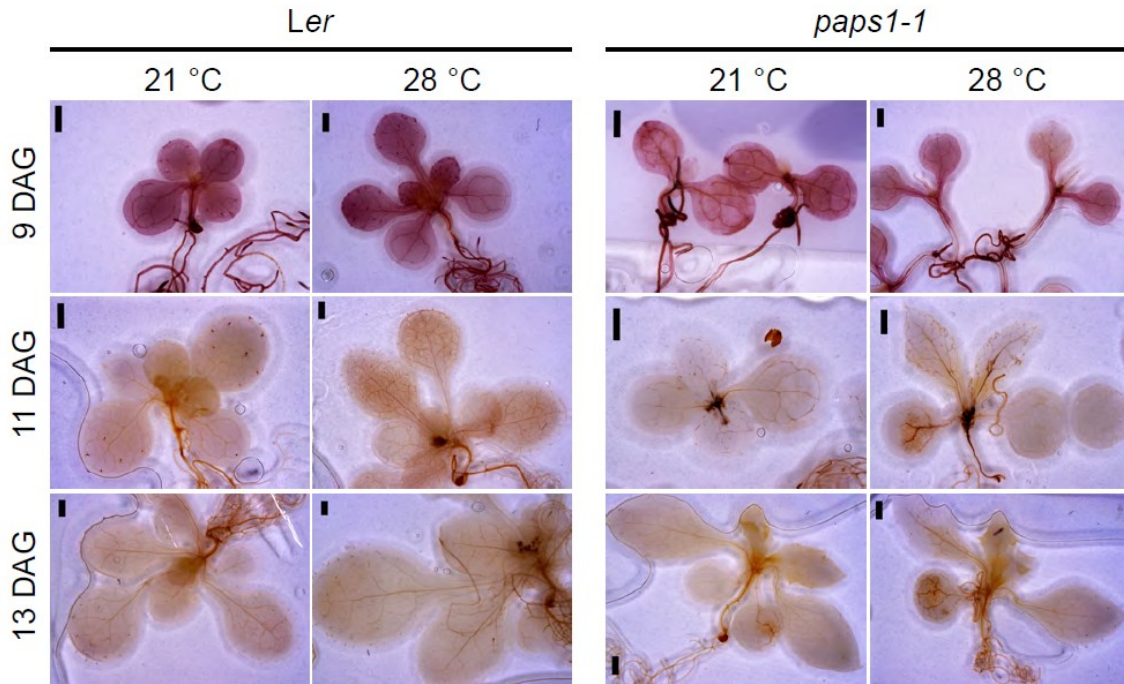
**Supporting Figure 1: Molecular characterization of *paps1* mutant alleles.**

(A) Schematic representation of the *PAPS1* locus indicating the positions of the primers used for the RT-PCRs shown in (B).

(B) Agarose-gel electrophoresis of RT-PCR products on RNA from the indicated genotypes. The primer combinations and the cycle numbers used are shown on the left.

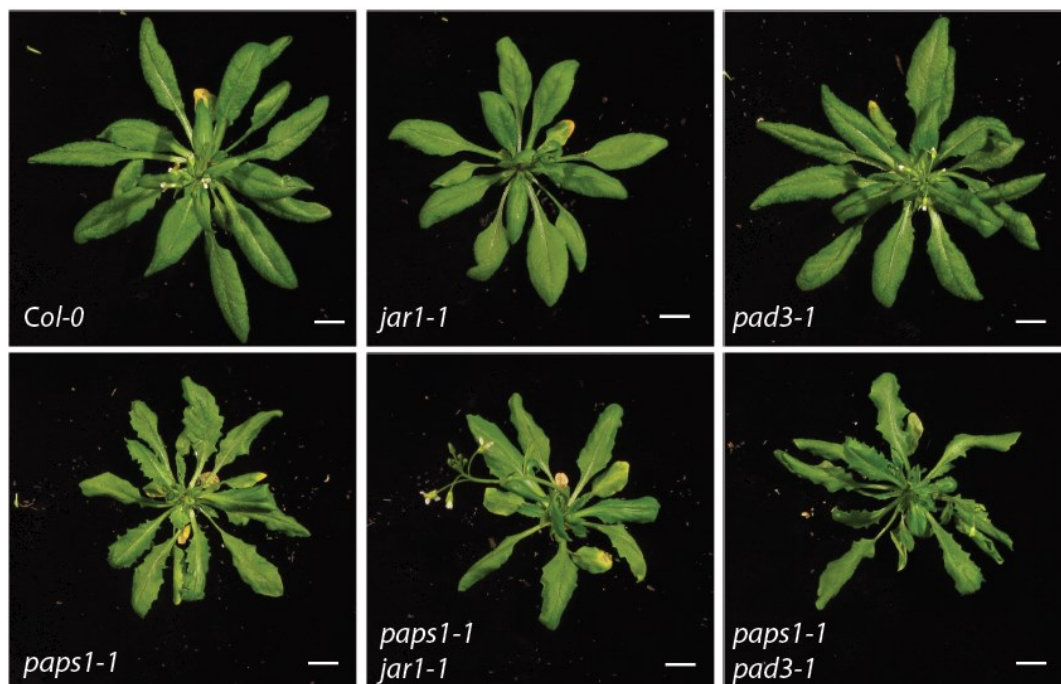
(C) Phenotype of Col-0 and *paps1-2* seedlings grown under different temperatures.

Results



Supporting Figure 2: *paps1-1* mutants do not accumulate hydrogen peroxide.

3'3' Diaminobenzidine staining of *Ler* and *paps1-1* plants of different ages grown in either 20 or 28 °C. Scale bars are 2 mm.



Supporting Figure 3: The constitutive immune response in *paps1-1* is independent of *JAR* and *PAD3* activities.

Whole-plant images of the indicated genotypes. Scale bars are 1 cm.

Supporting Experimental Procedures

Genotyping mutant alleles For genotyping point-mutant alleles, the following primers were used:

Name		Primer	length PCR product	cut by
<i>paps1-1</i>	dCAPS	oSV126/166	210	mutant by EcoRI
<i>pad4-1</i>	CAPS	GTO295/296	452	WT by BsmFI
<i>npr1-1</i>	dCAPS	GTO181/182	286	WT by NlaIII
<i>jar1-1</i>	dCAPS	GTO158/159	130	WT by BglI
<i>ap2-1</i>	dCAPS	GTO23/24	309	mutant by Hpy188I
<i>eds1-2</i>	Indel	GTO293/294	WT 1359, mutant 420	

For genotyping T-DNA insertion alleles, gene-specific primers (called LP and RP primer) that flank the T-DNA insertion site, and a T-DNA right border primer (BP) were used. These are listed below

Oligonucleotide name	Sequence	Description
oSV166	TAATGCCCATCATTACTCCTGCGAAT	genotype <i>paps1-1</i>
oSV126	GCTTTGTTTGATTCCATAGC	genotype <i>paps1-1</i>
GTO295	AGATTCAATGGTACAAAGATCGTT	genotype <i>pad4-1</i>
GTO296	TCTCGCCTCATCCAACCACTCTT	genotype <i>pad4-1</i>
GTO181	ATAAGGCACTTGACTCGGATG	genotype <i>npr1-1</i>
GTO182	AGTGCGGTTCTACCTTCCAA	genotype <i>npr1-1</i>
GTO158	TTTCTCAGTGTGTGTGTTTTTGATCATCAGAT	genotype <i>jar1-1</i>
GTO159	CTGTTTCTGAAGGCAAAAGCAGTGCAGAA	genotype <i>jar1-1</i>
GTO293	ATATTGTCCCTCGGATTATGCT	genotype <i>eds1-2</i>
GTO294	CTCCAAGCATCCCTTCTAATGT	genotype <i>eds1-2</i>
oSV100	TCTCGTACAATCCAACATCTTG	genotype <i>paps1-2</i> LP primer
oSV91	AGTGTCCAACCTCTCCAAGTTTC	genotype <i>paps1-2</i> RP primer
oSV126	GCTTTGTTTGATTCCATAGC	genotype <i>paps1-3</i> LP primer
oSV78	TGGGACCTAGACATGCAACTAG	genotype <i>paps1-3</i> RP primer
oSV77	TGTGAAGTAAACTCAACCCAGAC	genotype <i>paps1-4</i> LP primer
oSV79	GGTCTTCTATCAATGGAATTG	genotype <i>paps1-4</i> RP primer
oSV120	ACATGGAGATGTTGAACTGCC	genotype <i>paps2-3</i> LP primer
oSV121	CCACTGTTCCACGTATATCAAAC	genotype <i>paps2-3</i> RP primer
GTO151	TTGAAACCTTCGAAATATAAG	genotype <i>pad3-1</i> LP Primer
GTO152	GTGGTGAAGAAGCTTGAAGA	genotype <i>pad3-1</i> RP Primer
ML437	TGGTTCACGTAGTGGGCCATCG	BP primer for SALK-TDNA
oSV139	AACGTCCGCAATGTGTTATTAAGTTGTC	BP primer for Ws-TDNA
ML438	TTCATAACCAATCTCGATACAC	BP primer for SAIL-TDNA

Results

qRT-PCR Primers used for the different genes are listed below.

Gene Name	AGI code		Sequence
PDF2	At1g13320	fw	GCATTTCACTCCTCTGGCTAAG
		rev	GGCACTTGGGTATGCAATATG
PR1	AT2G14610	fw	TGTGCCAAAGTGAGGTGTAAC
		rev	TGATGCTCCTTATTGAAATACTGATAC
PR2	AT3G57260	fw	GGTGTCGAGACCGGTTGGC
		rev	CCCTGGCCTTCTCGGTGATCCA
SID2	AT1G74710	fw	TGAAGCAACAACATCTCTACAGGCG
		rev	CCCGAAAAGGCTCGGCCCAT
	AT5G62730	fw	TCTTCGCCGCTTCTATAAC
		rev	AACTCCATCATACCGGCTAGAG
	At1g09500	fw	CTCCTACAGAAACAAGCCTTAGAG
		rev	GACCTGCAAGGAATAACAAGTAAC
	At5g24780	fw	AATGGGCTGATTTGGTTGAG
		rev	GTGCCAAAACGGCTACAAAG

Phenotypic analysis, measurements of organ and cell sizes

Petals were dissected from the 6th to 15th flowers and used for measurements. For leaves, the 4th and 5th leaves of plants at the bolting stage or the entire rosette were taken for measurements. To measure organ size, the organs were placed with forceps onto Sellotape. Once all organs were collected, the tape was stuck onto a black Perspex sheet for petals or on a blank white paper sheet for leaves. The organs were scanned with a resolution of 3600 dpi in greyscale (8-bit, petals) or 1200 dpi colour image (leaves) using the HP Scanjet 4370. The organ size was then measured using the Image Processing and Analysis in Java (ImageJ) software (<http://rsbweb.nih.gov/ij/>).

2.3. Additional characterization of the *paps1-1* mutants

2.3.1. Double mutants with *ahg2-1* are embryo-lethal

As mentioned in the introduction deadenylation in plants is catalyzed by two enzymatic complexes: CCR4 and PARN, and it is believed that CCR4 is the major cytoplasmic deadenylase whereas PARN deadenylates only a subset of mRNAs (Reverdatto *et al.*, 2004). To address the question whether accumulation of the PARN targets has any effect on the *paps1-1* mutation, it was combined with the *ahg2-1* mutation.

In a population of 100 F2 plants of a cross of homozygous *paps1-1* and *ahg2-1* single mutants no homozygous double mutants could be found. This suggested embryo lethality of the double mutants. To confirm this, the offspring of *paps1-1/paps1-1; agh2-1/+* plants were examined. Approximately 25% (24 out of 96) of the seeds did not germinate on MS plates and also 25 % of the seeds inside the siliques appeared as dark-brown flat chips (Fig. 2.1), proving their lethality.

2.3.2. The BR pathway is not affected in *paps1-1* mutants

As shown in chapter 2.1 and 2.2 the *paps1-1* mutant leaves exhibit an ectopic pathogen response that is dependent on the *EDS1/PAD4* pathway, but not on the SA or JA pathway. An influence of a lack of phytoalexins (plant defense molecules) could not be observed either.

In addition to the tested mutants, we asked whether the brassinosteroid pathway, another important growth and defense hormone class, is altered in the *paps1-1* mutants. We therefore introgressed the *bes1-D* mutation into the *paps1-1* mutants (Fig. 2.2). BES1 is a semidominant suppressor of BRI1, a receptor kinase that transduces the BR signal to downstream signaling components. *Bes1-D* is a gain of function mutant that exhibits constitutive BR response phenotypes, including long and bending petioles, curly leaves, accelerated senescence, and constitutive expression of BR response genes (Yin *et al.*, 2002). As the *bes1-D paps1-1* double mutants showed only an additive phenotype of both single mutants, ectopic BR signalling cannot rescue the constitutive immune response in *paps1-1* mutants.



Fig. 2.1: *paps1-1 ahg2-1* double mutants are embryo lethal.

Seeds from one silique of a *paps1-1* homozygous *ahg2-1* heterozygous mutant, putative homozygous double mutant seeds right appear as brown chips. Scale bar is 500 μ m.

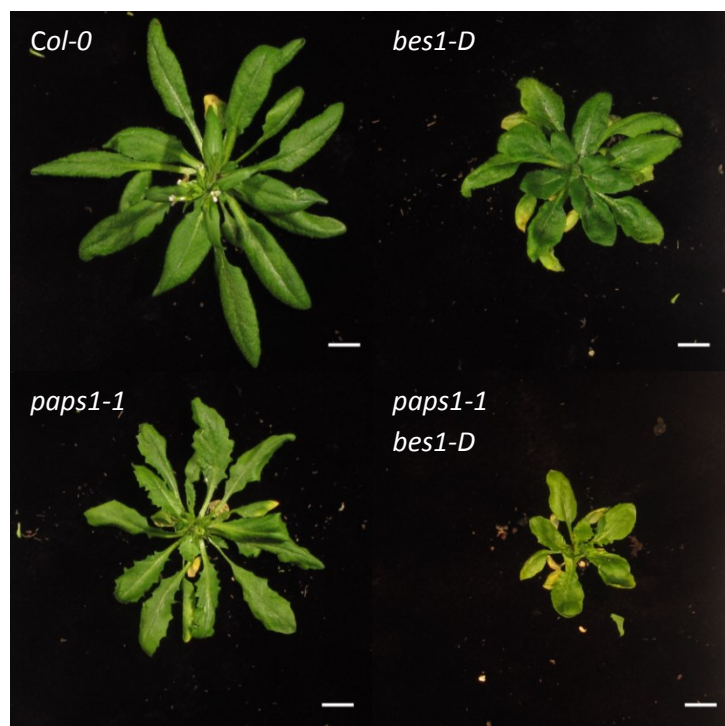


Fig. 2.2 The constitutive immune response in *paps1-1* is independent of BRI1

Whole plant images of the depicted genotypes. Scale bars are 1 cm.

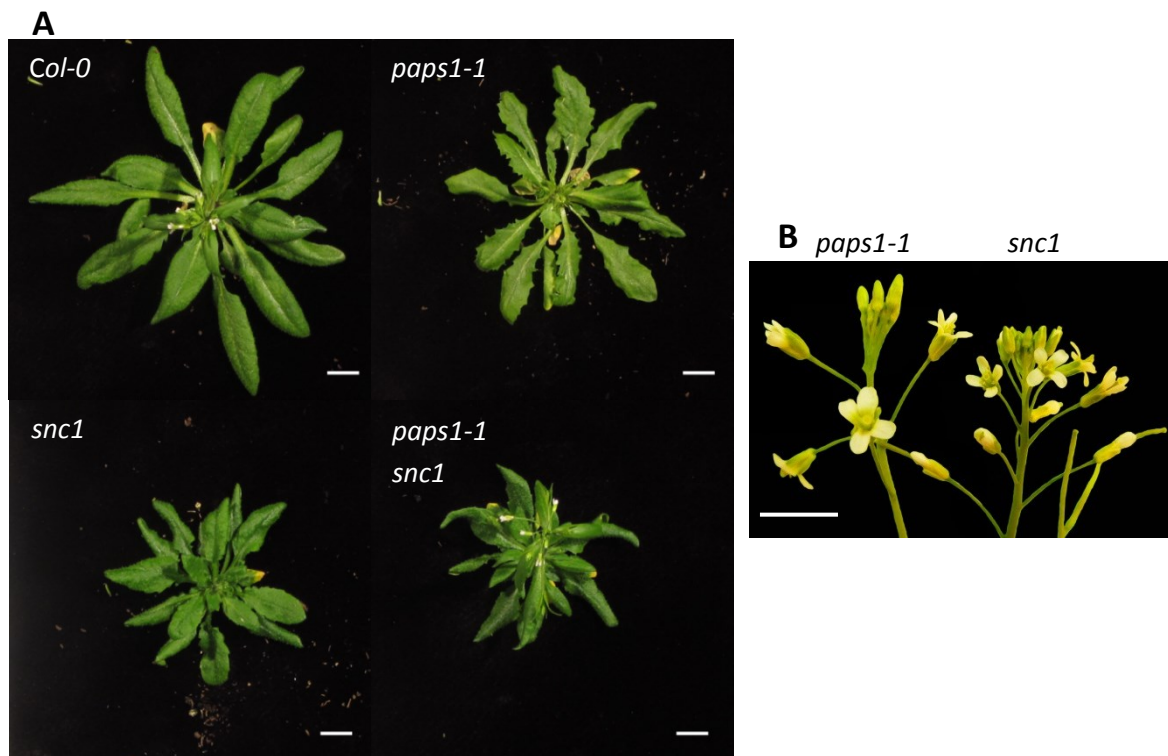


Fig. 2.3 phenotypic similarities of *paps1-1* to *snc1* mutants

(A) whole plant images of the indicated genotypes

(B) flowers of *paps1-1* and *snc1* plants

Scale bars are 1 cm

A constitutive immune response was already observed in the *suppressor of npr1, constitutive-1* (*snc1*) mutants (Li *et al.*, 2001). In *snc1*, one of the TIR-NB-LRR-type R genes of the *RPP5* resistance gene cluster, a receptor of pathogen-derived ligands, contains a point mutation. This mutation renders the receptor active and leads to constitutive expression of *PR* genes (Zhang *et al.*, 2003). The *RPP5* pathway is dependent on EDS1 function, therefore the *snc1* mutant phenotypes are suppressed completely by *eds1* mutations. However, this pathway also requires the signal molecule SA, but does not employ NPR1 function (Li *et al.*, 2001). Because of its molecular similarities to the *paps1-1* mutant we compared the phenotypes and combined the two mutations to see whether there is any effect. Certain phenotypic similarities were observed between the two mutants: both of them have a small stature with smaller leaves whereas flower size is increased in *paps1-1* mutants but not in *snc1* mutants (Fig. 2.3). This is likely due to the temperature sensitivity of the PAPS1 protein rather than temperature sensitivity of the affected process.

2.3.3. redox-sensitive GFP reveals more oxidized chloroplasts in *paps1-1* mutants

As already mentioned, pathogen-responses in plants are accompanied by massive transcriptional and metabolic reprogramming, where the change in the intracellular redox-status plays an important role. As described in chapter 2.2 no accumulation of H₂O₂ was observed in the *paps1-1* mutants by DAB staining. Could the changes in the intracellular redox-status be more subtle or only limited to cell compartments? This question was addressed by introducing a modified version of GFP, the redox-sensitive GFP (roGFP2) into the *paps1-1* mutants localized in either the cytoplasm or plastids (Hansons *et al.*, 2004; Dooley *et al.*, 2004; Schwarzländer *et al.*, 2008; Lehmann *et al.*, 2008). The emission maxima of this reporter depend on the excitation wavelength and the local redox potential. The reduced form emits most light when excited with light of a wavelength of 488 nm and the oxidized form at 405 nm. This makes it possible to use the ratio of fluorescence emission at 527 nm after excitation with 405 and 480 nm as a measure of the local redox potential. There was no difference in this ratio between mutant and wild-type leaves for the cytoplasmic reporter (Fig. 2.4A, Fig. 2.5). By contrast, the spectral ratio for the chloroplast-localized reporter was significantly altered in *paps1-1* mutant leaves. It changed by 50% towards the oxidized form, indicative of a more oxidizing environment in the mutant chloroplasts than in wild type (Fig. 2.6, Fig. 2.4B).

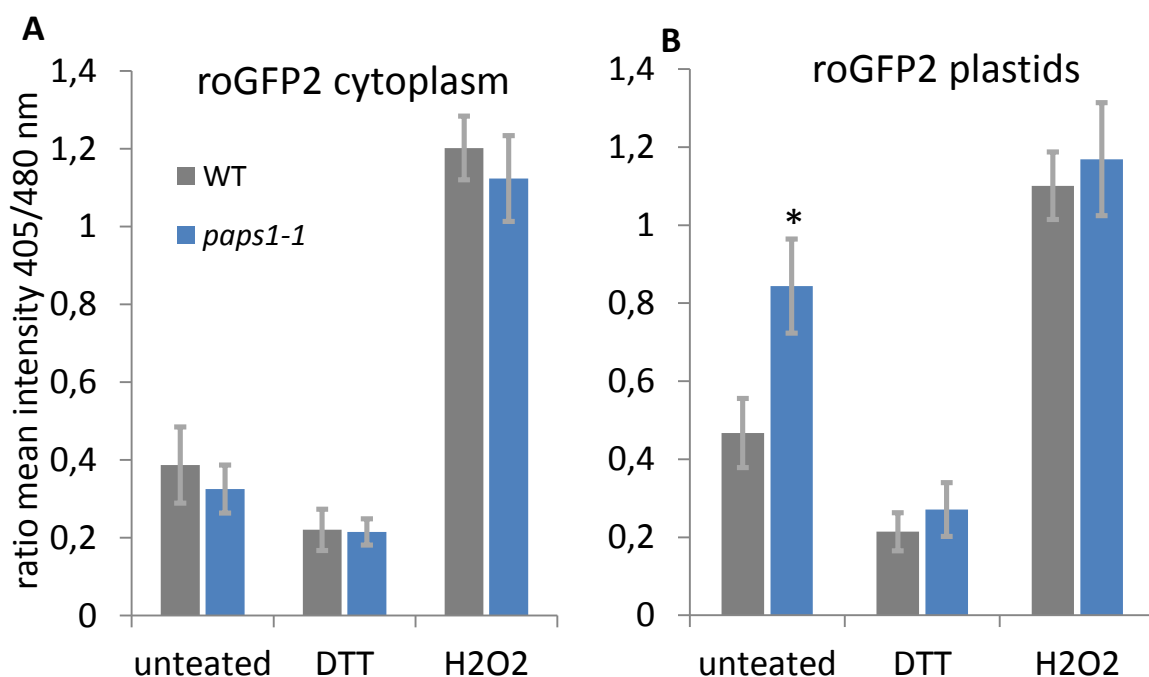


Fig. 2.4: Quantification of roGFP2 fluorescence in *paps1-1* and *Ler* leaves in cytoplasm (A) and plastids (B).

* Difference is significant at $p < 0.005$ (t-test), DTT – dithiothreitol treated leaves as control for reduced form, H₂O₂ – hydrogen peroxide treated leaves used as control for oxidized form

Results

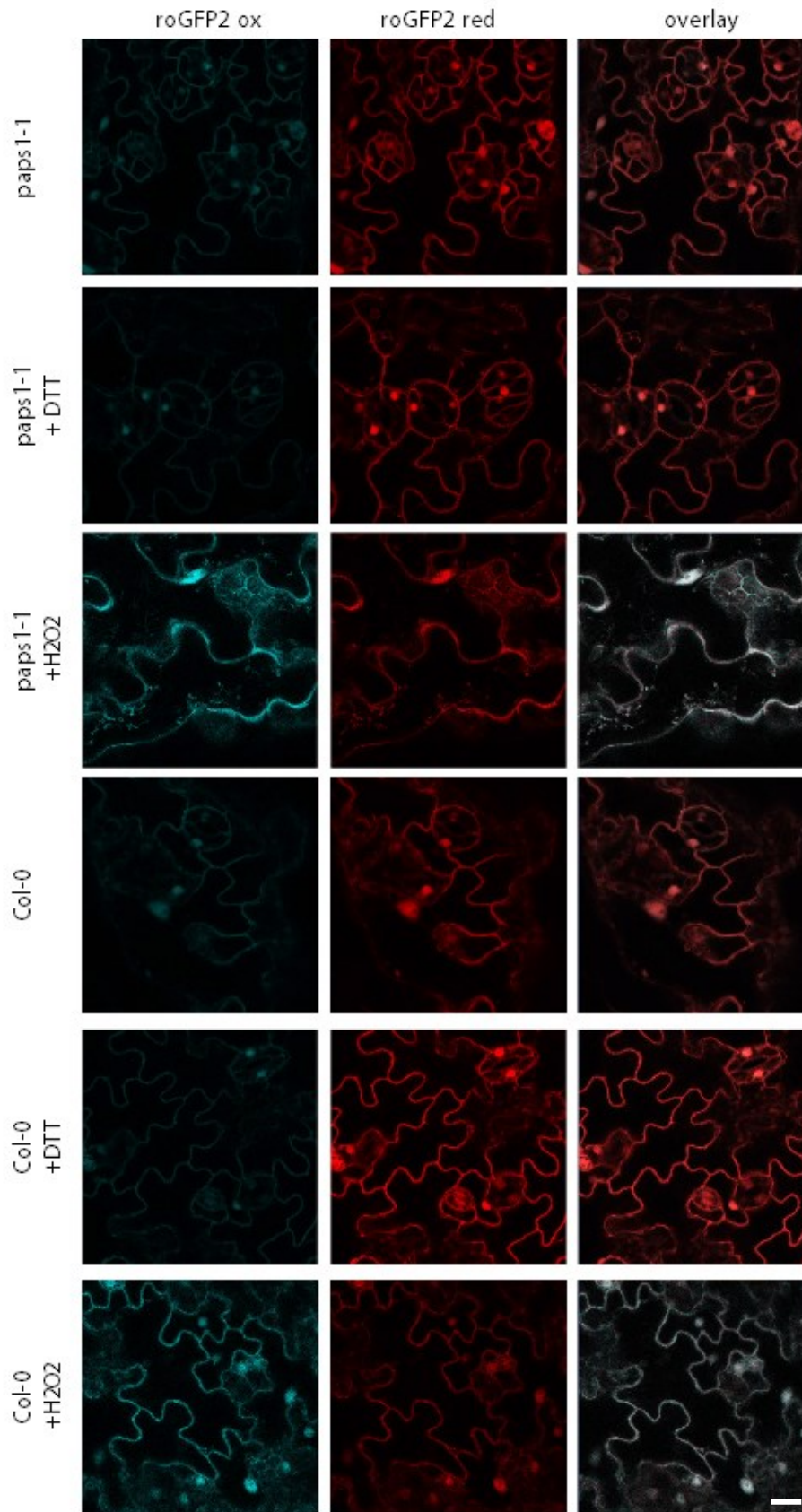


Fig. 2.5: False-colour images of cytoplasmic roGFP2 fluorescence in *Col-0* and *paps1-1* leaves.

ox – oxidized form (excitation wavelength 405 nm) red – reduced form (excitation wavelength 488 nm) Scale bar is 10 μ m.

Results

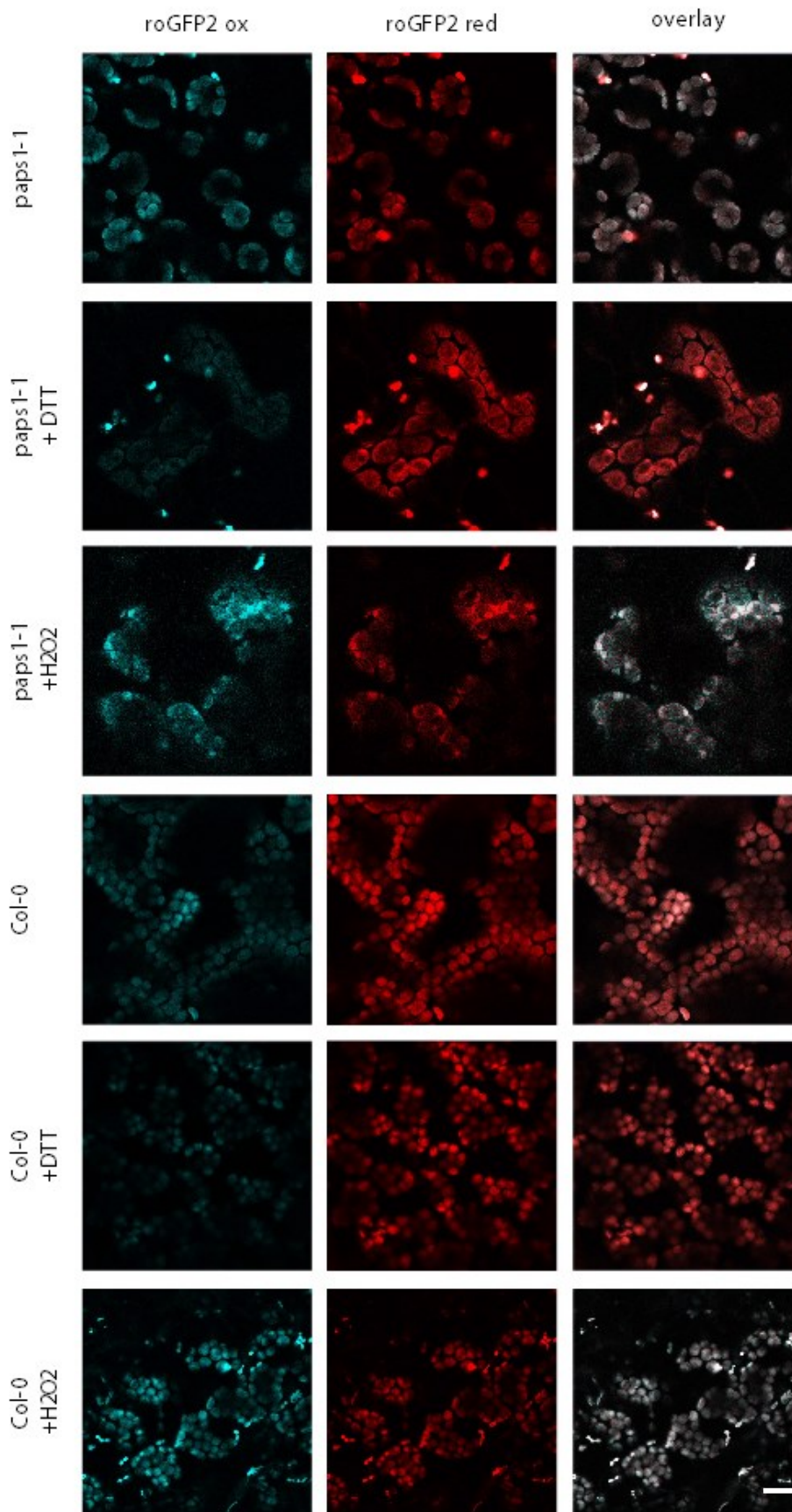


Fig. 2.6: False-colour images of plastidal roGFP2 fluorescence in *Col-0* and *paps1-1* leaves.
ox – oxidized form (excitation wavelength 405 nm) red – reduced form (excitation wavelength 488 nm) Scale bar is 10 μ m.

2.3.4. RNA sequencing

So far, only the *SAUR* genes were shown to be molecularly affected by the *paps1-1* mutation, changing their poly(A) tail and therefore influencing in part the growth phenotype (Chapter 2.1). However, considering the different growth defects in flowers and leaves, and the ectopic pathogen answer in the *paps1-1* mutant leaves it is likely that additional transcripts are affected by the *paps1-1* mutation changing their poly(A) tail. To address this question I made use of an RNA sequencing approach coupled with fractionation of the mRNA according to their poly(A) tail length. Total RNA is incubated with biotinylated oligod(T) primers and paramagnetic streptavidin beads. The biotin part of the primer binds the magnetic beads whereas the oligod(T) part hybridizes with the poly(A) tails of the mRNA. The beads can be captured with a magnet to remove unbound RNA or other molecules in the supernatant. Subsequently a low stringency elution buffer recovers mRNAs with only short (<50 adenosines [A]) poly(A) tails whereas a following elution with water recovers the remaining fraction (>50 A). As internal quality control we generated RNAs with defined poly(A) tail lengths of 30 A, 75 A and 134 A and added those to each sample before fractionation. As mentioned before, the *paps1-1* mutant protein is temperature sensitive. To reach more severe molecular effects, the plants were shifted from 21 °C to 28 °C two hours prior harvesting. After aligning the sequence reads to the *Arabidopsis* reference genome, fpkm (fragments per kilobase of exon per million fragments mapped) values were calculated for each transcript as a measure of its relative abundance in the fraction. The ratio of fpkm values from the fraction with short poly(A) tails and that with long poly(A) tails (termed the short and long fractions from here on) was then determined as a proxy for the distribution of poly(A)-tail lengths on each transcript.

To verify the success of the fractionation, the relative abundance of the three control RNAs was estimated by qRT-PCR in each fraction (Fig. 2.7). An equal volume of each fraction was reverse transcribed and the mean of the PCR efficiency for each primer pair to the power of $-ct$ (PCR_{eff}^{-ct}) was used as an approximate value for the abundance of the control RNAs in each fraction. As expected the 30A control was about 5.2 (wild type) and 5.1 (*paps1*) times more abundant in the short than in the long fraction. By contrast, the 75 A and 134 A fractions were about 4.1 (wild type), 4.9 (*paps1*) and 3.5 (wild type), 3.9 (*paps1*) times more abundant in the long fractions, respectively. For further verification 8 genes with an indication of altered long/short ratio based on the initial bioinformatic analysis were analysed by qPCR and their long/short ratio (as ratio of $PCR_{eff}^{-\Delta ct}$ of WT to *paps1-1*, whereas $\Delta ct = ct_{gene} - ct_{control}$) normalized to each of the spike-in control RNAs was compared to the values obtained from the RNAseq data (Fig. 2.8). Though to different extend, the trend of long/short ratio is the same in the qPCR data as in the RNAseq data. Thus, the RNA-seq values meaningfully reflect the transcript abundances in the fractions. The fractionation successfully

Results

resolved different populations of transcripts based on their poly(A)-tail lengths; the fpkm values determined by RNA-seq can then be used as estimates for the relative abundances of the transcripts in the two fractions; and the ratios of these fpkm values can be used as proxies for the poly(A)-tail length distributions of the transcripts.

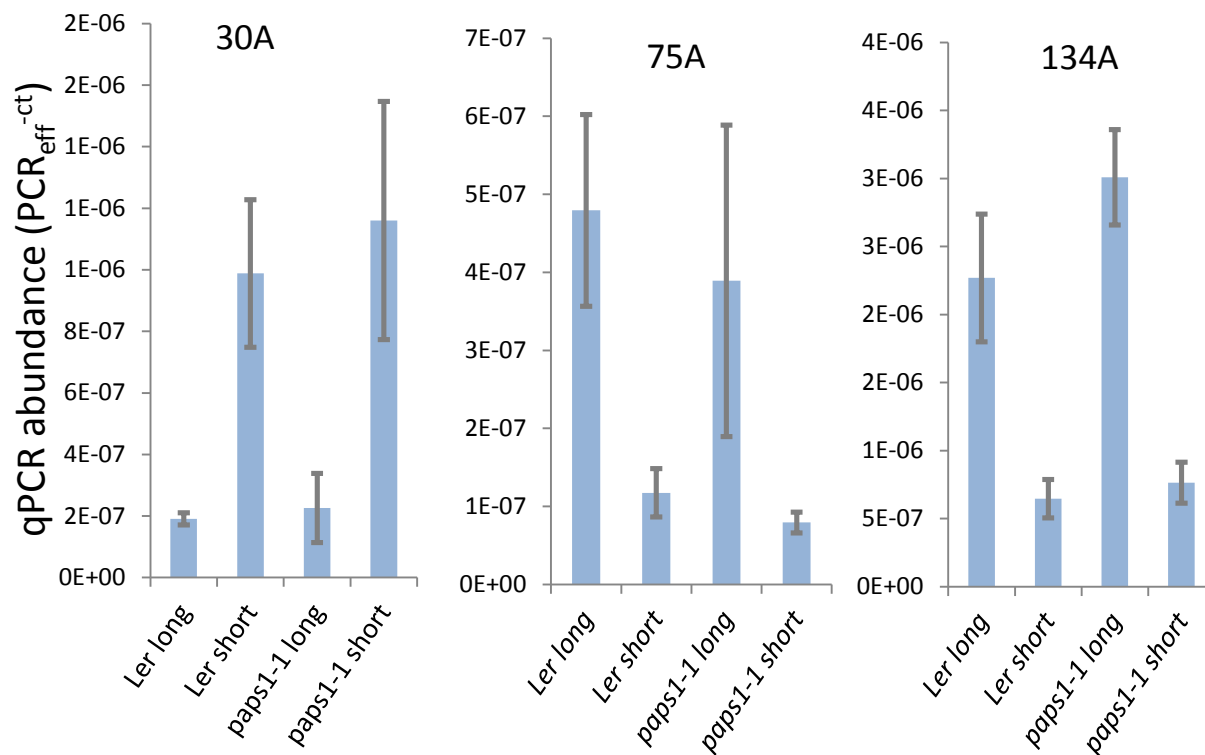


Fig. 2.7: qPCR abundance of three control RNAs in the fractionated mRNA pools

Control mRNAs with 30 As are most prominent in the short fraction whereas control mRNAs with 75 or 134 As are more prominent in the long fractions.

Values are PCR efficiency to the power of the raw ct values without any reference from 4 biological replicates.

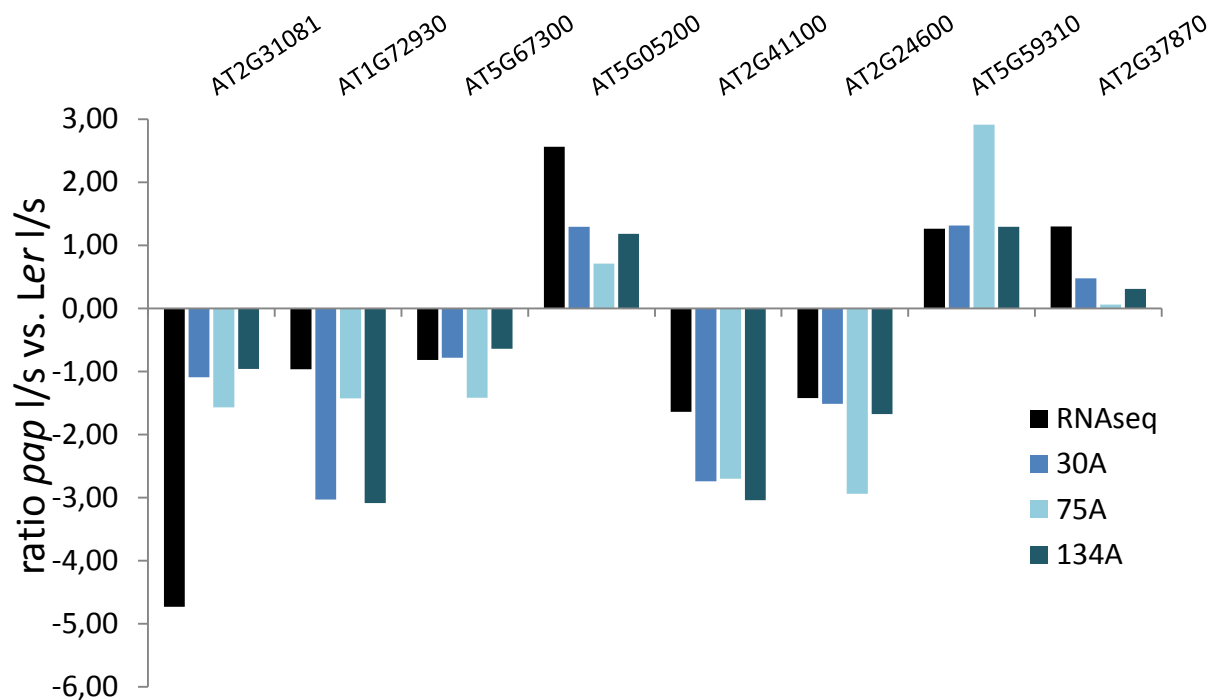


Fig. 2.8: Long/short mRNA ratios of 8 control genes in the fractionated mRNA pools

values are the ratio of *paps1-1/Ler* of the long/short ratio from each genotype from RNAseq data or qPCR values normalized to each of the three spike-in control RNAs.

If the set of transcripts with a predicted change in the poly(A)-tail length indeed reflects the biological role of PAPS1, it should be possible to identify additional functions of PAPS1 by analysing this set of transcripts. To this end, we compared both the set of 400 transcripts with the lowest P-value and the set of 400 transcripts with the strongest fold change with lists of the most strongly affected genes from published microarray experiments using MASTA (Reina-Pinto *et al.*, 2010). Amongst the 30 microarray experiments with the strongest overlap (top 5%), there were several using cold-stress treatment of plants. The most strongest overlap based on P-values was with a line involving overexpressing the thylakoid-localized form of ascorbate peroxidase (tAPX), a scavenging enzyme for the reactive oxygen species H₂O₂. Genes downregulated in tAPX overexpressing plants can be assumed to be induced by H₂O₂, while H₂O₂-repressed genes are expected to be upregulated in tAPX overexpressors. Of the 45 genes in the overlap, 41 are more strongly expressed in tAPX overexpressors than in wild-type, 4 are less strongly expressed, and all of these have a shorter poly(A) tail in *paps1* mutants. These findings are consistent with the more oxidized chloroplasts in *paps1-1* mutants shown by roGFP (Section 2.3.3) and suggest that *paps1-1* mutants accumulate more H₂O₂ in their chloroplasts contributing to the ectopic immune response.

The RNA seq data is attached as electronic file on a CD.

2.3.5. Methods and Material

Genotyping Mutant Alleles

Name		Primer	length PCR product	cut by
<i>paps1-1</i>	dCAPS	oSV126/166	210 bp	mutant cut by EcoRI
<i>ahg2-1</i>	dCAPS	oSV 292/293	168 bp	WT cut by BslI
<i>bes1-D</i>	CAPS	GTO 88/89	231 bp	WT cut by HpaII
<i>snc1</i>	CAPS	GTO 154/155	669 bp	WT cut by XbaI

For genotyping of T-DNA insertion alleles, gene-specific primers (called LP and RP primer) that flank the T-DNA insertion site, and a T-DNA right border primer (LBP) were used.

Oligonucleotide name	Sequence	Description
oSV166	TAATGCCCATCATTACTCCTGCGAAT	genotype <i>paps1-1</i>
oSV126	GCTTTGTTTGATTCCATAGC	genotype <i>paps1-1</i>
oSV292	GTGTATACTGATTGAGACCCCGA	genotype <i>ahg2-1</i>
oSV293	TAGCTACATCATCTCTCGAG	genotype <i>ahg2-1</i>
ML437	TGGTTCACGTAGTGGGCCATCG	BP primer for SALK-TDNA
GTO25	CGTAATGGCATTGTTGGGAAGT	<i>SIZ1</i> RP primer
GTO26	AGCTATGCTGTGTGGGTCCTC	<i>SIZ1</i> LP Primer
GTO88	AACCATTGCCTACTTGGGAAT	genotype <i>bes1-D</i>
GTO89	ATGGCTGTTGTTGTGCAAAT	genotype <i>bes1-D</i>
GTO154	ATTGTTGCCTCATGCGTAAT	genotype <i>snc1</i>
GTO155	GCAATCACTCATATCTAAATAGATCAG	genotype <i>snc1</i>

Molecular cloning and plant transformation For details on the construction of the plasmids for the control RNA see Appendix A.

oligo d(T) based mRNA fractionation: The mRNA fractionation was carried out with the Promega PolyAtract® System 1000 and the protocol modified as follows:

The GTC, DIL, β -mercaptoethanol (BME), biotinylated oligod(T), 0.5 x SSC and H₂O were allowed to reach room temperature. Forty-one microliter of BME were added per ml of GTC (GTC/BME) and 20.5 μ l BME were added per ml of DIL and preheated to 70 °C. The SSC buffer was diluted to a concentration of 0.085 x. In a 2 ml tube, 80 μ g of total RNA (in a maximum of 40 μ l) were mixed with 400 μ l GTC/BME, 15 μ l biotinylated oligo d(T) (Promega) and 816 μ l DIL/BME and heated to 70 °C for 5 min. Afterwards the samples were spun down at 13 000 rpm for 10 minutes at room temperature. In the meantime the paramagnetic beads were washed as suggested. The supernatant of the spun samples was added to the washed beads and the biotinylated oligod(T) was allowed to bind the beads by rotation at room temperature for 15 min. In the following step, the beads were captured

Results

and the supernatant transferred to a new tube (unbound fraction). The beads were washed three times with rotation for at least 5 min between each wash step. Afterwards, the beads were resuspended in 400 µl of 0.085 x SSC and rotated for 10 min at room temperature. The beads were captured and the eluate transferred to a new tube (short fraction). This step was repeated once (total of 800 µL). The beads were then washed with 400 µl nuclease free water (rotation for 10 min) twice and the eluates transferred to a new tube (800 µl, long fraction). All collected samples were centrifuged for 10 min at 13000 rpm, 4 °C to remove any transferred beads. Then 0.1 vol of Co-precipitant Pink buffer (BioLine) were added and the samples mixed well. Afterwards 30 µg of Co-precipitant Pink (BioLine) were added, mixed well, and 1 vol 100 % ethanol was added. The samples were incubated overnight (15 - 16 hours) at -20 °C. In the next step, the samples were centrifuged at 13000 rpm, 4 °C for 30 min. The supernatant was removed, the pellet washed with 500 µl 80 % ethanol, dried, and dissolved in 15 µl DEPC treated water.

In-vitro transcription One microgram of each linearized plasmid was diluted in 13.6 µl with water. Subsequently 2 µl 5 mM NTP solution (BioLine), 2 µl 10 x T7 transcription buffer (NEB) and 1 µl 2 mg/ml BSA (NEB) were added. The samples were mixed well and 1 µl RNase Inhibitor (Promega) and 0.4 µl T7 Polymerase (NEB) were added. The samples were incubated for 2 hours at 37 °C. Afterwards the reaction was stopped by adding 1.5 µl TURBO DNase (Ambion) and incubating for 30 min at 37 °C. Phenol:Chloroform extraction on the samples was carried out. RNA concentrations were measured with the Picodrop and a mix of all RNAs with a concentration of 1 ng/µl was made. 1 µl of this mix was added to each RNA sample before fractionation (see above).

RNA sequencing The fractionated RNA samples were sent to LGC Genomics (TGS Haus 8, Ostendstraße 25, 12459 Berlin) to be sequenced via channel single read (50 bp) on the Illumina HiSeq 2000. RNAseq evaluation (log fold change and counts per million values) as well as the top 400 list of the MASTA analysis that was done as described (Reina-Pinto *et al.*, 2010) are attached as electronic file on CD.

qRT-PCR Measurements 1 µl of each sample from the oligo d(T) fractionated mRNA was used for reverse transcription with oligo(dT)17 primers. Expression levels were analysed using a Roche LightCycler 480.

Following Primers were used:

Gene		Sequence
34A control	fw	CCGACAACCACTACCTGAGC
	rev	TCCATGCCGAGAGTGATCC

Results

75A control	fw	AGACGTTCCAACCACGTCTT
	rev	GAAGGATAGTGGGATTGTGCG
134A control	fw	CTTCGGGATAGTTCCGACCT
	rev	CAGTACCAGAAAGTGCTCCGT
At1g72930	fw	TCCGGCGATTGTTCAAGGTGATG
	rev	ATGCGAGTCCTTATGGGCCTTC
At2g31081	fw	GGAAGAGAGCCCTTCAGATTCAGG
	rev	AGAACCGTTTGGCCGTCTTTTCG
At5g67300	fw	GAAGCGTGTGGGACAAGTAAG
	rev	GACGTTGGAGTGGGCTATG
At2g41100	fw	TTCGACAAGAATGGTGTGTTCC
	rev	TCCGCTTCGTTTCATCAAGTCCTG
At2g24600	fw	TGGAAAGGGAAATCGCTTGTAGGG
	rev	TGCGGTATGGTCACCAAAGATGC
At5g59310	fw	AGTGTTTCATCGTTGCATCAGTGG
	rev	AGACATGGACTCAAGCTACTTGCC
At2g37870	fw	TCGGCGTTCCTAAACGCTGTAAC
	rev	TGTAACGTCCACATCGCTTGCC

Confocal imaging of roGFP

All images were taken with a LSM 710, AxioObserver (Zeiss) with the C-Apochromat 40x/1.20 W Korr M27 objective in multi-track mode with line switching between 405 nm and 488 nm excitation and constant emission acquisition at 527 nm wavelength. Settings were adjusted to untreated roGFP2 in the Col-0 background for cytoplasm and plastids separately and not changed for image acquisition of treated control or *paps1-1* mutant leaves in the respective compartment. Two pictures each from three different plants were taken.

Plant material were 11 day old *paps1-1/roGFP2* seedlings and 9 day old *roGFP2* seedlings grown on ½ MS plates under standard growth conditions. Dithiothreitol (DTT) and H₂O₂ controls were prepared as described in (Schwarzländer *et al.*, 2008).

Images were evaluated with the Carl Zeiss ZEN software in the following way: three different parts of each picture were selected and the values for the mean intensity and standard deviation for both channels were noted, then the ratio of oxidized/reduced mean intensity was calculated and averaged.

Results

References

- Box, M.S., Coustham, V., Dean, C. and Mylne, J.S.** (2011) Protocol: A simple phenol-based method for 96-well extraction of high quality RNA from Arabidopsis. *Plant Methods*, **7**, 7.
- Clough, S.J. and Bent, A.F.** (1998) Floral dip: a simplified method for Agrobacterium-mediated transformation of Arabidopsis thaliana. *Plant J*, **16**, 735-743.
- Dooley, C.T., Dore, T.M., Hanson, G.T., Jackson, W.C., Remington, S.J., Tsien, R.Y.** (2004) Imaging dynamic redox changes in mammalian cells with green fluorescent protein indicators. *J Biol Chem*, **279**, 22284-22293.
- Lehmann, M., Schwarzländer, M., Obata, T., Sirikantaramas, S., Burow, M., Olsen, C.E., Tohge, T., Fricker, M.D., Møller, B.L., Fernie, A.R., Sweetlove, L.J., Laxa, M.** (2008) The metabolic response of Arabidopsis roots to oxidative stress is distinct from that of heterotrophic cells in culture and highlights a complex relationship between the levels of transcripts, metabolites and flux. *Mol Plant*, **2**, 390-406.
- Li, X., Clarke, J.D., Zhan, Y., Dong, X.** (2001) Activation of an EDS1-mediated R-gene pathway in the *snc1* mutant leads to constitutive, NPR1-independent pathogen resistance. *Mol Plant-Microbe Interact*, **14**, 1131-1139.
- Reina- Pinto JJ, Voisin D, Teodor R, Yepremov A (2010)** Probing differentially expressed genes against a microarray database for in silico suppressor/enhancer and inhibitor/activator screens. *Plant J* **61**: 166-175.
- Schwarzländer, M., Fricker, M.D., Müller, C., Marty, L., Brach, T., Novak, J., Sweetlove, L.J., Hell, R., Mexer, A.J.** (2008) Confocal imaging of glutathione redox potential in living plant cells. *J Microsc*, **231**, 299-316.
- Vi, S.L., Trost, G., Lange, P., Czesnick, H., Rao, N., Lieber, D., Laux, T., Gray, W.M., Manley, J.L., Groth, D., Kappel, C. and Lenhard, M.** (2013) Target specificity among canonical nuclear poly(A) polymerases in plants modulates organ growth and pathogen response. *Proc Natl Acad Sci U S A*, **110**, 13994-13999.
- Yin, Y., Wang, Z.Y., Mora-Garcia, S., Asami, T., Chory, J.** (2002) BES1 accumulates in the nucleus in response to brassinosteroids to regulate gene expression and promote stem elongation. *Cell*, **109**, 181-191.

3. Discussion

Polyadenylation of mRNA is an essential process throughout the eukaryotic kingdom. The model plant *Arabidopsis thaliana* possesses four different poly(A) polymerases that catalyze the addition of the poly(A) tail to the pre-mRNA (Addepalli *et al.*, 2004). To our current understanding, it is not clear whether these isoforms fulfil different functions. Although poly(A) tails must exceed a minimal length to promote translation, an influence of tail length beyond this minimum is largely unknown, also it is unclear whether different PAPS are responsible for different tail-lengths (Eckmann *et al.*, 2011; Weill *et al.*, 2012). The identification of a mutant in the Poly(A) Polymerase 1 (*PAPS1*) gene led to the idea of a functional specialization amongst the different PAPS. The respective mutant plants exhibit an increase of floral organ size whereas the size of the leaves is reduced. By contrast, virtually all previously described mutants that affect organ size (except for *cincinnata* in *Antirrhinum majus*) either do so in the same manner in leaves and floral organs, or they only affect one type of organ, but not the other (Johnson and Lenhard 2011; Powell and Lenhard 2012).

3.1. Why is the *PAPS1* function different in flowers and leaves?

An intriguing feature of the *paps1-1* mutation is the opposite effect on the different plant organs. By converting sepals into ectopic leaves (through the *ap2-1* mutation) the organ-specificity of the *paps1-1* mutation was demonstrated as opposed to a position-dependent effect. It had been reported, that *PAPS1* is alternatively spliced between flowers and leaves which could be the possible reason for the opposite effects. The mRNA in flowers retains the sixth intron, leading to a truncated, putatively non-functional protein (Addepalli *et al.*, 2004). However, this result could not be confirmed, hence retention of the sixth intron is not likely to be the cause of the opposite phenotypes in flowers and leaves (Chapter 2.2). Additionally, at least for *SAUR19/24* transcripts defective polyadenylation was equally seen in leaves and flowers, arguing against wide-spread differences in isoform-target relations or suggesting that other transcripts besides growth-regulators are affected that do not or only make minor contributions to the mutant phenotype.

Two more likely explanations may account for the opposite phenotypes 1) due to different posttranslational modifications in flowers and leaves *PAPS1* forms different 3'-end processing complexes and gains differential substrate specificity or 2) the same PAPS complex targets different flower and leaf specific mRNAs in the respective organs. Amongst the targets of these modified *PAPS1* in flowers or flower-specific mRNAs might be growth repressors. When these are mis-polyadenylated, they get degraded faster and are not able to retain their growth repressing function

Discussion

in the flowers, hence these become bigger. In contrast, the modified PAPS1 in leaves targets *PR* genes. Mispolyadenylation of these leads to a constitutive activation of the *PR* genes which results in growth-retardation. Consistent with this, mutants that exhibit an ectopic pathogen response are well known to be impaired in growth as well, for example the *scn1* mutants (Li *et al.*, 2001; Chinchilla *et al.*, 2007). However, *PR1*, *PR2* and *PR5* expression levels were below the detection level in the RNA sequencing experiment but their overexpression was demonstrated by qPCR before. Consistent with this defense-related gene expression remains largely unchanged in *paps1-1* mutant flowers (Chapter 2.1). Additionally, it was shown, that when plants enter the reproductive phase, pathogen-responsive genes are downregulated by *LEAFY* (Winter *et al.*, 2011). Hence, it seems likely that floral organs have a low innate responsiveness to pathogens supporting the idea of differential mRNAs being affected in the different plant organs. As polyadenylation is an essential mechanism both explanations may be true to a certain extent: certain mRNAs are affected in both, flowers and leaves, as well as flower and leaf-specific mRNAs contributing to the phenotype in *paps1-1* mutants.

How does the *paps1-1* mutation affect gene expression? The 3'-end processing complex is in physical interaction with the transcription and splicing machinery (reviewed in [Bentley, 2014]). Mutations in PAPS1 can prevent the proper assembly of the 3'-end processing complex and therefore the interaction with either the splicing or transcription machinery and lead already to altered pre-mRNAs that can not be processed accurately. Another imaginable scenario is that the mutated PAPS protein produces poly(A) tails of the wrong length. The misregulation of flower- and leaf-specific mRNAs may result from the altered length of the poly(A) tail that inhibits proper translation as it is well known that 3'-end processing and translation are coupled. Alternatively the respective mRNAs are subject to faster degradation (Chapter 3.3) because of their incomplete poly(A) tail. A third possibility is that not only the change of poly(A) tail length, but also the choice of poly(A) site by the mutated PAPS1 protein may affect the growth regulating factors and the pathogenesis related genes. *oxt6* mutant plants lacking CPSF30 (Chapter 1.2.2), a component of the plant 3'-end processing complex, are more tolerant to oxidative stress (Zhang *et al.*, 2008). Additionally, a genome wide approach revealed a large number of Arabidopsis genes with altered poly(A) site choice in *oxt6* mutants. The authors analysed sequence motifs in and around the 3'-UTR and identified a subset of transcripts exclusively found in *oxt6* mutants that are polyadenylated on sites that lack the near upstream element (NUE, Chapter 1.2.1). Poly(A) site choice may also be changed in *paps1-1* mutant plants. Again, the poly(A) site choice of general growth repressing or enhancing factors can be altered or flower- and leaf-specific transcripts might be affected leading to the phenotype. Following this pathway, alternative polyadenylation can ultimately lead to removal or inclusion of novel regulatory elements as microRNA binding sites in the respective growth-

Discussion

influencing genes. At least for SAUR19/24 transcripts it was shown, that the poly(A) site is largely the same in wildtype and mutant plants and that the transcripts differ in their poly(A) tail length, arguing against APA.

In *paps1-1* mutant petals cell size is increased by 21%, yet overall the petals are almost two-fold larger than wild type. Mutant petals are growing and dividing for a longer period of time. Additionally the size of the early primordium and the number of founder cells appear to be increased in *paps1-1* mutants (Chapter 2.1). Therefore, PAPS1 limits the duration of the petal growth period and founder-cell recruitment into the emerging organs. Polyadenylation of cell-cycle gene mRNAs is a crucial feature for proper cell division. Mutations in RNA Pol II in *Drosophila melanogaster* lead to alternative polyadenylation of the cell cycle gene *polo*, a protein kinase with various functions in cell division. Transgenic flies lacking the distal *polo* pA site died with severe abdominal abnormalities (Moreira, 2011). As mentioned before, alternative poly(A) site choice by the mutated PAPS1 could lead to altered expression of cell-cycle regulating genes, causing the increase of cells in the petal primordia. Consistent with this, a change in expression or tail length of cell-cycle related genes could not be observed in the mutant leaves based on RNA sequencing. It will be interesting to analyse whether mispolyadenylation by the mutated PAPS1 may affect cell-cycle related genes in flowers and be the cause for the enlarged floral organs in *Arabidopsis*. Consistent with this idea, human CstF-77 level is important for the expression of cell-cycle related genes and its downregulation may help cells halt proliferation and launch differentiation (Luo *et al.*, 2013).

Additionally, it will be interesting to test whether this increase in floral organ size is reflected in a larger expression domain of the petal-anlagen marker *DORNRÖSCHEN-LIKE* (Chandler *et al.*, 2011) and whether it results from an overall increase in floral-meristem size.

The transcripts that are affected by reduced *PAPS1* activity in flowers seem to have different sensitivity to polyadenylation defects. This conclusion is based on the different phenotypes observed in the allelic series of *paps1* mutations. The weakest allele *paps1-4* shows only a moderate increase of floral organ size, indicating that only highly sensitive mRNAs to PAPS1 defects are affected. Amongst those may be cell cycle regulating genes or negative regulators of founder-cell recruitment and/or organ growth. A moderate reduction of PAPS1 activity can be seen in *paps1-1* mutants grown in 21 °C. In this mutant either the most sensitive transcripts are affected more strongly, or also less-sensitive mRNAs might be affected, or both causing even more strongly increased floral organs, but decreased leaf size. The strongest reduction of PAPS1 activity in viable mutants can be observed in *paps1-2* mutants likely causing polyadenylation defects of a larger number of transcripts, resulting in more pleiotropic effects with disorganized flowers. This idea is supported by the fact that *paps1-1* plants grown in high temperatures resemble *paps1-2* flowers (probably because higher

temperatures destabilize the *paps1-1* mutant protein) and that trans-heterozygous plants between *paps1-4* and *paps1-2* resemble *paps1-1* plants. A non-functional PAPS1 as in the *paps1-3* mutants, where the T-DNA insertion is in the catalytic domain, leads to male gametophytic lethality. This demonstrates that PAPS1 is an essential protein in plant development, but there exist different classes of mRNAs that show different sensitivity to PAPS1 activity.

It will be interesting to further evaluate the long/short RNAseq data to search for flower or leaf specific RNAs that change their poly(A) tail and could contribute to the opposite phenotypes. Additionally, affected mRNAs can be analysed at the level of sequence-motifs to identify possible unique motifs for PAPS1 target mRNAs that could explain the functional specificity amongst the different PAPS in *Arabidopsis*. A recent approach made use of the so-called PAL-seq, a method that accurately measures individual poly(A) tails of any physiological length (Subtelny *et al.*, 2014). Applying this method to the *paps1-1* mutants might be worthwhile to characterize poly(A) tail differences in greater detail.

3.2. The ectopic pathogen response in *paps1* mutant leaves

A global transcriptome analysis revealed that an ectopic pathogen response is activated in *paps1-1* mutant leaves (Chapter 2.1). As already known, constitutive activation of pathogen responses results in reduced leaf growth due to reduced cell expansion (Bowling *et al.*, 1994) and thus smaller leaves. However, pathogen-responses in plants involve massive transcriptional reprogramming and a complex network of receptors, resistance-proteins and phytohormones as reaction on pathogen attack (Chapter 1.3).

Reactive oxygen species (ROS) in general and hydrogen peroxide (H₂O₂) in particular are well known signalling components in response to pathogens, elicitors, wounding or heat (Slesak *et al.*, 2007). No accumulation of H₂O₂ in *paps1-1* leaves was observed by DAB staining. To discover potentially more subtle changes in the intra-cellular or intra-cell organellar redox status I made use of a redox-sensitive form of green fluorescent protein (GFP). This method revealed that the plastids (chloroplasts) in *paps1-1* mutant leaves are more oxidized. During photosynthesis, redox intermediates with extraordinarily negative redox potentials are generated that can convert oxygen into superoxide radicals, H₂O₂ and other ROS species. Plants have evolved complex mechanisms to control the redox poise of the electron transport chain and the redox environment in the chloroplasts like production of low-molecular weight antioxidants and antioxidant enzymes (Baier and Dietz, 2005). However, during evolution of plants, chloroplasts have lost the exclusive genetic control over redox regulation and antioxidant gene expression. Together with many other genes, all genes encoding antioxidant enzymes and enzymes involved in the biosynthesis of low molecular

Discussion

weight antioxidants were transferred to the nucleus. It sounds reasonable that nucleus-encoded chloroplast-localized proteins responsible for photosynthesis and/or antioxidant enzymes are susceptible to poly(A) tail changes by the mutated PAPS1 protein. Therefore a proper regulation of photosynthesis and detoxification of ROS can not be ensured. Consistent with this, *paps1-1* mutants are lighter green than wild-type plants and show severe bleaching when grown under high temperatures. This hypothesis is further supported by the fact that RNA sequencing revealed a profile of mis-regulated genes that overlaps with those seen in plant overexpressing a thylakoid-localized form of ascorbate peroxidase. In addition to their photosynthetic function, chloroplast development directly influences growth of the whole organ. Inhibition of chloroplast differentiation by norflurazon showed that retrograde signals from the chloroplasts are key factors driving the transition from cell proliferation to cell expansion (Andriankaja *et al.*, 2012). Leaf cells in the *paps1-1* mutants are smaller than in the wildtype, a fact that could be also caused by the misdeveloped chloroplasts, but this remains to be analysed.

Besides their photosynthetic function, chloroplasts are the starting point of ABA synthesis. ABA levels are reduced in the *paps1-1* mutants, a probably secondary effect that results from the mis-balanced redox status of the chloroplasts. Nevertheless, this ABA deficiency may also contribute to the aggravation of the *paps1-1* phenotype under higher temperatures where the *paps1-1* encoded protein is less active and chloroplast function/ABA biosynthesis are more severely impaired. ABA plays a major role in controlling stomatal closure. Evaporation through the stomata increases under higher temperatures and *paps1-1* mutants can probably not react on this properly by closing their stomata due to the ABA deficiency. It will be interesting to analyse whether the chloroplast morphology is changed in *paps1-1* mutants and whether the stomatal conductance is increased. Another open question is whether application of exogenous ABA can somehow rescue the mutant phenotype at least under high temperatures.

JAs regulate *Arabidopsis thaliana* wound and defense responses, pollen development and stress-related growth inhibition. JA is synthesized starting from linolenic acid via OPDA. *OPDA REDUCTASE3* (*OPR3*) reduces OPDA and the resulting intermediate undergoes three rounds of β -oxidation in the peroxisomes to yield JA. JA itself can then be metabolized to the volatile Methyl Jasmonate (MeJA) by a JA carboxy methyl transferase (*JMT*) or to the bioactive conjugate Ja-Ile by JA amino acid synthetase *JAR1* (*JASMONATE RESISTANT1*) that conjugates isoleucine (Ile) to JA or other jasmonyl-amino acid conjugates as for example jasmonyl-tryptophan (JA-Trp) by other conjugating enzymes. Overall OPDA levels were unchanged in *paps1-1* mutants, whereas JA levels were reduced. This indicates either a disturbed biosynthesis downstream of OPDA or a preferential metabolism to one or the other derivate downstream of JA. As shown by double mutant analysis, the *jar1-1 paps1-1*

Discussion

double mutants were indistinguishable from the *paps1-1* single mutants and JA-Ile levels were reduced in the *paps1-1* mutant leaves. A preferential production of JA-Ile and its influence on the phenotype can therefore be excluded. It will be interesting to analyse mutants impaired in metabolizing OPDA to JA like the *opr3* mutant (Stintzi and Browse, 2000) or mutants impaired in converting JA to MeJA or other jasmonyl-amino acid conjugates. The latter is particularly interesting because it was shown that MeJA delays the switch from the mitotic cell cycle to the endoreduplication cycle, which accompanies cell expansion and inhibits the mitotic cycle itself, arresting cells in G1 phase prior to the S-phase transition (Noir *et al.*, 2013). Additionally class I and class II TCP proteins regulate leaf development antagonistically via the jasmonate signaling pathway (Danisman *et al.*, 2012). Misregulation of the JA pathway as a direct effect from the *PAPS1* mutations or as indirect effect from the ectopic pathogen response may therefore influence the growth phenotype as well.

An influence of two other phytohormones involved in growth and pathogen responses, brassinosteroids and salicylic acid was excluded (see below). It is the SA-independent branch of the EDS1/PAD4-signalling pathway that is involved in the ectopic pathogen-response in leaves. This conclusion is based on three lines of evidence: (1) Loss of *npr1* function, a major downstream component of SA-dependent EDS1/PAD4-signalling, does not suppress the constitutive immune response in *paps1*. (2) SA levels are not increased in *paps1* mutants relative to wild type. (3) Reducing SA levels by overexpressing the SA-degrading enzyme NahG does not rescue the *paps1* mutant leaf phenotype. While overall little is known about the SA-independent functions of EDS1/PAD4, two important modulators of this process have been identified: the flavin-containing monooxygenase FMO1 and the Nudix hydrolase NUDT7 (Bartsch *et al.*, 2006). Consistent with the above interpretation, the expression of *FMO1*, which positively regulates the EDS1 pathway, is strongly upregulated in *paps1-1* mutant leaves (Chapter 2.1). The Arabidopsis *SNC1* gene encodes a TIR-NB-LRR receptor protein of the *RPP5* resistance gene cluster upstream of the EDS1 regulatory node. Mutations in this gene lead to a constitutive immune response with phenotypic changes comparable to *paps1-1* mutant leaves, whereas flowers are essentially unchanged. In the *nudt6-2 nudt7* double mutants autoimmunity is activated in an *SNC1* (*suppressor of npr1-1, constitutive1*) dependent and independent pathway, which are both temperature sensitive and dependent on *EDS1* (Wang *et al.*, 2013). It remains to be analysed, whether poly(A) tail changes in the *SNC1* mRNA are responsible for the leaf phenotype in *paps1-1* mutants and whether NUDT7 or FMO1 are involved. The double mutant between *paps1-1* and *snc1* appears similar to both single mutants. It is therefore likely that *snc1* and *paps1-1* act in a common pathway. It will be interesting to find out whether EDS1 or PAD4 are subject to the *paps1-1* mispolyadenylation, changing their poly(A) tail and

Discussion

therefore are the cause of the ectopic pathogen response. Indeed, EDS1 and PAD4 tend to have shorter poly(A) tails based on the RNAseq data. Alternatively TIR-NB-LRR receptor proteins upstream of the EDS1/PAD4 regulatory node or factors of the SA independent branch of the EDS1/PAD4 pathway could be affected by mispolyadenylation and be the underlying reason for the phenotype.

As mentioned before, immune responses are often accompanied by ROS production and resulting oxidative stress. A link between polyadenylation and oxidative stress has been reported in mutant plants deficient in CPSF30 expression. These are more tolerant to oxidative stresses than the wild type and imply a link between calcium and redox signaling pathways and alternative polyadenylation (Zhang *et al.*, 2008). Maybe the *paps1* mutations affects the same set of transcripts as in the CPSF30 mutants, demonstrating a general effect of disturbed 3'-end processing on oxidative stress tolerance.

Overexpression of the yeast poly(A)-binding protein Pab1p in tobacco or *A. thaliana* leads to a constitutive immune response and increased resistance (Li *et al.*, 2000). Another example is the plant RNA binding protein FPA, which regulates 3'-end mRNA polyadenylation and negatively regulates basal resistance to bacterial pathogen *Pseudomonas syringae* in *Arabidopsis* (Lyons *et al.*, 2013). The connection between polyadenylation or poly(A)-tail length control and immune response has been reported in other species as well. Blocking polyadenylation by cordycepin treatment inhibits the induction of inflammatory mRNAs by cytokines in human airway smooth muscle cells (Kondrashov *et al.*, 2012). However, critical immune response-related molecular targets for poly(A)-tail length control have not been defined yet.

3.3. Influence of *paps* mutations on deadenylation and RNA decay

As mentioned before, deadenylation and mRNA decay are important features of maintaining the transcriptional homeostasis inside the cells. The first step, deadenylation, is carried out by three major deadenylases in eukaryotes: the CCR4-POP2-Not complex, PAN and PARN complex (Chapter 1.2.5). CCR4 is the main cytoplasmic deadenylase while PARN deadenylates only a subset of transcripts in *Arabidopsis* (Reverdatto *et al.*, 2004). Additionally, a recent study showed that PARN directly regulates the poly(A) tail of mitochondrial RNAs (Hirayama *et al.*, 2013). These findings suggest a distinct regulation of deadenylation for different transcripts in *Arabidopsis*. Interestingly, the poly(A) binding protein (PABP) in yeast can activate deadenylation by recruiting PAN2-PAN3 to trim off poly(A) tails from pre-mRNAs (~80 nt) to mRNA specific poly(A) tails (55-70 nt) (Brown and Sachs, 1998). Although it is believed that this is a special feature of yeast, similar mechanisms may exist in plants as PAN has not been examined in *Arabidopsis* yet. It is therefore interesting whether

Discussion

mispolyadenylation of certain transcripts prevents trimming of the poly(A) tail to a proper length by the different deadenylases in *Arabidopsis* as well.

A mutation in the AtPARN complex termed *ABA hypersensitive germination 2 (ahg2-1)* leads to embryo lethality when introgressed into *paps1-1* mutants. This suggests that nucleus-encoded mitochondrial genes are mispolyadenylated in *paps1-1* mutants which are normally degraded by the PARN complex. In double mutants, the mispolyadenylated transcripts accumulate and disturb the transcriptional balance inside the mitochondria leading to lethality. A functional link between deadenylation defects and immune response was shown before. Mutations in *AtCAF1a* and *AtCAF1b*, the two homologues of the yeast CCR4-associated factor, result in defective poly(A)-tail shortening of stress-associated mRNAs and in reduced expression of the *PATHOGENESIS-RELATED1 (PR1)* gene (Liang *et al.*, 2009). By contrast, overexpressing *AtCAF1a* upregulates *PR1* expression and increases pathogen resistance. It will be interesting to analyse whether only accumulation of PARN targets in *paps1-1* mutants leads to embryo lethality or if an accumulation of mis-polyadenylated transcripts in general causes this severe phenotype by introgressing *ccr4 knock-out* mutations into the *paps1-1* background.

After removal of the poly(A) tail mRNAs can be degraded by two different pathways. One pathway degrades RNA in the 5'- to 3'-direction through the action of exoribonucleases (XRN). In the case of mRNA, this process is preceded by decapping. *Arabidopsis* has three XRN-like proteins *XRN2*, *XRN3* and *XRN4*. AtXRN2 and AtXRN3 are localized to the nucleus and involved in pre-rRNA processing while AtXRN4 is cytoplasmic and acts as the main mRNA degrading enzyme. It will be interesting to analyse whether mispolyadenylated mRNAs in *paps* mutants are subject to faster degradation in the cytoplasm because of their incomplete poly(A) tail. If this holds true, inhibition of mRNA degradation in the cytoplasm by blocking XRN4 activity through the *xrn4-6* mutation (Gy *et al.*, 2007) should restore the wildtype phenotype.

The second degradation pathway utilizes the exosome complex to degrade RNA in the 3' to 5' direction. The two types of exosomes are categorized based on localization, i.e., nuclear or cytoplasmic. The nuclear exosome degrades aberrant pre-mRNAs such as nonsense transcripts, rRNA, snRNA and snoRNA by-products, while the cytoplasmic exosome is responsible for the 3'- to 5'-exoribonucleolytic degradation of mRNAs. The exosome is a multiprotein complex where only the RRP41 subunit retained the catalytic activity (Chekanova *et al.*, 2000). The RNA- destabilizing role of polyadenylation seems paradoxical given that poly(A) tails are best known for stabilizing mRNAs in eukaryotes. Polyadenylation by canonical PAPS stabilizes RNAs whereas polyadenylation by a set of noncanonical PAPS triggers degradation of a variety of RNAs because these poly(A) tails serve as 'landing platforms' for exoribonucleases. The key feature that distinguishes between stabilizing and

destabilizing poly(A) tails is probably the length of the tail (Eckmann *et al.*, 2010). Polyadenylation assisted RNA degradation in the nucleus is mediated by the exosome (Schmidt and Jensen, 2006). This suggests that mispolyadenylated transcripts with short poly(A) tails in the *paps1-1* mutants may already be target of degradation by the nuclear exosome. However, blocking exosome function by mutating the RRP4 or RRP41 subunit is not suitable because they cause embryo lethality and severe female gametophytic defects, respectively (Chekanova *et al.*, 2002; Chekanova *et al.*, 2007). A more useful tool is the deployment of estradiol inducible *rrp4* and *rrp41* RNAi lines (Chekanova *et al.*, 2007) and their effect on *paps1-1* mutants should be analysed.

3.4. Functional specialization amongst PAPS in Arabidopsis

Only mutations in *PAPS1* cause an increase of floral organ size and decrease of leaf size. Mutations in *PAPS2* or *PAPS4* cause only a late-flowering phenotype. This defect is not a general phenotype for plants impaired in 3'-end processing since *cstf64-1* mutants do not show decreased leaf or increased flower size. This fact suggests a potential specialized function amongst the different PAPS in *Arabidopsis*. As shown in chapter 2.1 the different PAPS share high similarity in their N-terminal catalytic domain but differ in their C-terminal domains. Introduction of chimaeric proteins with the *PAPS4* N-terminus and the *PAPS1* C-terminus can nearly fully rescue the phenotype. All three PAPS show non-specific polyadenylation activity in vitro (Hunt *et al.*, 2000; Addepalli *et al.*, 2004) and are expressed ubiquitously in all tissues throughout all developmental stages (Meeks *et al.*, 2009). Bulk-poly(A) tail distribution is equal in mutant and wildtype plants, suggesting that the majority of mRNAs is properly polyadenylated and the different PAPS have in part redundant functions. It is therefore more likely that the specificity arises from post-translational modifications or substrate-specificity rather than differential expression.

The diverging C-terminal domains of the different PAPS may provide a platform for different C-terminal modifications. It is already known that human PAP α and PAP γ are subject to numerous post-translational modifications that change their activity (phosphorylation), binding ability to other 3'-end processing complex factors (acetylation) or intracellular localization (acetylation, sumoylation) (Colgan *et al.*, 1996; 1998; Mouland *et al.*, 2002; Shimazu *et al.*, 2007; Vethantham *et al.*, 2007). This may also hold true for the different PAPS in *Arabidopsis*: *PAPS1* is phosphorylated on several residues in its C-terminal domain [<http://phosphat.mpimp-golm.mpg.de>; (Durek *et al.*, 2010)]. However, the biological function remains unknown. An example for diverse 3'-end processing complexes is shown by pull-down assay of FY, which revealed two complexes of different sizes (Manzano *et al.*, 2009). This supports the idea that the different PAPS form different 3'-end

Discussion

processing complexes that fulfil different functions. This idea is supported by the fact that *SAUR19/24* transcripts have shorter poly(A) tails in *paps1*, but not *paps2* or *paps4* mutants.

Although the different PAPS have different functions, it is not clear where the specificity comes from and which genes are targets of the one PAPS or the other. Clearly *SAUR19/24* transcripts are targets for PAPS1 mediated polyadenylation, but only have a minor contribution to the mutant phenotype. Additionally PAPS1 function seems to be different in the different plant organs: an ectopic pathogen response is activated in the *paps1-1* mutant leaves that involves the SA-independent EDS1/PAD4 pathway and contributes to the reduced leaf size. This constitutive immune response that was apparent at the transcriptomic level as different *PR* genes were overexpressed. The phenotype and the *PR* gene expression was rescued by introducing the chimaeric PAPS4^N-PAPS1^C construct into the *paps1-1* mutants. This argues for the responsibility of the C-terminal PAPS domains in regulating specialized functions amongst the different PAP isoforms. In accordance, *paps1-1* and *paps1-4* mutants are more resistant to the biotrophic oomycete *Hyaloperonospora arabidopsidis* whereas the *paps2-3 paps4-3* double mutant are not. The size of the mutant flowers is increased, probably because negative-regulators of founder cell recruitment are very susceptible to polyadenylation defects. It is likely that several generally expressed genes are impaired by mispolyadenylation through the mutated PAPS1 all of whom make additional minor contributions to the phenotype. Employing different PAPS to react on different environmental conditions or during different developmental stages enables the plant to generate transcripts with different poly(A) tail lengths. As the poly(A) tail length affects transcription and splicing, stability of the transcript, contributes to efficient nuclear export and influences translation, regulation of its length appears to be a novel layer of gene regulation in plants that has not been reported so far. Future research is necessary to find out how exactly and under which conditions plants modulate the balance of activities amongst the PAPS isoform, which genes are susceptible to differential polyadenylation and how this differentiation is regulated.

Appendix A: Cloning strategies

poly(A) Tail control vectors for RNA Sequencing

short fraction (30As)

Plasmid pJill_SV1 (35S::omega Leader::YFP in pBlueML) was linearized with BsrGI (NEB) and Gel-purified. A equimolar mixture of GTO277 and GTO278 (1/2 BsrGI restriction site + 30 As) was heated to 95 °C in a heating block. Afterwards the heating block was carried to the cold room (8 °C) and the samples slowly cooled down to room temperature. This Primer mixture was used as insert and ligated to the linearized pJill_SV1. After transformation, clones where tested by colony-PCR (GTO279, HBo116) for absence or presence of the insert. Positive clones where sent for sequencing and one with the right orientation of the insert was termed pGT2c and further used. pGT2c was digested with NcoI to remove the omega leader and religated. The resulting plasmid was termed pGT2d. pGT2d was linearized with BamHI, phenol:chloroform purified, and used as template for *in-vitro* transcription (see 2.3.4.).

intermediate fraction (75As)

Plasmid pJill_SV1 (35S::omega Leader::YFP in pBlueML) was linearized with KpnI (NEB) and Gel-purified. A equimolar mixture of GTO289 and GTO290 (1/2 KpnI restriction site + 75 As) was heated to 95 °C in a heating block. Afterwards the heating block was carried to the cold room (8 °C) and the samples slowly cooled down to room temperature. This Primer mixture was used as insert and ligated to the linearized pJill_SV1. This Primer mixture was used as insert and ligated to the linearized pJill_SV1. After transformation, clones where tested by colony-PCR (GTO291, GTO292) for absence or presence of the insert. Positive clones where sent for sequencing and one with the right orientation of the insert was termed pGT3b. pGT3b was linearized with XmaI, phenol:chloroform purified and used as template for *in-vitro* transcription.

long fraction (134As)

Plasmid ML1004 (AlcA::omega Leader in pBlueML) was digested with Sall and XhoI to remove the omega leader and religated. The resulting plasmid was termed pGT4. The plasmid pGT3a was digested with KpnI and the 150 bp fragment gel-purified and ligated into the KpnI linearized pGT4. Clones where screened by colony-PCR (HBo006 and HBo116). Positive clones where sent for sequencing and one with the right orientation of the insert was termed pGT5 and further used. pGT5 was linearized with BamHI, phenol:chloroform purified, and used as template for *in-vitro* transcription (see 2.3.4.).

Appendix B: Instruments

Name	Model/Type	Company
Camera	AxioCam MRm	Zeiss
Camera I	Powershot	Canon
Confocal Microscope	AxioObserver	Zeiss
Cooling centrifuge	5417R	eppendorf
Electroporator	Micropulser	BioRad
Fluorescence lamp	HxP120c	Zeiss
Fluorescence Microscope	SteREO Lumar V.12	Zeiss
Geldocumentation	BioDoc Analyze	Biometra
Plant growth chamber		Percival
Microscope	BX51	Olympus
Mini Centrifuge	Biofuge pico	Heraeus
PCR Machine	PTC200	MJ Research
Photometer	BioPhotometer	eppendorf
Picodrop	Pico100	Picodrop
Plate centrifuge	4K15	Sigma
RF camera	F14532	Marlin
geldocumentation		
Rotator	SB3	stuart
shaking Incubator	Ecotron	Infors HT
Thermomixer	Thermomixer comfort	eppendorf
Vortex	Vortex Genie 2	scientific industries

Abbreviations

35S	promoter of the 35S gene from cauliflower mosaic virus
AA	amino acid
ABA	abscisic acid
<i>Agrobacterium</i>	<i>Agrobacterium tumefaciens</i>
<i>ahg2-1</i>	<i>ABA hypersensitive germination 2-1</i>
Amp	ampicillin
ANT	<i>AINTEGUMENTA</i>
APA	alternative polyadenylation
APS	ammoniumperoxysulfate
AP2	APETALA2
<i>At</i>	<i>Arabidopsis thaliana</i>
<i>Arabidopsis</i>	<i>Arabidopsis thaliana</i>
ATP	adenosine 5'-triphosphate
BB	<i>BIG BROTHER</i>
bp	basepairs
BR	brassinosteroid
Ca	calcium
CaMV	cauliflower mosaic virus
CCR4	carbon catabolite repressor 4
CDK	cyclin dependent kinase
cDNA	complementary DNA
CF	cleavage factor
CFP	cyan fluorescent protein
CLV	<i>CLAVATA</i>
COI	coronatine insensitive
<i>Col-0</i>	<i>Columbia-0</i>
CPSF	cleavage and polyadenylation specificity factor
CSTF	cleavage stimulation factor
CTD	carboxyterminal domain
C-terminal	carboxyterminal
DAB	3'3' diaminobenzidine
DNA	deoxyribonucleic acid
DNase	deoxyribonuclease
dNTPs	deoxynucleoside triphosphates
<i>E. coli</i>	<i>Escherichia coli</i>
EDS	enhanced disease susceptibility
e.g.	for example
EMS	ethylmethanesulfonate
<i>et al.</i>	<i>et alii</i>
EtOH	ethanol
<i>FLC</i>	<i>FLOWERING LOCUS C</i>
fw	forward
x g	gravity, 9.81 m/s ²
g	gramme
GA	giberellic acid

Abbreviations

GFP	green fluorescent protein
GRF	growth regulating factor
GUS	β-Glucoronidase
h	hour
H ₂ O	water
i.e.	id est
JA	jasmonic acid
JAR	jasmonic acid receptor
Kana	kanamycin
kg	kilogram
LB	lysogeny broth
<i>Ler</i>	<i>Landsberg erecta</i>
LFY	LEAFY
LRR	leucin rich repeat
M	molar
Me-JA	methyl-jasmonate
min	minute
mRNA	messenger RNA
MS	medium after Murashige & Skoog
μl	microliter
ng	nanogram
NLS	nuclear localization signal
NPR1	NONEXPRESSOR OF PATHOGENESIS RELATED GENES 1
N-terminal	amino-terminal
nt	nucleotides
OD	optical density
PABN	nuclear poly(A) binding protein
PAD	phytoalexin deficient
PAN	poly(A) nuclease
PAP/PAPS	poly(A)polymerase
PARN	poly(A) specific ribonuclease
PCR	polymerase chain reaction
PPT	phosphinotricin
PR genes	pathogenesis related genes
qPCR	quantitative PCR
rev	reverse
RNA	ribonucleic acid
roGFP	redox sensitive GFP
rpm	rotations per minute
rRNA	ribosomal RNA
RT	room temperature (20-24 °C)
s	second
SA	salicylic acid
SAG101	senescence associated gene 101
SAM	shoot apical meristem
SAUR	small auxin upregulated RNA
<i>S. cerevisiae</i>	<i>Sacchaomyces cerevisiae</i>
<i>snc-1</i>	<i>suppressor of npr1, constitutive-1</i>
STM	SHOOT MERISTEMLESS
TCA	trichlor acetic acid

Abbreviations

TCP	TEOSINTE-BRANCHED1/CYCLOIDEA/PCF
TIR	toll-interleukin-receptor
T-DNA	transferred DNA
vol, v	volume
w	weight
WT	wildtype
<i>WUS</i>	<i>WUSCHEL</i>
XRN	exoribonuclease
YFP	yellow fluorescent protein

References

- Aarts N, Metz M, Holub E, Staskawicz BJ, Daniels MJ, Parker JE (1998)** Different requirements for EDS1 and NDR1 by disease resistance genes define at least two R gene-mediated signaling pathways in Arabidopsis. *Proc Natl Acad Sci USA* 95: 10306-10311.
- Abbasi N, Park YI, Choi SB (2013)** RNA deadenylation and decay in plants. *J Plant Biol* 56:198-207.
- Addepalli B, Meeks LR, Forbes KP, Hunt AG (2004)** Novel alternative splicing of mRNAs encoding poly(A) polymerases in Arabidopsis. *Biochim Biophys Acta* 1679: 117-128.
- Addepalli B and Hunt AG (2007)** A novel endonuclease activity associated with the Arabidopsis ortholog of the 30-kDa subunit of cleavage and polyadenylation specificity factor. *Nucleic Acids Res* 35:4453-4463.
- Al Husini N, Kudla P, Ansari A (2013)** A Role for CF1A 3' end processing complex in promoter-associated transcription. *PLoS Gen* 9(8):e1003722
- Anastasiou E, Kenz S, Gerstung M, MaxLean D, Timmer J, Flack C, Lenhard M (2007)** Control of plant organ size by KLUH/CYP78A5-Dependent intercellular signaling. *Dev Cell* 13: 843-856.
- Anderson JP, Badruzsafari E, Schenk PM, Manners JM, Desmond OJ, Ehlert C, Maclean DJ, Ebert PR, Kazan K (2004)** Antagonistic interaction between abscisic acid and jasmonate-ethylene signaling pathways modulates defense gene expression and disease resistance in Arabidopsis. *Plant Cell* 16: 3460–3479.
- Ansari A and Hampsey M (2005)** A role for the CPF 3'-end processing machinery in RNAP II-dependent gene looping. *Genes & Dev* 19: 2969-2978.
- Ausubel FM (2005)** Are innate immune signaling pathways in plants and animals conserved? *Nature Immunol* 6(10): 973-979.
- Baier M and Dietz KJ (2005)** Chloroplasts as source and target of cellular redox regulation: a discussion on chloroplast redox signals in the context of plant physiology. *J Exp Bot* 56: 1449-1462.
- Balbo PB, Meinke G, Bohm A (2005)** Kinetic studies of Yeast Poly(A) Polymerase indicate an induced fit mechanism for nucleotide specificity. *Biochemistry* 44: 7777-7786.
- Bard J, Zhelkovsky AM, Helmling S, Earnest TN, Moore CL, Bohm A (2000)** Structure of yeast poly(A) polymerase alone and in complex with 3'-dATP. *Science* 289: 1346-1349.
- Becker JD, Boavida LC, Carneiro J, Haury M, Feijó JA (2003)** Transcriptional profiling of Arabidopsis Tissue Reveals the Unique Characteristics of the Pollen Transcriptome. *Plant Phys* 133(2): 713-725.
- Beilharz TH and Preiss T (2007)** Widespread use of poly(A) tail length control to accentuate expression of the yeast transcriptome. *RNA* 13: 982-987.
- Benková E, Michniewicz M, Sauer M, Teichmann T, Seifertová D, Jürgens G, Friml J (2003)** Local, efflux-dependent auxin gradients as a common module for plant organ formation. *Cell* 29: 591-602.
- Bentley DL (2014)** Coupling mRNA processing with transcription in time and space. *Nat Rev Gen* 15: 163-175.
- Berchowitz LE, Copenhaver GP (2008)** Fluorescent Arabidopsis tetrads: a visual assay for quickly developing large crossover and crossover interference data sets. *Nat Protoc* 3: 41–50.
- Berchowitz LE, Copenhaver GP (2009)** Visual markers for detecting gene conversion directly in the gametes of Arabidopsis thaliana. *Methods Mol Biol* 557: 99–114.
- Berry M and Sachar RC (1982)** Expression of conserved message of poly(A) polymerase through hormonal control in wheat aleurone layers. *FEBS Letters* 141: 164-168.
- Bhattacharjee S, Halane MK, Kim SH, Gassmann W (2011)** Pathogen effectors target Arabidopsis EDS1 and alter its interactions with immune regulators. *Science* 334:1405-1408.

- Bleckmann A and Simon R (2009)** Interdomain signaling in stem cell maintenance of plant shoot meristems. *Mol Cells* 27: 615-620.
- Bleckmann A, Weidtkamp-Peters S, Seidel CAM, Simon R (2010)** Stem cell signaling in *Arabidopsis* requires CRN to localize CLV2 to the plasma membrane. *Plant Physiol* 152: 166-176.
- Bowling SA, Guo A, Cao H, Gordon S, Klessing DF, Dong X (1994)** A mutation in *Arabidopsis* that leads to constitutive expression of systemic acquired resistance. *Plant Cell* 6: 1845-1857.
- Brand U, Grunewald M, Hobe M, Simon R (2002)** Regulation of CLV3 expression by two homeobox genes in *Arabidopsis*. *Plant Physiol* 129: 565-575.
- Braybrook SA and Kuhlemeier C (2010)** How a plant builds leaves. *Plant Cell* 22: 1006-1018.
- Brown KM and Gilmartin GM (2003)** A mechanism for the regulation of pre-mRNA 3' end processing by human cleavage factor Im. *Mol Cell* 12: 1467-1476.
- Brown CE and Sachs AB (1998)** Poly(A) tail length control in *Saccharomyces cerevisiae* occurs by message-specific deadenylation. *Mol Cell Biol* 18: 6548-6559.
- Chandler JW, Jacobs B, Cole M, Comelli P, Werr W (2011)** DORNROSCHEN-LIKE expression marks *Arabidopsis* floral organ founder cells and precedes auxin response maxima. *Plant Molecular Biology*, 76: 171-185.
- Chekanova JA, Shaw RJ, Wills MA, Belostotsky DA (2000)** Poly(A) tail-dependent exonuclease AtRrp41 from *Arabidopsis thaliana* rescues 5.8 S rRNA processing and mRNA decay defects of the yeast ski6 mutant and is found in an exosome sized complex in plant and yeast cells. *J Biol Chem* 275: 33158-33166.
- Chekanova JA, Dutko JA, Mian IS, Belostotsky DA (2002)** *Arabidopsis thaliana* exosome subunit AtRrp4p is a hydrolytic 3' → 5' exonuclease containing S1 and KH RNA binding domains. *Nucleic Acids Res* 30:695-700.
- Chekanova JA, Belostotsky DA (2006)** MicroRNAs and messenger RNA turnover. *Methods Mol Biol* 342: 73–85.
- Chekanova JA, Gregory BD, Reverdatto SV, Chen H, Kumar R, Hooker T, Yazaki J, Li P, Skiba N, Peng Q, Alonso J, Brukhin V, Grossniklaus U, Ecker JR, Belostotsky DA (2007)** Genomewide high-resolution mapping of exosome substrates reveals hidden features in the *Arabidopsis* transcriptome. *Cell* 131 : 1340–1353.
- Chen R and Baluška F (2013)** Signaling and communication in plants: Polar Auxin Transport. Springer
- Chen F and Wilusz J (1998)** Auxiliary downstream elements are required for efficient polyadenylation of mammalian pre-mRNAs. *Nucleic Acids Res* 26: 2891-1898.
- Cheng H, Qin LJ, Lee SC, Fu XD, Richards DE, Cao DN, Luo D, Harberd NP, Peng JR (2004)** Giberellin regulates *Arabidopsis* floral development via suppression of DELLA protein function. *Development* 131: 1055-1064.
- Cheng YT, Germain H, Wiermer M, Bi DL, Xu F, Garcia AV, Wirthmueller L, Despres C, Parker JE, Zhang YL, Li X (2009)** Nuclear pore complex component MOS7 / Nup88 is required for innate immunity and nuclear accumulation of defense regulators in *Arabidopsis*. *Plant Cell* 21: 2503–2516.
- Chinchilla D, Zipfel C, Robatzek S, Kemmerling B, Nurnberger T, Jones JD, Felix G, Boller T (2007)** A flagellin-induced complex of the receptor FLS2 and BAK1 initiates plant defence. *Nature* 448: 497-500.
- Choi J, Choi D, Lee S, Ryu CM, Hwang I (2011)** Cytokinins and plant immunity: old foes or new friends? *Trends Plant Sci* 16: 388-394.
- Chory J, Nagpal P, Peto CA (1991)** Phenotypic and genetic analysis of det2, a new mutant that affects light-regulated seedling development in *Arabidopsis*. *Plant Cell* 3: 445-459.
- Clark SE (2001)** Cell signaling at the shoot meristem. *Nature Rev Mol Cell Biol* 2: 276-284.
- Colgan DF, Murthy KG, Prives C, Manley JL (1996)** Cell-cycle related regulation of poly(A) polymerase by phosphorylation. *Nature* 384: 282-285.

- Colgan DF, Murthy KG, Zhao W, Prives C, Manley JL (1998)** Inhibition of poly(A) polymerase requires p34cdc2/cyclin B phosphorylation of multiple consensus and non-consensus sites. *EMBO J* 17: 1053-1062.
- Collart MA and Panasenko OO (2012)** The Ccr4-Not complex. *Gene* 492: 42-53.
- Cooke C, Hans H, Alwine JC (1999)** Utilization of splicing elements and polyadenylation signal elements in the coupling of polyadenylation and last-intron removal. *Mol Cell Biol* 19: 4971-4979.
- Cosgrove DJ (2005)** Growth of the plant cell wall. *Nat Rev Mol Cell Biol* 6: 850-861.
- Cowling RJ and Harberd NP (1999)** Gibberellins control *Arabidopsis* hypocotyl growth via regulation of cellular elongation. *J exp Bot* 50: 1351-1357.
- Danisman S, van der Wal F, Dhondt S, Waites R, de Folter S, Bimbo A, van Dijk AD, Muino JM, Cutri L, Dornelas MC, Angenent GC, Immink RG (2012)** *Arabidopsis* class I and class ITCP transcription factors regulate jasmonic acid metabolism and leaf development antagonistically. *Plant Physiol* 159: 1511-1523.
- Dehlin E, Wormington M, Korner CG & Wahle E (2000)** Cap-dependent deadenylation of mRNA. *EMBO J* 19: 1079-1086.
- Denis CL & Chen J (2003)** The CCR4-NOT complex plays diverse roles in mRNA metabolism. *Prog Nucleic Acid Res Mol Biol* 73: 221-250.
- De Vos M, Van Zaanen W, Koornneef A, Korzelius JP, Dicke M, et al. (2006)** Herbivore-induced resistance against microbial pathogens in *Arabidopsis*. *Plant Physiol* 142: 352-363.
- Disch S, Anastasiou E, Sharma VK, Laux T, Fletcher JC, Lenhard M (2006)** The E3 ubiquitin ligase BIG BROTHER controls *Arabidopsis* organ size in a dosage-dependent manner. *Curr Biol* 16: 272-279.
- Dong X (2004)** NPR1, all things considered. *Curr Op Plant Biol* 7:547-552.
- Donnelly PM, Bonetta D, Tsukaya H, Dengler RE, Dengler NG (1999)** Cell Cycling and Cell enlargement in Developing Leaves of *Arabidopsis*. *Dev Biol* 215: 407-419.
- Dubois M, Skirycz A, Claeys H, Maleux K, Dhondt S, De Bodt S, Vanden Bossche R, De Milde L, Yoshizumi T, Matsui M, Inzé D (2013)** Ethylene Response Factor 6 acts as a central regulator of leaf growth under water-limiting conditions in *Arabidopsis*. *Plant Physiol* 162: 319-332.
- Eckmann CR, Rammelt C, Wahle E (2011)** Control of poly(A) tail length. *Wiley Interdiscip Rev RNA* 2: 348-361.
- Edmonds M (1990)** Polyadenylate Polymerases. *Methods Enzymol* 181: 161-170.
- Efroni I, Han SK, Kim HJ, Wu MF, Steiner E, Birnbaum KD, Hong JC, Eshed Y, Wagner D (2013)** Regulation of leaf maturation by chromatin-mediated modulation of cytokinin responses. *Dev Cell* 24: 438-445.
- Elkon R, Ugalde AP, Agami R (2013)** Alternative cleavage and polyadenylation: extent, regulation and function. *Nature Rev Gen* 14: 496-506.
- Elliot BJ, Dattaroy T, Meeks-Midkiff LR, Forbes KP, Hunt AG (2003)** An interaction between an *Arabidopsis* poly(A) polymerase and a homologue of the 100 kDa subunit of CPSF. *Plant Mol Biol* 51: 373-384.
- El Oirdi M, Abd El Rahman T, Rigano L, El Hadrami A, Rodriguez MC, Daayf F, Vojnov A, Bouarab K (2011)** *Botrytis cinerea* manipulates the antagonistic effects between immune pathways to promote disease development in tomato. *Plant Cell* 23: 2405-2421.
- Eloy NB, de Freitas Lima M, Van Damme D, Vanhaeren H, Gonzalez N, De Milde L, Hemerly AS, Beemster GT, Inzé D, Ferreira PC (2011)** The APC/C subunit 10 plays an essential role in cell proliferation during leaf development. *Plant J* 68(2): 351-363.
- Evsyukova I, Bradrick SS, Gregory SG, Garcia-Blanco MA (2013)** Cleavage and polyadenylation specificity factor 1 (CPSF1) regulates alternative splicing of interleukin 7 receptor (ILR7) exon 6. *RNA* 19: 103-115.
- Felix G, Duran JD, Volko S, Boller T (1999)** Plants have a sensitive perception system for the most conserved domain of bacterial flagellin. *Plant J* 18(3): 265-276.
- Fernandez-Calvo P, Chini A, Fernandez-Barbero G, Chico JM, Gimenez-Ibanez S, Geerinck J, Eeckhout D, Schweizer F, Goday M, Franco-Zorrilla JM, Pauwels L, Witters E, Puga MI, Paz-Ares,**

- Goossens A, Rexmond P, De Jaeger G, Solano R (2011)** The *Arabidopsis* bHLH transcription factors MYC3 and MYC4 are targets of JAZ repressors and act additively with MYC2 in the activation of jasmonate responses. *Plant Cell* 23: 701–715.
- Ferreira P, Hemerly A, de Almeida Engler J, Bergounioux C, Burssens S, Van Montagu M, Engler G, Inzé D (1994a)** Three discrete classes of *Arabidopsis* cyclins are expressed during different intervals of the cell cycle. *Proc Natl Acad Sci USA* 91: 11313–11317.
- Ferreira PCG, Hemerly AS, de Almeida Engler J, VanMontagu M, Engler G, Inzé D (1994b)** Developmental expression of the *Arabidopsis* cyclin gene *cyc1At*. *Plant Cell* 6: 1763–1774.
- Feys BJ, Moisan LJ, Newman MA, Parker JE (2001)** Direct interaction between the Arabidopsis disease resistance signaling proteins, EDS1 and PAD4. *EMBO J* 20:5400-5411.
- Feys BJ, Wiermer M, Bhat RA, Moisan LJ, Medina-Escobar N, Neu C, Cabral A, Parker JE. (2005)** *Arabidopsis* SENESCENCEASSOCIATED GENE101 stabilizes and signals within an ENHANCED DISEASE SUSCEPTIBILITY1 complex in plant innate immunity. *Plant Cell* 17: 2601–2613.
- Fisher K and Turner S (2007)** PXY, a receptor-like kinase essential for maintaining polarity during plant vascular-tissue development. *Curr Biol* 17: 1061–1066.
- Ford LP, Bagga PS, Wilusz J (1997)** The poly(A) tail inhibits the assembly of a 3'-to-5' exonuclease in an in vitro RNA stability system. *Mol Cell Biol* 17: 398–406.
- Francis KE, Lam SY, Harrison BD, Bey AL, Berchowitz LE, Copenhaver GP (2007)** Pollen tetrad-based visual assay for meiotic recombination in Arabidopsis. *Proc Natl Acad Sci USA* 104: 3913–3918.
- Fridman Y and Savaldi-Goldstein S (2013)** Brassinosteroids in growth control: How, when and where. *Plant Sci* 209: 24-31.
- Gao M, Fritz DT, Ford LP & Wilusz J (2000)** Interaction between a poly(A)-specific ribonuclease and the 5'cap influences mRNA deadenylation rates *in vitro*. *Mol Cell* 5:479-488
- Garcia AV, Blanvillain-Baufume S, Huibers RP, Wiermer M, Li GY, Gobbato E, Rietz S, Parker JE (2010)** Balanced nuclear and cytoplasmic activities of EDS1 are required for a complete plant innate immune response. *PLoS Pathogens* 6: e1000970.
- Garneau NL, Wilusz J, Wilusz CJ (2007)** The highways and byways of mRNA decay. *Nature Rev Mol Biol* 8: 113-126.
- Glazebrook J (2005)** Contrasting mechanisms of defense against biotrophic and necrotrophic pathogens. *Annu Rev Phytopathol* 43: 205-227.
- Gómez-Gómez L and Boller T (2000)** FLS2: An LRR Receptor-like Kinase Involved in the Perception of the Bacterial Elicitor Flagellin in Arabidopsis. *Mol Cell* 5(1): 1003-1011.
- Gonzalez N, De Bodt S, Sulpice R, Jikumaru Y, Chae E, Dhondt S, Van Daele T, De Milde L, Weigel D, Kamiya Y, Stitt M, Beemster GT, Inzé D (2010)** Increased leaf size: different means to an end. *Plant Physiol* 153: 1261-1279.
- Gonzalez N, Vanhaeren H, Inzé D (2012)** Leaf size control: complex coordination of cell division and expansion. *Trends Plant Sci* 17(6): 332-340.
- Green C and Besharse JC (1996)** Identification of a novel vertebrate circadian clock-regulated gene encoding the protein nocturnin. *Proc Natl Acad Sci USA* 93: 14884-14888.
- Guenot B, Bayer E, Kierzkowski D, Smith RS, Mandel T, Žádníková P, Benková E, Kuhlemeier C (2012)** PIN1-independent leaf initiation in Arabidopsis. *Plant Physiol* 159(4): 1501-1510.
- Gy I, Gascolli V, Laressergues D, Morel JB, Gombert J, Proux F, Vaucheret H, Mallory AC (2007)** *Arabidopsis* FIERY1, XRN2 and XRN3 are endogenous RNA silencing suppressors. *Plant Cell* 19: 3451-3461.
- Haracska L, Johnson RE, Prakash L, Prakash S (2005)** Trf4 and Trf5 proteins of *Saccharomyces cerevisiae* exhibit poly(A) polymerase activity but no DNA polymerase activity. *Mol Cell Biol* 25: 10183-
- Hemerly A, Bergounioux C, Van Montagu M, Inzé D, Ferreira P (1992)** Dominant negative mutants of the Cdc2 kinase gene uncouple cell division from iterative plant development. *EMBO J* 14: 3925-3963.

- Heidrich K, Wirthmueller L, Tasset C, Pouzet C, Deslandes L, Perker JE (2011)** *Arabidopsis* EDS1 connects pathogen effector recognition to cell compartment-specific immune responses. *Science* 334: 1401-1404.
- Hirayama T, Matsuura T, Ushiyama S, Narusaka M, Kurihara Y, Yasuda M, Ohtani M, Seki M, Demura T, Nakashita H, Yoshihiro N, Hayashi S (2013)** A poly(A)-specific ribonuclease directly regulates the poly(A) status of mitochondrial mRNA in *Arabidopsis*. *Nature Communications* 4:2247.
- Hirose Y and Manley JL (1998)** RNA polymerase II is an essential mRNA polyadenylation factor. *Nature* 395: 93–96.
- Hofmeister W (1868)** Allgemeine Morphologie der Gewächse. In: *Handbuch der Physiologischen Botanik*, Band 1, Abteilung 2. W. Engelmann, Leipzig, Germany: 405-664.
- Holm L and Sander C (1995)** DNA Polymerase β belongs to an ancient nucleotidyltransferase superfamily. *Trends Biochem Sci* 20: 345-347.
- Horiguchi G, Kim GT, Tsukaya H (2005)** The transcription factor AtGRF5 and the transcription coactivator AN3 regulate cell proliferation in leaf primordia of *Arabidopsis thaliana*. *Plant J* 43: 68-78.
- Horiguchi G and Tsukaya H (2011)** Organ size Regulation in plants: insights from compensation. *Front Plant Sci* 2:24.
- Horniyk C, Terzi LC, Simpson GG (2010)** The Spen family protein FPA controls alternative cleavage and polyadenylation of RNA. *Dev Cell* 18:172-174.
- Hunt AG, Addepalli B (2008)** The Interaction between two *Arabidopsis* polyadenylation factor subunits involves an evolutionarily-conserved motif and has implications for the assembly and function of the polyadenylation complex. *Protein and Peptide Letters* 15: 76-88.
- Hunt A, Meeks LR, Forbes KP, Das Gupta J, Mogen BD (2000)** Nuclear and chloroplast poly(A) polymerases from plants share a novel biochemical property. *Biochem Biophys Res Commun* 272: 174-181.
- Hunt AG (2012)** RNA regulatory elements and polyadenylation in plants. *Front Plant Sci* 2: 109.
- Hunt AG, Xing D, Li QQ (2012)** Plant polyadenylation factors: conservation and variety in the polyadenylation complex in plants. *BMC genomics* 13: 641.
- Janeway CA Jr. (1989)** Approaching the Asymptote? Evolution and Revolution in Immunology. *Quant Biol* 54: 1–13.
- Jiang CJ, Shimono M, Sugano S, Kojima M, Liu X, Inoue H, Sakakibara H, Takatsuji H (2013)** Cytokinin act synergistically with Salicylic Acid to activate defense gene expression in rice. *Mol Plant Microbe Int* 26: 287-296.
- Johnson K and Lenhard M (2011)** Genetic control of plant organ growth. *New Phytol* 191: 319-333.
- Jones JDG and Dangl JL (2006)** The plant immune system. *Nature* 444: 323-329.
- Junge F, Zaessinger S, Temme C, Wahle E, Simonelig M (2002)** Control of poly(A) polymerase level is essential to cytoplasmic polyadenylation and early development in *Drosophila*. *EMBO J* 21(23): 6603-6613.
- Kaufmann I, Martin G, Friedlein A, Langen H, Keller W (2004)** Human Fip1 is a subunit of CPSF that binds to U-rich RNA elements and stimulates poly(A) polymerase. *EMBO J* 23: 616-626.
- Kashiwabara S, Zhuang T, Yamagata K, Noguchi J, Fukamizu A, Baba T (2000)** Identification of a novel isoform of poly(A) polymerase, TPAP, specifically present in the cytoplasm of spermatogenic cells. *Dev Biol* 228: 106-115.
- Kawade K, Horiguchi G, Tsukaya H (2010)** Non-cell-autonomously coordinated organ size regulation in leaf development. *Development* 15: 4221-4227.
- Kazan K and Manners JM (2012)** JAZ repressors and the orchestration of phytohormone crosstalk. *Trends Plant Sci.* 17: 22–31
- Kerwitz Y, Kühn U, Lilie H, Knoth A, Scheuermann T, Friedrich H, Schwarz E, Wahle E (2003)** Stimulation of poly(A) polymerase through a direct interaction with the nuclear poly(A) binding protein allosterically regulated by RNA. *EMBO J* 22: 3705-3714.

- Kieffer M, Master V, Waites R, Davies B (2011)** TCP14 and TCP15 affect internode length and leaf shape in Arabidopsis. *Plant J Cell Mol Biol* 68: 147-158.
- Kim H and Lee Y (2001)** Interaction of poly(A) polymerase with the 25-kDa subunit of cleavage factor I. *Biochem Biophys Res Communications* 289: 513-518.
- Kim JH, Choi D, Kende H (2003)** The AtGRF family of putative transcription factors involved in leaf and cotyledon growth in Arabidopsis. *Plant J* 36: 94-104.
- Kinkema m, Fan W, Dong X (2000)** Nuclear localization of NPR1 is required for activation of PR gene expression. *Plant Cell* 12:2339-2350.
- Koch E and Slusarenko A (1990)** Arabidopsis is susceptible to infection by a downy mildew fungus. *Plant Cell* 2: 437-445.
- Korner C, Menendez-Riedl S Pelaez, John PCL (1989)** Why are Bonsai plants small? A consideration of cell size. *Funct Plant Biol* 16: 443-448.
- Korneef M and Vanderveen JH (1980)** Induction and analysis of giberellin sensitive mutants in Arabidopsis thaliana (L.) heyneh. *Theor Appl Genet* 58: 257-263.
- Koornneef A, Leon-ReyesA, Ritsema T, VerhageA, Den Otter FC, et al. (2008)** Kinetics of salicylate-mediated suppression of jasmonate signaling reveal a role for redox modulation. *Plant Physiol.* 147: 1358–1368.
- Kuhlemeier C (2007)** Phyllotaxis. *Trends Plant Sci* 12: 143-150.
- Kühn U, Gündel M, Knoth A, Kerwitz Y, Rüdell S, Wahle E (2009)** Poly(A) tail length in controlled by the nuclear poly(A)-binding protein regulating the interaction between poly(A) polymerase and the cleavage and polyadenylation specificity factor. *J Biol Chem* 284: 22803-22814.
- Kunkel BN, Brooks DM (2002)** Cross talk between signaling pathways in pathogen defense. *Curr Opin Plant Biol* 5: 325-331.
- Kyburz A, Friedlein A, Langen H, Keller W (2006)** Direct interactions between subunits of CPSF and the U2 snRNP contribute to the coupling of pre-mRNA 3' end processing and splicing. *Mol Cell* 23: 195-205.
- Kyriakopoulou CB, Nordvarg H, Virtanen A (2001)** A novel nuclear human poly(A) polymerase (PAP) PAP γ . *J Biol Chem* 276: 33504-33511.
- Lee LYC, Hou X, Fang L, Fan S, Kumar PP, Yu H (2012)** STUNTED mediates the control of cell proliferation by GA in Arabidopsis. *Development* 139: 1568-1576.
- Leung J and Giraudat J (1998)** Abscisic acid signal transduction. *Annu Rev Plant Physiol Plant Mol Biol* 49: 199-222.
- Lenhard M and Laux T (2003)** Stem cell homeostasis in the Arabidopsis shoot meristem is regulated by intercellular movement of CLAVATA3 and its sequestration by CLAVATA1. *Development* 130: 3163-3173.
- Liang W, Li C, Liu F, Jiang H, Li S, Sun J, Wu X & Li C (2009)** The Arabidopsis homologs of CCR4-associated factor 1 show mRNA deadenylation activity and play a role in plant defence responses. *Cell Res* 19:307-316.
- Li QQ, Hunt AG (1997)** The polyadenylation of RNA in plants. *Plant Physiol* 115: 321–325
- Li Y, Zheng L, Corke F, Smith C, Bevan MW (2008)** Control of final seed and organ size by the DA1 gene family in Arabidopsis thaliana. *Genes Dev.* 22: 1331–1336.
- Ligner J, Kellermann J, Keller W (1991)** Cloning and expression of the essential gene for poly(A) polymerase from *S. cerevisiae*. *Nature* 354: 496-498.
- Liu D, Song Y, Chen Z, Yu D (2009)** Ectopic expression of miR396 suppresses GRF target gene expression and alters leaf growth in Arabidopsis. *Physiol Plantarum* 136: 223-236.
- Liu F, Marquardt S, Lister C, Swiezeswki S, Dean C (2010)** Targeted 3' end processing of antisense transcripts triggers Arabidopsis FLC chromatin silencing. *Science* 327: 94-97.
- Livak KJ and TD Schmittgen (2001)** Analysis of relative gene expression data using real-time quantitative PCR and the 2(-Delta Delta C(T)) Method. *Methods* 25(4): 402-408.

- Loke JC, Stahlberg EA, Strenski DG, Haas BJ, Wood PC, Li QQ (2005)** Compilation of mRNA polyadenylation signals in *Arabidopsis* revealed a new signal element and potential secondary structures. *Plant Physiol* 138: 1457-1468.
- Lorenzo O, Piqueras R, Sánchez-Serrano JJ, Solano R (2003)** ETHYLENE RESPONSE FACTOR1 integrates signals from ethylene and jasmonate pathways in plant defense. *Plant Cell* 15: 165–78
- Lukasik E, Takken FI (2009)** STANDING strong, resistance proteins instigators of plant defence. *Curr Opin Plant Biol* 12: 427-436.
- Luo W, Ji Z, Pan Z, You B, Hoque M, Li W, Gunderson AI, Tian B (2013)** The conserved intronic cleavage and polyadenylation site of Cstf-77 gene imparts control of 3' end processing activity through feedback autoregulation and by U1 snRNP. *PLoS Gen* 9: e1003613.
- Lutz CS, Murthy KGK, Schek N, O'Connor JP, Manley JL, Alwine JC (1996)** Interaction between U1 snRNP-A and the 160-kD subunit of cleavage-polyadenylation specificity factor increases polyadenylation efficiency in vitro. *Genes Dev* 10: 325-337.
- Lutz CS and Moreira A (2011)** Alternative mRNA polyadenylation in eukaryotes: an effective regulator of gene expression. *WIREs RNA* 2: 23-31.
- Lyons R, Iwase A, Gänsewig T, Sherstnev A, Duc C, Barton GJ, Hanada K, Higuchi-Takeuchi M, Matsui M, Sugimoto K, Kazan K, Simpson GG, Shirasu K (2013)** The RNA-binding protein FPA regulates flg22-triggered defense responses and transcription factor activity by alternative polyadenylation. *Sci Rep* 3:2866.
- Mandel CR, Bai Y, Tong L (2008)** Protein factors in pre-mRNA 3'-end processing. *Cell Mol Life Sci* 65: 1099-1122.
- Manley JL (1995)** A complex protein assembly catalyzes polyadenylation of mRNA precursors. *Curr Opin Genetics & Dev* 5: 222-228.
- Mans RJ and Huff NJ (1997)** Utilization of ribonucleic acid and deoxyoligomer primers for polyadenylic acid synthesis by adenosine triphosphate: polynucleotidylexotransferase from maize. *J Biol Chem* 250: 3672-3678.
- Manzano D, Marquardt S, Jones AM, Bäurle I, Liu F, Dean C (2009)** Altered interactions within FY/AtCPSF complexes required for Arabidopsis FCA-mediated chromatin silencing. *Proc Natl Acad Sci USA* 106: 8772-8777.
- Marrocco K, Bergdoll M, Achard P, Crigui MC, Genschik P (2010)** Selective proteolysis sets the tempo of the cell cycle. *Curr Opin Plant Biol* 13: 631-639.
- Martin G and Keller W (1996)** Mutational analysis of mammalian poly(A) polymerase identifies a region for primer binding and catalytic domain, homologous to the family X polymerases and to other nucleotidyltransferases. *EMBO J* 15: 2593-2603.
- Martin G, Jenö P, Keller W (1999)** Mapping of ATP binding regions in poly(A) polymerases by photoaffinity labeling and by mutational analysis identifies a domain conserved in many nucleotidyltransferases. *Protein Sci* 8: 2380-2391.
- Martin G, Keller W, Doublé S (2000)** Crystal structure of mammalian poly(A) polymerase in complex with an analog of ATP. *EMBO J* 19: 4193-4203.
- Martinez J, Ren YG, Nilsson P, Ehrenberg M & Virtanen A (2001)** The mRNA cap structure stimulates rate of poly(A) removal and amplifies processivity of degradation. *J Biol Chem* 276: 27923–27929.
- Mayr C and Bartel DP (2009)** Widespread shortening of 3'-UTRs by alternative cleavage and polyadenylation activates oncogenes in cancer cells. *Cell* 138:673-684.
- McDowell, JM (2011)** Beleaguered Immunity. *Science* 334: 1354-1355.
- Medler S, Al Husini N, Raghunayakula S, Mukundan B, Aldea A, Ansari A (2011)** Evidence for a complex of transcription factor IIB (TFIIB) with Poly(A) Polymerase and Cleavage Factor 1 subunits required for gene looping. *J Biol Chem* 286: 33709-22718.
- Medzhitov R and Janeway CA Jr. (1997)** Innate immunity: The Virtues of a Nonclonal System of Recognition. *Cell* 91(3): 295-298.
- Meeks LR, Addepalli B & Hunt AG (2009)** Characterization of genes encoding poly(A) polymerases in plants: evidence for duplication and functional specialization. *PLoS One* 4: e8082.

- Meijer HA, Bushell M, Hill K, Gant TW, Willis AE, Jones P, De Moor C (2007)** A novel method for poly(A) fractionation reveals a large population of mRNAs with a short poly(A) tail in mammalian cells. *Nucleic Acids Res* 35: e132.
- Meyerowitz Em (1997)** Control of cell division patterns in developing shoots and flowers of *Arabidopsis thaliana*. *Cold Spring Harb Symp Quant Biol* 62: 369-375.
- Millevoi S & Vagner S (2010)** Molecular mechanisms of eukaryotic pre-mRNA 3' end processing regulation. *Nucleic Acids Res* 38: 2757-2774.
- Mizukami Y and Fischer RL (2000)** Plant organ size control: *AINTEGUMENTA* in *Arabidopsis* plants results in increased growth of floral organs. *Dev Genet* 25: 224-236.
- Mogen BD, MacDonald MH, Leggewie G, Hunt AG (1992)** Several distinct types of sequence elements are required for efficient mRNA 3' end formation in a pea *rbcS* gene. *Mol Cell Biol* 12: 5406-5414
- Moreira A (2011)** Integrating transcription kinetics with alternative polyadenylation and cell cycle control. *Nucleus* 2: 556-561.
- Mori M, Nomura T, Ooka H, Ishizaka M, Yokota T, Sugimoto K, Okabe K, Kajiwara H, Satoh K, Yamamoto K, Hirochika h & Kikuchi S (2002)** Isolation and Characterization of a rice dwarf mutant with a defect in Brassinosteroid Biosynthesis. *Plant Physiol* 130: 1152-1161.
- Mouland AJ, Coady M, Yao XJ, Cohen EA (2002)** Hypophosphorylation of poly(A) polymerase and increased polyadenylation activity are associated with human immunodeficiency virus type I expression. *Virology* 292: 321-330.
- Muller R, Bleckmann A, Simon R (2008)** The receptor kinase CORYNE of *Arabidopsis* transmits the stem cell-limiting signal CLAVATA3 independently of CLAVATA1. *Plant Cell* 20: 934-946.
- Murthy and Manley (1995)** The 160-kDa subunit of human cleavage-polyadenylation specificity factor coordinates pre-mRNA 3'-end formation. *Genes & Dev* 9: 2672-2683.
- Nadeau JA and Sack FD (2002)** Stomatal development in *Arabidopsis*. *The Arabidopsis Book* 1, e0066.
- Nagaike T, Logan C, Hotta I, Rozenblatt-Rosen O, Meyerson M, Manley JL (2011)** Transcriptional activators enhance polyadenylation of mRNA precursors. *Mol Cell* 41: 409-418.
- Nakayama N, Smith RS, Mandel T, Robinson S, Kimura S, Boudaoud A, Kuhlemeier C (2012)** Mechanical regulation of Auxin-mediated Growth. *Curr Biol* 22: 1468-1476.
- Nath U, Crawford BCW, Carpenter R, Coen E (2003)** Genetic control of surface curvature. *Science* 299: 1404-1407.
- Navarro L, Zipfel C, Rowland O, Keller I, Robatzek S, Boller T, Jones JDG (2004)** The transcriptonal innate immune response to flg22. interplay and Overlap with Avr Gene-dependent defense responses and bacterial pathogenesis. *Plant Physiol* 135: 1113-1128.
- Navarro L, Bari R, Achard P, Lison P, Nemri A, Harberd NP, Jones JDG (2008)** DELLAs control plant immune responses by modulating the balance of jasmonic acid and salicylic acid signaling. *Curr Biol* 18: 650-655.
- Niu Y, Figueroa P, Browse J. (2011)** Characterization of JAZ-interacting bHLH transcription factors that regulate jasmonate responses in *Arabidopsis*. *J Exp Bot* 62: 2143-2154.
- Nishimura N, Kitahata N, Seki M, Narusaka Y, Narusaka M, Kuromori T, Asami T, Shinozaki K & Hirayama T (2005)** Analysis of *ABA hypersensitive germination2* revealed the pivotal functions of PARN in stress responses in *Arabidopsis*. *Plant J* 44(6): 972-984.
- Niwa M and Berget SM (1991)** Mutation of the AAUAAA polyadenylation signal depresses in vitro splicing of proximal but not distal introns. *Genes Dev* 5:2086-2095.
- Noir S, Börner M, Takahashi N, Ishida T, Tsui TL, Nalbi V, Shanahan H, Sugimoto K, Devoto A (2013)** Jasmonate controls leaf growth by repressing cell proliferation and the onset of endoreduplication while maintaining a potential stand-by-mode. *Plant Physiol* 161: 1930-1951.
- Ogawa T, Ueda Y, Yoshimura K, Shigeoka S (2006)** Comprehensive analysis of Nudix hydrolases in *Arabidopsis thaliana*. *J Biol Chem* 280: 25277-25238.

- Oszolak F, Kapranov P, Foissac S, Kim SW, Fishilevich E, Monaghan AP, John B, Milos PM (2010)** Comprehensive polyadenylation site maps in yeast and human reveal pervasive alternative polyadenylation. *Cell* 143:1018-1029.
- Park MY, Wu G, Gonzalez-Sulser A, Vaucheret H, Poething RS (2005)** Nuclear Processing and export of microRNAs in *Arabidopsis*. *Proc Nat Acad Sci USA* 102: 3691-3696.
- Pauwels L, Goossens A (2011)** The JAZ proteins: a crucial interface in the jasmonate signaling cascade. *Plant Cell* 23: 3089–3100.
- Peng J, Murray EL, Schönberg DR (2005)** The poly(A)-limiting element enhances mRNA accumulation by increasing the efficiency of pre-mRNA 3' end processing. *RNA* 11: 958-965.
- Perumal K, Sinha K, Henning D, Reddy R (2001)** Purification, characterization, and cloning of the cDNA of human signal recognition particle RNA 3'-adenylating enzyme. *J Biol Chem* 276: 21791-21796.
- Peterson KM, Rychel AL, Torii KU (2010)** Out of the mouths of plants: the molecular basis of the evolution and diversity of stomatal development. *Plant Cell* 22: 296–306.
- Pieterse CMJ, Van der Does D, Zamioudis C, Leon-Reyes A, Van Wees SCM (2012)** Hormonal modulation of plant immunity. *Annu Rev Cell Dev Biol* 28: 489-521.
- Pré M, Atallah M, Champion A, De Vos M, Pieterse CMJ, Memelink J (2008)** The AP2/ERF domain transcription factor ORA59 integrates jasmonic acid and ethylene signals in plant defense. *Plant Physiol* 147: 1347–1357.
- Powell AE and Lenhard M (2011)** Control of Organ size in Plants. *Curr Biol* 22(9): R360-R367.
- Pullen N, Jaeger KE, Wigge PA, Morris RJ (2013)** Simple network motifs can capture characteristics of the floral transition in *Arabidopsis*. *Plant Signal Behav* 8: 11.
- Quesada V, Macknight R, Dean C, Simpson G (2003)** Autoregulation of FCA pre-mRNA processing controls *Arabidopsis* flowering time. *EMBO J* 22: 3142-3152.
- Ramakers C, Ruijter JM, Deprez RH, Moorman AFM (2003)** Assumption-free analysis of quantitative real-time PCR data. *Neuroscience Letters* 339: 62-66.
- Raabe T, Bollum FL, Manley JL (1991)** Primary structure and expression of bovine poly(A) polymerase. *Nature* 353: 229-234.
- Rédei GP (1962)** Single locus heterosis. *Zeitschrift für Vererbungslehre* 93: 164-170.
- Reina- Pinto JJ, Voisin D, Teodor R, Yepremov A (2010)** Probing differentially expressed genes against a microarray database for in silico suppressor/enhancer and inhibitor/activator screens. *Plant J* 61: 166-175.
- Reinhardt D, Pesce ER, Stieger P, Mandel T, Baltensperger K, Bennett M, Traas J, Friml J, Kuhlemeier C (2003)** Regulation of phyllotaxis by polar auxin transport. *Nature* 426: 255-260.
- Reverdatto SV, Dutko JA, Chekanova JA, Hamilton DA & Belostotsky DA (2004)** mRNA deadenylation by PARN is essential for embryogenesis in higher plants. *RNA* 10: 1200-1214.
- Rietz S, Stamm A, Malonek S, Wagner S, Becker D, Medina-Escobar N, Vlot AC, Feys BJ, Niefind K, Parker JE (2011)** Different roles of Enhanced Disease Susceptibility1 (EDS1) bound to and dissociate from Phytoalexin Deficient4 (PAD4) in *Arabidopsis* immunity. *New Phytol* 191: 107-119.
- Robert-Seilaniantz A, Grant M, Jones JDG (2011a)** Hormone crosstalk in plant disease and defense: more than just jasmonate-salicylate antagonism. *Annu Rev Phytopathol* 49: 317–343.
- Robert-Seilaniantz A, MacLean D, Jikumaru Y, Hill L, Yamaguchi S, Kamiya Y, Jones JDG (2011b)** The microRNA miR393 re-directs secondary metabolite biosynthesis away from camalexin and towards glucosinolates. *Plant J* 67: 218–231.
- Rodriguez RE, Mecchia MA, Debernardi JM, Schommer C, Weigel D, Palatnik JF (2010)** Control of cell proliferation in *Arabidopsis thaliana* by microRNA miR396. *Development* 137: 103-112.
- Rothnie HM(1996)** Plant mRNA 3'-end formation. *PlantMol Biol* 32: 43-61
- Rothnie HM, Chen G, Futterer J, Hohn T (2001)** Polyadenylation in rice tungro bacilliform virus: cis-acting signals and regulation. *J Virol* 75: 4184–4194

- Ruijter JM, Ramakers C, Hoogaars WMH, Karlen Y, Bakker O, van den Hoff MJB, Moorman AFM (2009)** Amplification efficiency: linking baseline and bias in the analysis of quantitative PCR data. *Nucleic Acids Research* 37(6): e45.
- Rupp HM, Frank M, Werner T, Strnad M, Schmülling T (1999)** Increase steady state mRNA levels of the STM and KNAT1 homeobox genes in cytokinin overproducing *Arabidopsis thaliana* indicate a role for cytokinins in the shoot apical meristem. *Plant J* 18: 557-563.
- Sanfacon H, Brodmann P, Hohn T (1991)** A dissection of the cauliflower mosaic virus polyadenylation signal. *Genes Dev* 5: 141-149
- Sachs AB, Sarnow P, Hentze MW (1997)** Starting at the beginning, middle, and end: translation initiation in eukaryotes. *Cell* 89: 831-838.
- Sawicki SG, Jelinek W, Darnell JE (1977)** 3'-terminal addition to HeLa cell nuclear and cytoplasmic poly(A). *J Mol Biol* 113: 219-235.
- Schmidt M and Jensen TH (2006)** The exosome: a multipurpose RNA-decay machine. *Trends Biochem Sci* 33: 501-510.
- Schoof H, Lenhard M, Haecker A, Mayer KFX, Jürgens G, Laux T (2000)** The stem cell population of *Arabidopsis* shoot meristems is maintained by a regulatory loop between the CLAVATA and WUSCHEL genes. *Cell* 100: 635-644.
- Schönberg DR, Moskaitis JE, Smith LHJ, Pastori RL (1989)** Extranuclear Estrogen-regulated destabilization of *Xenopus laevis* Serum Albumin mRNA. *Mol Endocrinol* 3: 805-815.
- Shaul O, Mironov V, Bursens S, Van Montagu M, Inzé D (1996)** Two *Arabidopsis* cyclin promoters mediate distinctive translational oscillation in synchronized tobacco BY-2 cells. *Proc Natl Acad Sci USA* 93: 4868-4872.
- Sherstnev A, Duc C, Cole C, Zacharaki V, Hornyik C, Ozsolak F, Milos PM, Barton GJ, Simpson GG (2012)** Direct sequencing of *Arabidopsis thaliana* RNA reveals patterns of cleavage and polyadenylation. *Nat Struct Mol Biol* 19: 845-852.
- Shi Y, Giammartino DC, Taylor D, Sarkeshik A, Rice WJ, Yates JR 3rd, Frank J, Manley JL (2009)** Molecular architecture of the human pre-mRNA 3'end processing complex. *Mol Cell* 33(3): 365-376.
- Spartz AK, Lee SH, Wenger JP, Gonzalez N, Itoh H, Inzé D, Peer WA, Murphy AS, Overvoorde PJ, Gray WM (2012)** The SAUR19 subfamily of SMALL AUXIN UP RNA genes promote cell expansion. *Plant J* 70: 978-990
- Spoel SH, Koornneef A, Claessens SMC, Korzelius JP, Van Pelt JA, Mueller MJ, Buchala AJ, Métraux JP, Brown R, Kazan K, VanLoon LC, Dong X, Pieterse CMJ (2003)** NPR1 modulates cross-talk between salicylate- and jasmonate-dependent defense pathways through a novel function in the cytosol. *Plant Cell* 15: 760-770.
- Spoel SH, Johnson JS, Dong X (2007)** Regulation of tradeoffs between plant defenses against pathogens with different lifestyles. *Proc Natl Acad Sci USA* 104: 18842-18847.
- Spoel SH and Loake GJ (2011)** Redox-based protein modifications: the missing link in plant immune signalling. *Curr Opin Plant Biol* 14: 358-364.
- Stebbins GL (1974)** Flowering plants: evolution above the species level. *Belknap Press, Cambridge, Mass.*
- Steiner E, Efroni I, Gopalraj M, Saathoff K, Tseng TS, Kieffer M, Eshed Y, Olszewski N, Weiss D (2012)** The *Arabidopsis* O-linked n-acetylglucosamine transferase spindly interacts with class I TCPs to facilitate cytokinin responses in leaves and flowers. *Plant Cell* 24: 96-108.
- Steitz TA (1998)** A mechanism for all polymerases. *Nature* 391: 231-232.
- Stintzi A and Browse J (2000)** The *Arabidopsis* male-sterile mutant, opr3, lacks the 12-oxophytodenoic acid reductase required for jasmonate synthesis. *Proc Natl Acad Sci USA* 97: 10625-10630.
- Stransfeld L, Eriksson S, Adamski NM, Breuninger H, Lenhard M (2010)** KLUH/CYP78A5 promotes organ growth without affecting the size of the early primordium. *Plant Signaling Behav* 5: 982-984.

- Straus MR, Rietz S, van Thernaat EVL, Bartsch M, Parker JE (2010)** Salicylic acid antagonism of EDS1-driven cell death is important for immune and oxidative stress responses in *Arabidopsis*. *Plant J* 62: 628-640.
- Subtelny AO, Eichhorn SW, Chen GR, Sive H, Bartel DP (2014)** Poly(A)-tail profiling reveals an embryonic switch in translational control. *Nature* 2014/01/29/online.
- Sullivan M and Morgan DO (2007)** Finishing mitosis, one step at a time. *Nat Rev Mol Cell Biol* 8: 894-903.
- Szekeres M, Németh K, Koncz-Kálmán Z, Mathur J, Kauschmann A, Altmann T, Rédei GP, Nagy F, Schell J, Koncz C (1996)** Brassinosteroids rescue the deficiency of CYP90, a cytochrome P450, controlling cell elongation and de-etiolation in *Arabidopsis*. *Cell* 85: 171-182.
- Tada Y, Spoel SH, Pajerowska-Mukhtar K, Mou Z, Song J**
- Tao Y, Xie Z, Chen W, Glazebrook J, Chang H-S, Han B, Zhu T, Zou G, Katagiri F (2003)** Quantitative nature of *Arabidopsis* responses during compatible and incompatible interactions with the bacterial pathogen *Pseudomonas syringae*. *Plant Cell* 15: 317-330.
- Thomas PE, Xiaohui W, Liu M, Gaffney B, Guoli J, Qingshun QL, Hunt AG (2012)** Genome-wide control of polyadenylation site choice by CPSF30 in *Arabidopsis*. *Plant Cell* 24: 4376-4388.
- Thordal-Christensen H, Zhang Z, Wei C, Collinge DB (1997)** Subcellular localization of H₂O₂ in plants. H₂O₂ accumulation in papillae and hypersensitive response during barley-powdery mildew interaction. *Plant J* 11: 1187-1194.
- Thureson A, Astrom J, Astrom A, Grovnik K, Virtanen A (1994)** Multiple forms of poly(A) polymerases in human cells. *Proc Natl Acad Sci USA* 91: 979-983.
- Tian B, Hu H, Zhang H, Lutz CS (2005)** A large scale analysis of mRNA polyadenylation of human and mouse genes. *Nucl Acids Res* 33: 201-212.
- Topalian SL, Kaneko S, Gonzales MI, Bond GI, Ward Y, Manley JL (2001)** Identification and characterization of neo-poly(A) polymerase, an RNA processing enzyme overexpressed in human tumors. *Mol Cell Biol* 21:5614-5623.
- Tsuda K, Sato M, Stoddard T, Glazebrook J, Katagiri F (2009)** Network properties of robust immunity in plants. *PLoS Genetics* 5:e1000772.
- Twell, D., Wing, R., Yamagushi, J., McCormick, S. (1989)** Isolation and expression of an anther-specific gene from tomato. *Mol Gen Genet* 217: 240-245.
- Tzafrir I, Pena-Muralla R, Dickermann A, Berg M, Rogers R, Hutchens S, Sweeney TC, McElver J, Aux G, Patton D, Meinke D (2004)** Identification of genes required for embryo development in *Arabidopsis*. *Plant Physiol* 135: 1206-1220.
- Venthatham V, Roa N, Manley JL (2007)** Sumoylation regulates multiple aspects of mammalian poly(A) polymerase function. *Genes & Dev* 22: 499-511.
- Verberne MC, Hoekstra J, Bol JF, Linthorst HJM (2003)** Signaling of systemic acquired resistance in tobacco depends on ethylene perception. *Plant J* 35: 27-32.
- Vlot AC, Dempsey DA, Klessig DF (2009)** Salicylic acid, a multifaceted hormone to combat disease. *Annu Rev Phytopathol* 47: 177-206.
- Vi, Lang-Son (2011)** The role of a canonical Poly(A) Polymerase in organ-identity dependent size regulation in *Arabidopsis thaliana*. *PhD Thesis*, University of East Anglia.
- Vi LS, Trost G, Lange P, Czesnick H, Rao N, Lieber D, Laux T, Gray WM, Manlex JL, Groth D, Kappel C, Lenhard M (2013)** Target specificity among nuclear poly(A) polymerases in plants modulates organ growth and pathogen response. *Proc Natl Acad Sci USA* 110: 13994-13999.
- Vinciguerra P and Stutz F (2004)** mRNA export: an assembly line from genes to nuclear pores. *Curr Opin Cell Biol* 2004 16: 285-292.
- Wagner E, Clement SL, Lykke-Andersen J (2007)** An unconventional human CCR4-CAF1 deadenylase complex in nuclear cajal bodies. *Mol Cell Biol* 27: 1686-1695.
- Wahle E, Martin G, Schiltz, Keller W (1991)** Isolation and expression of cDNA clones encoding mammalian poly(A) polymerase. *EMBO J* 10:4251-4257.

- Wahle E (1991)** Purification and characterisation of mammalian polyadenylate polymerase involved in 3' end processing of messenger RNA precursors. *J Biol Chem* 226:3131-3139.
- Wahle E (1995)** Poly(A) tail length control is caused by termination of processive synthesis. *J Biol Chem* 270: 2800-2808.
- Wahle E and Rügsegger U (1999)** 3'-end processing of pre-mRNA in eukaryotes. *FEMS Microbiol Rev* 23: 277-295.
- Wahle E and Winkler GS (2013)** RNA decay machines: deadenylation by the Ccr4-Not and Pan2-Pan3 complexes. *Biochim Biophys Acta* 1829: 561-579
- Wang D, Pajeroska-Mukhtar K, Hendrickson Culler A, Dong X (2007)** Salicylic acid inhibits pathogen growth in plants through repression of the auxin signaling pathway. *Curr Biol* 17: 784–1790.
- Wang L, Gu X, Xu D, Wand W, Wang H, Zeng M, Chang Z, Huang H, Cui X (2011)** miR396-targeted AtGRF transcription factors are required for coordination of cell division and differentiation during leaf development in *Arabidopsis*. *J Exp Bot* 62: 761–773.
- Wang H, Lu Y, Liu P, Wen W, Zhang J, Ge X, Xia Y (2013)** The ammonium/nitrate ratio is a input signal in the temperature modulated, SNC1-mediated and EDS1-dependent autoimmunity of *nudt6-1 nudt7*. *Plant J* 73: 262-275.
- Walley JW, Kelley DR, Nestorova G, Hirschberg DL, Dehesh K (2010a)** *Arabidopsis* deadenylases AtCAF1a and AtCAF1b play overlapping and distinct roles in mediating environmental stress responses. *Plant Physiol* 152: 866-875.
- Walley JW, Kelley DR, Savchenko T, Dehesh K (2010)** Investigating the function of CAF1 deadenylases during plant stress responses. *Plant Signal Behav* 5: 802-805.
- Wasternack C and Hause B (2013)** Jasmonates: biosynthesis, perception, signal transduction and action in plant stress response, growth and development. An update to the 2007 review in *Annals of Botany*. *Annals of Botany* 111(6): 1021-1058.
- Weill L, Belloc E, Bava FA, Mendez R (2012)** Translational control by changes in poly(A) tail length. *Nature Struct Mol Biol* 19: 577-585.
- Werner T, Motyka V, Strnad M, Schmülling T (2001)** Regulation of plant growth by cytokinin. *Proc Natl Acad Sci USA* 98: 10487-10492.
- Wickens M, Anderson P, Jackson RJ (1997)** Life and death in the cytoplasm: messages from the 3'end. *Curr Opin Genetics Develop* 7: 220–232.
- Wiermer M, Feys BJ, Parker JE (2005)** Plant immunity: the EDS1 regulatory node. *Curr Opin Plant Biol* 8: 383-389.
- Wilusz CJ, Wormington M, Peltz SW (2001)** The cap-to-tail guide to mRNA turnover. *Nat Rev Mol Cell Biol* 2:237–246.
- Winter CM, Austin RS, Blanvillan-Baufume S, Reback MA, Monniaux M, Wu MF, Sang Y, Yamaguchi A, Yamaguchi N, Parker JE, Parcy F, Jiensen ST, Li H, Wagner D (2011)** LEAFY target genes reveal floral regulatory logic, cis motifs, and a link to biotic stimulus responses. *Dev Cell* 20: 430-443.
- Wu X, Liu M, Downie B, Liang C, Ji G, Li QQ, Hunt AG (2011)** Genome-wide landscape of polyadenylation in *Arabidopsis* provides evidence for extensive alternative polyadenylation. *Proc Natl Acad Sci USA* 108: 12533-12538.
- Xing D and Li QQ (2010)** Alternative polyadenylation and gene expression regulation in plants. *RNA* 2: 445–458.
- Xu R, Ye X, Quinn Li Q (2004)** AtCPSF-II gene encoding an *Arabidopsis* homolog of CPSF 73 kDa subunit is critical for early embryo development. *Gene* 324: 35-45.
- Xu R, Zhao H, Dinkins RD, Cheng X, Carberry G, Li QQ (2006)** The 73 kDa subunit of the cleavage and polyadenylation specificity factor (CPSF) complex affects reproductive development in *Arabidopsis*. *Plant Mol Biol* 61: 799-815.

- Yamashita A, Chang TC, Yamashita Y, Zhu W, Zhong Z, Chen CYA, Shyu AB (2005)** Concerted action of poly(A) nucleases and decapping enzymes in mammalian mRNA turnover. *Nature Struct Mol Biol* 12: 1054-1063.
- Yang T, Davies PJ, Reid JB (1996)** Genetic dissection of the relative roles of auxin and giberellin in the regulation of stem elongation in intact light-grown peas. *Plant Physiol* 110: 1029-1034.
- Yanisch-Perron, C., Vieira, J., Messing, J. (1985)** Improved M13 phage cloning vectors and host strains: nucleotide sequences of the M13mp18 and pUC19 vectors. *Gene* 33: 103-119.
- Yao Y, Song L, Katz Y, Galili G (2002)** Cloning and characterization of Arabidopsis homologues of the animal CstF complex that regulates 3' mRNA cleavage and polyadenylation. *J Exp Bot* 53: 2277-2278.
- Yasuda M, Ishikawa A, Jikumaru Y, Seki M, Umezawa T, Asami T, Maruyama-Nakashita A, Kudo T, Shinozaki K, yoshida S, Nakashita H (2008)** Antagonistic interaction between systemic acquired resistance and the abscisic acid-mediated abiotic stress response in *Arabidopsis*. *Plant Cell* 20: 1678–1692.
- Ye Z, Ting JPY (2008)** NLR, the nucleotide-binding domain leucine-rich repeat containing family. *Curr Opin Immun* 20: 3-9.
- Yuan M, Shaw PJ, Warn RM, Lloyd CW (1994)** Dynamic reorientation of cortical microtubules, from transverse to longitudinal, in living plant cells. *Proc Natl Acad Sci USA* 91: 6050-6053.
- Zhao W and Manley JL (1996)** Complex alternative RNA processing generates unexpected diversity of poly(A) polymerase isoforms. *Mol Cell Biol* 16:2378-2386.
- Zipfel C (2008)** Pattern-recognition receptors in plant innate immunity. *Curr Opin Immun* 20: 10-16.